3.3 MECHANICAL PROPERTIES OF MATERIALS

This section provides the mechanical properties used in the structural evaluation. The properties include yield stress, ultimate stress, modulus of elasticity, Poisson's ratio, weight density, and coefficient of thermal expansion. Values are presented for a range of temperatures which envelopes the maximum and minimum temperatures under all service conditions applicable to the HI-STORM FW system components.

The materials selected for use in the MPC, HI-STORM FW overpack, and HI-TRAC VW transfer cask are presented on the drawings in Section 1.5. In this chapter, the materials are divided into two categories, structural and nonstructural. Structural materials are materials that act as load bearing members and are, therefore, significant in the stress evaluations. Materials that do not support mechanical loads are considered nonstructural. For example, the HI-TRAC VW inner shell is a structural material, while the lead between the inner and outer shell is a nonstructural material. For nonstructural materials, the principal property that is used in the structural analysis is weight density. In local deformation analysis, however, such as the study of penetration from a tornado-borne missile, the properties of lead in HI-TRAC VW and plain concrete in HI-STORM FW are included.

3.3.1 Structural Materials

a. Alloy X

A hypothetical material termed Alloy X is defined for the MPC pressure retaining boundary. The material properties of Alloy X are the least favorable values from the set of candidate alloys. The purpose of a least favorable material definition is to ensure that all structural analyses are conservative, regardless of the actual MPC material. For example, when evaluating the stresses in the MPC, it is conservative to work with the minimum values for yield strength and ultimate strength. This guarantees that the material used for fabrication of the MPC will be of equal or greater strength than the hypothetical material used in the analysis.

Table 3.3.1 lists the numerical values for the material properties of Alloy X versus temperature. These values, taken from the ASME Code, Section II, Part D [3.3.1], are used in all structural analyses. As is shown in Chapter 4, the maximum metal temperature for Alloy X used at or within the Confinement Boundary remains below 1000°F under all service modes. As shown in ASME Code Case N-47-33 (Class 1 Components in Elevated Temperature Service, 2007 Code Cases, Nuclear Components), the strength properties of austenitic stainless steels do not change due to exposure to 1000°F temperature for up to 10,000 hours. Therefore, there is no risk of a significant effect on the mechanical properties of the confinement or boundary material during the short time duration loading. A further description of Alloy X, including the materials from which it is derived, is provided in Appendix 1.A.

Two properties of Alloy X that are not included in Table 3.3.1 are weight density and Poisson's ratio. These properties are assumed constant for all structural analyses, regardless of temperature. The values used are shown in the table below.

PROPERTY	VALUE
Weight Density (lb/in^3)	0.290
Poisson's Ratio	0.30

b. Metamic-HT

Metamic-HT is a composite of nano-particles of aluminum oxide (alumina) and finely ground boron carbide particles dispersed in the metal matrix of pure aluminum. Metamic-HT is the principal constituent material of the HI-STORM FW fuel baskets. Metamic-HT neutron absorber is an enhanced version of the Metamic (classic) product widely used in dry storage fuel baskets [3.1.4, 3.3.2] and spent fuel storage racks [1.2.11]. The enhanced properties of Metamic-HT derive from the strengthening of its aluminum matrix with ultra fine-grained (nano-particle size) alumina (Al_2O_3) particles that anchor the grain boundaries. The strength properties of Metamic-HT have been characterized through a comprehensive test program, and Minimum Guaranteed Values suitable for structural design are archived in [Table 1.2.8]. The Metamic-HT metal matrix composite thus exhibits excellent mechanical strength properties (notably creep resistance) in addition to the proven thermal and neutron absorption properties that are intrinsic to borated aluminum materials. The specific Metamic-HT composition utilized in this FSAR has 10% (min.) B_4C by weight.

Section 1.2.1.4.1 provides detailed information on Metamic-HT. Mechanical properties are provided in Table 1.2.8

c. Carbon Steel, Low-Alloy and Nickel Alloy Steel

The carbon steels in the HI-STORM FW system are SA516 Grade 70, SA515 Grade 70, and SA36. The low alloy steel is SA350-LF3. The material properties of SA516 Grade 70 and SA515 Grade 70 are shown in Tables 3.3.2. The material properties of SA350-LF2 and SA350-LF3 are given in Table 3.3.3. The material properties of SA36 are shown in Table 3.3.6.

Two properties of these steels that are not included in Tables 3.3.2, 3.3.3 and 3.3.6 are weight density and Poisson's ratio. These properties are assumed constant for all structural analyses. The values used are shown in the table below.

PROPERTY	VALUE
Weight Density (lb/in^3)	0.283
Poisson's Ratio	0.30

d. Bolting Materials

Material properties of the bolting materials used in the HI-STORM FW system are given in Table 3.3.4.

e. Weld Material

All weld materials utilized in the welding of the Code components comply with the provisions of the appropriate ASME subsection (e.g., Subsection NB for the MPC enclosure vessel) and Section IX. All non-code welds will be made using weld procedures that meet Section IX of the ASME Code. The minimum tensile strength of the weld wire and filler material (where applicable) will be equal to or greater than the tensile strength of the base metal listed in the ASME Code.

3.3.2 Nonstructural Materials

a. Concrete

The primary function of the plain concrete in the HI-STORM FW storage overpack is shielding. Concrete in the HI-STORM FW overpack is not considered as a structural member, except to withstand compressive, bearing, and penetrant loads. Therefore the mechanical behavior of concrete must be quantified to determine the stresses in the structural members (steel shells surrounding it) under accident conditions. Table 3.3.5 provides the concrete mechanical properties. Allowable, bearing strength in concrete for normal loading conditions is calculated in accordance with ACI 318-05 [3.3.5]. The procedure specified in ASTM C-39 is utilized to verify that the assumed compressive strength will be realized in the actual in-situ pours. Appendix 1.D in the HI-STORM 100 FSAR [3.1.4] provides additional information on the requirements on plain concrete for use in HI-STORM FW storage overpack.

To enhance the shielding performance of the HI-STORM FW storage overpack, high density concrete can be used during fabrication. The permissible range of concrete densities is specified in Table 1.2.5. The structural calculations consider the most conservative density value (i.e., maximum or minimum weight), as appropriate.

b. Lead

Lead is not considered as a structural member of the HI-STORM FW system. Its load carrying capacity is neglected in all structural analysis, except in the analysis of a tornado missile strike where it acts as a missile barrier. Applicable mechanical properties of lead are provided in Table 3.3.5.

c. Fuel Basket Shims

The fuel basket shims (basket shims), as presented on the drawings in Section 1.5, are made of an aluminum alloy to ensure a high thermal conductivity and to ensure stable mechanical properties in the temperature range obtained in the peripheral region of the fuel basket. Nominal mechanical properties for the basket shims are tabulated in Table 3.3.7.

Strictly speaking, the shim is not a structural material because it does not withstand any tensile loads and is located in a confined space which would prevent its uncontrolled deformation under load. The simulation of the shim in the basket's structural model, however, utilizes its mechanical properties of which only the Yield Strength has a meaningful (but secondary) role. Accordingly, in this FSAR, the nominal value of the Yield Strength specified in Table 3.3.7 herein, is set down as a "critical characteristic" for the shim material. The minimum value of the Yield Strength reported in the material supplier's CoC must be at least 90% of the nominal value in the above referenced table to ensure that the non-mechanistic tip-over analysis will not have to be revisited.

Table 3.3.1

ALLOY X MATERIAL PROPERTIES

Temp. (Deg. F)	Alloy X			
	S_y	S_u[†]	α	E
-40	30.0	75.0 (70.0)	--	28.88
100	30.0	75.0 (70.0)	8.6	28.12
150	27.5	73.0 (68.1)	8.8	27.81
200	25.0	71.0 (66.3)	8.9	27.5
250	23.7	68.6 (64.05)	9.1	27.25
300	22.4	66.2 (61.8)	9.2	27.0
350	21.55	65.3 (60.75)	9.4	26.7
400	20.7	64.4 (59.7)	9.5	26.4
450	20.05	63.9 (59.45)	9.6	26.15
500	19.4	63.4 (59.2)	9.7	25.9
550	18.85	63.35 (59.1)	9.8	25.6
600	18.3	63.3 (59.0)	9.8	25.3
650	17.8	62.85 (58.6)	9.9	25.05
700	17.3	62.4 (58.3)	10.0	24.8
750	16.9	62.1 (57.9)	10.0	24.45
800	16.5	61.7 (57.6)	10.1	24.1

Definitions:

S_y = Yield Stress (ksi)
α = Mean Coefficient of thermal expansion (in./in. per degree F x 10^{-6})
S_u = Ultimate Stress (ksi)
E = Young's Modulus (psi x 10^6)

Notes:

1. Source for S_y values is Table Y-1 of [3.3.1].
2. Source for S_u values is Table U of [3.3.1].
3. Source for α values is Table TE-1 of [3.3.1].
4. Source for E values is material group G in Table TM-1 of [3.3.1].

[†] The ultimate stress of Alloy X is dependent on the product form of the material (i.e., forging vs. plate). Values in parentheses are based on SA-336 forged materials (type F304, F304LN, F316, and F316LN), which are used solely for the one-piece construction MPC lids. All other values correspond to SA-240 plate material.

Table 3.3.2

SA516 AND SA515, GRADE 70 MATERIAL PROPERTIES

Temp. (Deg. F)	SA516 and SA515, Grade 70			
	S_y	S_u	α	E
-40	38.0	70.0	---	29.98
100	38.0	70.0	6.5	29.26
150	35.7	70.0	6.6	29.03
200	34.8	70.0	6.7	28.8
250	34.2	70.0	6.8	28.55
300	33.6	70.0	6.9	28.3
350	33.05	70.0	7.0	28.1
400	32.5	70.0	7.1	27.9
450	31.75	70.0	7.2	27.6
500	31.0	70.0	7.3	27.3
550	30.05	70.0	7.3	26.9
600	29.1	70.0	7.4	26.5
650	28.2	70.0	7.5	26.0
700	27.2	70.0	7.6	25.5
750	26.3	69.1	7.7	24.85

Definitions:

S_y = Yield Stress (ksi)
α = Mean Coefficient of thermal expansion (in./in. per degree F x 10^{-6})
S_u = Ultimate Stress (ksi)
E = Young's Modulus (psi x 10^6)

Notes:
1. Source for S_y values is Table Y-1 of [3.3.1].
2. Source for S_u values is Table U of [3.3.1].
3. Source for α values is material group 1 in Table TE-1 of [3.3.1].
4. Source for E values is "Carbon steels with C less than or equal to 0.30%" in Table TM-1 of [3.3.1]

Table 3.3.3

SA350-LF3 AND SA350-LF2 MATERIAL PROPERTIES

Temp. (Deg. F)	SA350-LF3 (SA350-LF2)			SA350-LF3 (SA350-LF2)	
	S_m	S_y	S_u	E	α
-20	23.3	37.5 (36.0)	70.0	28.22 (29.88)	---
100	23.3	37.5 (36.0)	70.0	27.64 (29.26)	6.5
200	22.9 (22.0)	34.3 (33.0)	70.0 (70.0)	27.1 (28.8)	6.7
300	22.1 (21.2)	33.2 (31.8)	70.0 (70.0)	26.7 (28.3)	6.9
400	21.4 (20.5)	32.0 (30.8)	70.0 (70.0)	26.2 (27.9)	7.1
500	20.3 (19.6)	30.4 (29.3)	70.0 (70.0)	25.7 (27.3)	7.3
600	18.8 (18.4)	28.2 (27.6)	70.0 (70.0)	25.1 (26.5)	7.4
700	16.9 (17.2)	25.3 (25.8)	66.5 (70.0)	24.6 (25.5)	7.6

Definitions:

S_m = Design Stress Intensity (ksi)
S_y = Yield Stress (ksi)
S_u = Ultimate Stress (ksi)
α = Mean Coefficient of Thermal Expansion (in./in. per degree F x 10^{-6})
E = Young's Modulus (psi x 10^6)

Notes:

1. Source for S_m values is Table 2A of [3.3.1].
2. Source for S_y values is Table Y-1 of [3.3.1].
3. Source for S_u values is ratioing S_m values.
4. Source for α values is group 1 alloys in Table TE-1 of [3.3.1].
5. Source for E values is material group B (for SA350-LF3) and "Carbon steels with C less than or equal to 0.30%" (for SA350-LF2) in Table TM-1 of [3.3.1].
6. Values for LF2 are given in parentheses where different from LF3.

Table 3.3.4

BOLTING MATERIAL PROPERTIES

SB637-N07718 (less than or equal to 6 inches diameter)					
Temp. (Deg. F)	S_y	S_u	E	α	S_m
-100	150.0	185.0	29.9	---	50.0
-20	150.0	185.0	29.43	---	50.0
70	150.0	185.0	28.9	7.1	50.0
100	150.0	185.0	28.76	7.1	50.0
200	144.0	177.6	28.3	7.2	48.0
300	140.7	173.5	27.9	7.3	46.9
400	138.3	170.6	27.5	7.5	46.1
500	136.8	168.7	27.2	7.6	45.6
600	135.3	166.9	26.8	7.7	45.1
SA193 Grade B7 (2.5 to 4 inches diameter)					
Temp. (Deg. F)	S_y	S_u	E	α	S_m
100	95.0	115.0	29.46	6.5	31.7
200	88.5	115.0	29.0	6.7	29.5
300	85.1	115.0	28.5	6.9	28.4
400	82.7	115.0	28.0	7.1	27.6
500	80.1	115.0	27.4	7.3	26.7
600	77.1	115.0	26.9	7.4	25.7

Definitions:

S_m = Design stress intensity (ksi)
S_y = Yield Stress (ksi)
α = Mean Coefficient of thermal expansion (in./in. per degree F x 10^{-6})
S_u = Ultimate Stress (ksi)
E = Young's Modulus (psi x 10^6)

Notes:

1. Source for S_m values is Table 4 of [3.3.1].
2. Source for S_y values is ratioing design stress intensity values and Table Y-1 of [3.3.1], as applicable.
3. Source for S_u values is ratioing design stress intensity values and Table U of [3.3.1], as applicable.
4. Source for α values is Tables TE-1 and TE-4 of [3.3.1], as applicable.
5. Source for E values is Tables TM-1 and TM-4 of [3.3.1], as applicable.

Table 3.3.4 (CONTINUED)

BOLTING MATERIAL PROPERTIES

Temp. (Deg. F)	S_y	S_u	E	α	S_m
SA193 Grade B7 (less than or equal to 2.5 inches diameter)					
100	105.0	125.0	29.46	6.5	35.0
200	98.0	125.0	29.0	6.7	32.6
300	94.1	125.0	28.5	6.9	31.4
400	91.5	125.0	28.0	7.1	30.5
500	88.5	125.0	27.4	7.3	29.5
600	85.3	125.0	26.9	7.4	28.4
SA564 630 H1150					
100	105.0	135.0	28.33	6.4	45.0
200	97.1	135.0	27.8	6.6	45.0
300	93.0	135.0	27.2	6.7	45.0
400	89.7	131.2	26.7	6.9	43.7
500	87.0	128.6	26.1	7.0	42.9
600	84.7	126.7	25.5	7.1	42.2

Definitions:

S_m = Design stress intensity (ksi)
S_y = Yield Stress (ksi)
α = Mean Coefficient of thermal expansion (in./in. per degree F x 10^{-6})
S_u = Ultimate Stress (ksi)
E = Young's Modulus (psi x 10^6)

Notes:
1. Source for S_y values is Table Y-1 of [3.3.1].
2. Source for S_u values is Table U of [3.3.1].
3. Source for α values is group 1 alloys and Condition 1150 precipitation hardened stainless steel in Table TE-1 of [3.3.1].
4. Source for E values is material group C and S17400 in Table TM-1 of [3.3.1].
5. Source for S_m values is Table 4 and Table 2A of [3.3.1] for SA-193 Grade B7 and SA-564 630 H1150 respectively.

Table 3.3.5

CONCRETE AND LEAD MECHANICAL PROPERTIES

PROPERTY	**VALUE**					
CONCRETE:						
Compressive Strength (psi)	3,300 psi					
Nominal Density (lb/ft^3)	150 lb/cubic feet					
Allowable Bearing Stress (psi)	1,543†					
Allowable Axial Compression (psi)	1,042†					
Allowable Flexure, extreme fiber tension (psi)	158†,††					
Allowable Flexure, extreme fiber compression (psi)	1,543†					
Mean Coefficient of Thermal Expansion (in/in/deg. F)	5.5E-06					
Modulus of Elasticity (psi)	57,000 (compressive strength (psi))$^{1/2}$					
LEAD:	-40°F	-20°F	70°F	200°F	300°F	600°F
Yield Strength (psi)	700	680	640	490	380	20
Modulus of Elasticity (ksi)	2.4E+3	2.4E+3	2.3E+3	2.0E+3	1.9E+3	1.5E+3
Coefficient of Thermal Expansion (in/in/deg. F)	15.6E-6	15.7E-6	16.1E-6	16.6E-6	17.2E-6	20.2E-6
Poisson's Ratio	0.40					
Density (lb/cubic ft.)	708					

Notes:
1. Concrete allowable stress values based on ACI 318-05.
2. Lead properties are from [3.3.7].

† Values listed correspond to concrete compressive stress = 3,300 psi.
†† No credit for tensile strength of concrete is taken in the calculations.

Table 3.3.6

SA36 MATERIAL PROPERTIES

Temp. (Deg. F)	SA36			
	S_y	S_u	α	E
-40	36.0	58.0	---	29.98
100	36.0	58.0	6.5	29.26
150	33.8	58.0	6.6	29.03
200	33.0	58.0	6.7	28.8
250	32.4	58.0	6.8	28.55
300	31.8	58.0	6.9	28.3
350	31.3	58.0	7.0	28.1
400	30.8	58.0	7.1	27.9
450	30.05	58.0	7.2	27.6
500	29.3	58.0	7.3	27.3
550	28.45	58.0	7.3	26.9
600	27.6	58.0	7.4	26.5
650	26.7	58.0	7.5	26.0
700	25.8	58.0	7.6	25.5

Definitions:

S_y = Yield Stress (ksi)
α = Mean Coefficient of thermal expansion (in./in./^{0}F x 10^{-6})
S_u = Ultimate Stress (ksi)
E = Young's Modulus (psi x 10^6)

Notes:
1. Source for S_y values is Table Y-1 of [3.3.1].
2. Source for S_u values is Table U of [3.3.1].
3. Source for α values is group 1 alloys in Table TE-1 of [3.3.1].
4. Source for E values is "Carbon steels with C less than or equal to 0.30%" in Table TM-1 of [3.3.1].

Table 3.3.7

FUEL BASKET SHIMS – NOMINAL MECHANICAL PROPERTIES

Temp. °C (°F)	Aluminum Alloy (B221 2219-T8511)				
	S_y	S_u	E	α	% Elongation
25 (75)	290 (42)	400 (58)	7.2 (10.5)	–	5
150 (300)	243 (35)	307 (44)	6.8 (9.8)	23.9 (13.3)	6.4
204 (400)	188 (27)	231 (34)	6.3 (9.1)	24.5 (13.6)	8.2
230 (450)	171 (25)	209 (30)	6.1 (8.8)	24.8 (13.8)	8.6
260 (500)	154 (22)	182 (26)	5.9 (8.5)	25.0 (13.9)	8.6
290 (550)	98 (14)	116 (17)	5.5 (8.0)	25.4 (14.1)	10.5

Definitions:

S_y = Yield Stress, MPa (ksi)
α = Mean Coefficient of thermal expansion, cm/cm-°C x 10^{-6} (in/in-°F x 10^{-6})
S_u = Ultimate Stress, MPa (ksi)
E = Young's Modulus, MPa x 10^4 (psi x 10^6)

Notes:

1. Source for E values is "Properties of Aluminum Alloys", page 82 [3.3.3] (properties listed in the table above are not affected by time at temperature).
2. Source for Sy, Su, and % Elongation values at room temperature is ASTM Specification B221M [3.3.8]. Values at elevated temperatures are obtained by scaling the room temperature values using the data from [3.3.3].
3. Source for α is Table TE-2 of [3.3.1] (values listed in TE-2 are also considered representative of Aluminum Alloy (2219-T8511) (UNS No. A92219)).
4. The optional solid shims have no mechanical property requirements.

3.4 GENERAL STANDARDS FOR CASKS

3.4.1 Chemical and Galvanic Reactions

Chapter 8 provides discussions on chemical and galvanic reactions, material compatibility and operating environments. Section 8.12 provides a summary of compatibility all HI-STORM FW system materials with the operating environment.

3.4.2 Positive Closure

There are no quick-connect/disconnect ports in the Confinement Boundary of the HI-STORM FW system. The only access to the MPC is through the storage overpack lid, which weighs over 10 tons (see Table 3.2.5). The lid is fastened to the storage overpack with large bolts. Inadvertent opening of the storage overpack is not feasible because opening a storage overpack requires mobilization of special tools and heavy-load lifting equipment.

3.4.3 Lifting Devices

3.4.3.1 Identification of Lifting Devices and Required Safety Factors

The safety of the lifting and handling operations involving HI-STORM FW system components is considered in this section. In particular, the compliance of the appurtenances integral to the cask components used in the lifting operations to NUREG-0612, Reg. Guide 3.61, and the ASME Code is evaluated.

The following design features of Threaded Anchor Locations (TALs) are relevant to their stress analysis:

i. Except for the HI-TRAC VW Version P and HI-STORM FW Version XL lids, all HI-STORM FW system components have TALs, which consist of vertically tapped penetrations in the solid metal blocks. For example, the HI-STORM FW overpack body and standard overpack lid (like all HI-STORM models) have tapped holes in the "anchor blocks" that are engaged for lifting. The loaded MPC is lifted at eight threaded penetrations in the top lid as depicted on the licensing drawings in Section 1.5. However, the MPC lifting analysis in this section conservatively takes credit for only 4 TALs. Likewise, eight vertically tapped holes in the top flange provide the lift points for HI-TRAC VW transfer cask.

   Lifting trunnions are used only for lifting of the HI-TRAC VW Version P.

ii. Operations involving loaded HI-STORM FW system components involve handling evolutions in the vertical orientation (except as described in Subsection 4.5.1). While the lifting devices used by a specific nuclear site shall be custom engineered to meet the architectural constraints of the site, all lifting devices are required to engage the tapped connection points using a vertical

tension member such as a threaded rod. Thus, the loading on the cask during lifting is purely vertical.

iii. There are no rotation trunnions in the HI-STORM FW components. All components are upended and downended at the nuclear plant site using "cradles" of the same design used at the factory (viz., the Holtec Manufacturing Division) during their manufacturing.

The stress analysis of the HI-STORM FW components, therefore, involves applying a vertical load equal to D*/n at each of the n TALs or lifting trunnions. Thus, for the case of the HI-STORM FW overpack, n = 4 (four "anchor blocks" as shown in the licensing drawings in Section 1.5).

The stress limits during a lift for individual components are as follows:

i. Lift points (MPC and HI-TRAC VW): The stress in the TALs and lifting trunnions must be the lesser of $1/3^{rd}$ of the material's yield strength and $1/10^{th}$ of its ultimate strength pursuant to NUREG-0612 and Reg. Guide 3.61.

ii. Lift points (HI-STORM FW): The stress in the threads must be less than $1/3^{rd}$ of the material's yield strength pursuant to Reg. Guide 3.61. This acceptance criterion is consistent with the stress limits used for the lifting evaluation of the HI-STORM 100 overpack in [3.1.4].

iii. Balance of the components: The maximum primary stresses (membrane and membrane plus bending) must be below the Level A service condition limit using ASME Code, Section III, Subsections NB and NF (2007 issues), as applicable, as the reference codes.

To incorporate an additional margin of safety in the reported safety factors, the following assumptions are made:

i. As the system description in Chapter 1 indicates, the heights of the MPCs, HI-STORM FW and HI-TRAC VW are variable. Further, the quantity of lead shielding installed in HI-TRAC VW and the density of concrete can be increased to maximize shielding. All lift point capacity evaluations are performed using the maximum possible weights for each component, henceforth referred to as the "heaviest weight configuration". Because a great majority of site applications will utilize lower weight components (due to shorter fuel length and other architectural limitations such as restricted crane capacity or DAS slab load bearing capacity, or lack of floor space in the loading pit), there will be an additional margin of safety in the lifting point's capacity at specific plant sites.

ii. All material yield strength and ultimate strength values used are the minimum from the ASME Code. Actual yield and tensile data for manufactured steel usually have up to 20% higher values.

The stress analysis of the lifting operation is carried out using the load combination D+H, where H is the "handling load". The term D denotes the dead load. Quite obviously, D must be taken as the

bounding value of the dead load of the component being lifted. In all lifting analyses considered in this document, the handling load H is assumed to be 0.15D. In other words, the inertia amplifier during the lifting operation is assumed to be equal to 0.15g. This value is consistent with the guidelines of the Crane Manufacturer's Association of America (CMAA), Specification No. 70, 1988, Section 3.3, which stipulates a dynamic factor equal to 0.15 for slowly executed lifts. Thus, the "apparent dead load" of the component for stress analysis purposes is $D^* = 1.15D$. Unless otherwise stated, all lifting analyses in this FSAR use the "apparent dead load", D^*, as the lifted load.

Unless explicitly stated otherwise, all analyses of lifting operations presented in this FSAR follow the load definition and allowable stress provisions of the foregoing. Consistent with the practice adopted throughout this chapter, results are presented in dimensionless form, as safety factors, defined as

$$\text{Safety Factor, } \beta = \frac{\text{Allowable Stress}}{\text{Computed Stress}}$$

In the following subsections, the lifting device stress analyses performed to demonstrate compliance with regulations are presented. Summary results are presented for each of the analyses.

3.4.3.2 Analysis of Lifting Scenarios

In the following, the safety analyses of the HI-STORM FW components under the following lifting conditions are summarized.

a. MPC Lifts

The governing condition for the MPC lift is when it is being raised or lowered in a radiation shielded space defined by the HI-TRAC VW or HI-STORM FW stack. In this condition, as stated in Section 3.4.3.1, only four tapped holes in the MPC lid (Alloy X material) are credited to carry the weight. The holes may be tapped using Unified Screw Thread (3.0" min. thread engagement) or ACME Screw Thread (3.75" min. thread engagement) forms.

The criteria derived from NUREG-0612, Reg. Guide 3.61, and the ASME Code Level A condition, stated earlier, apply. The stress analysis is carried out in two parts.

i. Strength analysis of the TALs (connection points) using classical strength-of-materials.

ii. A finite element analysis of the MPC as a cylindrical vessel with the weight of the fuel and basket applied on its baseplate which along with the weight of the Confinement Boundary metal is equilibrated by the reaction loads at the our lift points.

    The primary stress intensities must meet the Level A stress limits for "NB" Class 3 plate and shell structures.

Case (i): Stress Analysis of MPC Threaded Anchor Locations (TALs)

Per Table 3.2.8, the maximum weight of a loaded MPC is

D = 116,400 lb

Per the above, the apparent dead load of the MPC during handling operations is

D* = 1.15 x D = 133,860 lb

The MPC lid has 8 TALs as shown on the drawings in Section 1.5, but as stated in Section 3.4.3.1, only four tapped holes in the MPC lid are credited to carry the weight. Therefore, the lifted load per TAL is equal to

$$\frac{D^*}{4} = 33{,}465 lb$$

For Unified Screw Threads, the shear area of the internal threads (1 3/4" - 5UNC x 3.0" min. engagement) at each TAL is computed per Machinery's Handbook [3.4.12] as

A = 11.8 in^2

Finally, the shear stress on the TALs using Unified Screw Threads is computed as follows

$$\tau = \frac{D^*}{4A} = 2{,}836 psi$$

The MPC lid is made from Alloy X material, whose mechanical properties are listed in Table 3.3.1. Based on the design temperature listed in Table 2.2.3, and assuming the yield and ultimate strengths in shear to be 60% of the corresponding tensile strengths, the allowable stress in the threads is determined as follows

$$Sa = 0.6 \times \min\left(\frac{Sy}{3}, \frac{Su}{10}\right) = 3{,}540 psi$$

Therefore, the safety factor against shear failure of the TALs using Unified Screw Threads in the MPC lid is

$$SF = \frac{Sa}{\tau} = 1.248$$

For ACME Screw Threads, the shear area of the internal threads (1 3/4" – 4 ACME-2G x 3-3/4" min. engagement) at each TAL is computed per Machinery's Handbook [3.4.12] as

$A = 12.13 \text{ in}^2$

The shear stress on the TALs using ACME Screw Threads is computed as follows

$$\tau = \frac{D^*}{4A} = 2{,}759\, psi$$

Therefore, the safety factor against shear failure of the TALs using ACME Screw Threads in the MPC lid is

$$SF = \frac{Sa}{\tau} = 1.283$$

Case (ii): Finite Element Analysis of MPC Enclosure Vessel

The stress analysis of the MPC Enclosure Vessel under normal handling conditions is performed using ANSYS [3.4.1]. The finite element model, which is shown in Figure 3.4.1, is ¼ -symmetric, and it represents the maximum height MPC as defined by Tables 3.2.1 and 3.2.2. The maximum height MPC is analyzed because it is also the heaviest MPC. The key attributes of the ANSYS finite element model of the MPC Enclosure Vessel are described in Subsection 3.1.3.2.

The loads are statically applied to the finite element model in the following manner. The self-weight of the Enclosure Vessel is simulated by applying a constant acceleration of 1.15g in the vertical direction. The apparent dead weight of the stored fuel inside the MPC cavity (which includes a 15% dynamic amplifier) is accounted for by applying a uniformly distributed pressure of 23.1 psi on the top surface of the MPC baseplate. The amplified weight of the fuel basket and the fuel basket shims is applied as a ring load on the MPC baseplate at a radius equal to the half-width of the fuel basket cross section. The magnitude of the ring load is equal to 101.8 lbf/in. All internal surfaces of the MPC storage cavity are also subjected to a bounding normal condition internal pressure of 120 psig, which exceeds the normal operating pressures per Tables 4.4.5 and 4.5.5. Finally, the model is constrained by fixing one node on the top surface of the ¼-symmetric MPC lid, which coincides with the TAL. Symmetric boundary conditions are applied to the two vertical symmetry planes. The boundary conditions and the applied loads are graphically depicted in Figure 3.4.28.

The resulting stress intensity distribution in the Enclosure Vessel under the applied handling loads is shown in Figure 3.4.2. Figures 3.4.29 and 3.4.30 plot the thru-thickness variation of the stress intensity at the baseplate center and at the baseplate-to-shell juncture, respectively. The maximum primary stress intensities in the MPC Enclosure Vessel are compared with the applicable stress intensity limits from Subsection NB of the ASME Code [3.4.4]. The allowable stress intensities are conservatively taken at 500°F for the shell, 600°F for the lid, 450°F for the baseplate, and 450°F at

the baseplate-to-shell juncture. These temperatures bound the operating temperatures for these parts under normal operating conditions (Tables 4.4.3 and 4.5.2). The maximum calculated stress intensities and the corresponding safety factors are summarized in Table 3.4.1.

The shear stress in the MPC lid-to-shell weld under normal handling conditions is independently calculated, as shown below.

Per Table 3.2.8, the maximum weight of a loaded MPC is

W_{MPC} = 116,400 lb

The diameter and weight of the MPC lid assembly are

D = 74.375 in

W_{lid} = 11,500 lb

From Table 2.2.1, the bounding pressure inside the MPC cavity under normal operating conditions is

P = 120 psig

Thus, the total force acting on the MPC lid-to-shell weld is

$$F = 1.15 \cdot \left(W_{MPC} - W_{lid}\right) + P \cdot \left(\frac{\pi \cdot D^2}{4}\right) = 641{,}980 lb$$

which includes a 15% dynamic amplifier. The MPC lid-to-shell weld is a ¾" partial groove weld, which has an effective area equal to

$$A = \pi \cdot D \cdot \left(t_w - \frac{1}{8} in\right) \cdot 0.8 = 116.8 in^2$$

where t_w is the weld size (= 0.75in). The calculated weld area includes a strength reduction factor of 0.8 per ISG-15 [3.4.17]. Thus, the average shear stress in the MPC lid-to-shell weld is

$$\tau = \frac{F}{A} = 5{,}495 psi$$

The MPC Enclosure Vessel is made from Alloy X material, whose mechanical properties are listed in Table 3.3.1. Based on a bounding normal condition temperature of 600ºF (Tables 4.4.3 and 4.5.2),

and assuming that the weld strength is equal to the base metal ultimate strength, the allowable shear stress in the weld under normal conditions is

$$\tau_a = 0.3 \times S_u = 18{,}990\, psi$$

Therefore, the safety factor against shear failure of the MPC lid-to-shell weld is

$$SF = \frac{\tau_a}{\tau} = 3.46$$

b. Heaviest Weight HI-TRAC VW Lift

The HI-TRAC VW transfer cask is at its heaviest weight when it is being lifted out of the loading pit with the MPC full of fuel and water and the MPC lid lying on it for shielding protection (Table 3.2.8). The threaded lift points provide for the anchor locations for lifting. For the HI-TRAC VW Version P, the lifting trunnions serve as the lift points.

The stress analysis of the transfer cask consists of three steps:

i. A strength evaluation of the tapped connection points to ensure that it will not undergo yielding at 3 times D* and failure at 10 times D*.

ii. A strength evaluation of the HI-TRAC VW vessel using strength of materials formula to establish the stress field under D*. The primary membrane plus primary bending stresses throughout the HI-TRAC VW body and the bottom lid shall be below the Level A stress limits for "NF" Class 3 plate and shell structures.

iii. A strength evaluation of the lifting trunnions on the HI-TRAC VW Version P to ensure that it will not undergo yielding at 3 times D* and failure at 10 times D*.

Case (i): Stress Analysis of HI-TRAC VW Threaded Anchor Locations (TALs)

Per Table 3.2.8, the maximum lifted weight of a loaded HI-TRAC VW is

D = 270,000 lb

Per the above, the apparent dead load of the HI-TRAC VW during handling operations is

D* = 1.15 x D = 310,500 lb

The HI-TRAC VW top flange has 8 TALs as shown on the drawing in Section 1.5. Therefore, the lifted load per TAL is equal to

$$\frac{D^*}{8} = 38{,}813 lb$$

Per Machinery's Handbook [3.4.12], the shear area of the internal threads (2 1/4" - 4.5UNC x 2.25" min length.) at each TAL is

A = 12.228 in^2

Finally, the shear stress on the TALs is computed as follows

$$\tau = \frac{D^*}{8A} = 3{,}174 psi$$

The HI-TRAC VW top flange is made from SA-350 LF3 material, whose mechanical properties are listed in Table 3.3.3. Based on the design temperature listed in Table 2.2.3, and assuming the yield and ultimate strengths in shear to be 60% of the corresponding tensile strengths, the allowable stress in the threads is determined as follows

$$Sa = 0.6 \times \min\left(\frac{Sy}{3}, \frac{Su}{10}\right) = 4{,}200 psi$$

Therefore, the safety factor against shear failure of the TALs in the HI-TRAC VW top flange is

$$SF = \frac{Sa}{\tau} = 1.323$$

Case (ii): Stress Analysis of HI-TRAC VW Body

The stress analysis of the HI-TRAC VW steel structure during lifting operations is performed using strength of materials. All structural members in the load path are evaluated for the maximum lifted weight (Table 3.2.8). In particular, the following stresses are calculated:

- the shear stress in the welds between the top flange and the inner and outer shells
- the primary membrane stress in the inner and outer shells
- the tensile stress in the bottom lid bolts
- the primary bending stress in the bottom lid

To determine the bending stress in the bottom lid, the weight of the loaded MPC (Table 3.2.8) plus the weight of the water inside the HI-TRAC VW cavity (Table 3.2.4) is applied as a uniformly distributed pressure on the top surface of the lid. The bending stress is calculated at the center of the bottom lid assuming that the lid is simply supported at the bolt circle diameter. The calculated stresses are compared with the Level A stress limits for "NF" Class 3 plate and shell structures. The detailed calculations are documented in [3.4.13]. Table 3.4.2 summarizes the stress analysis results for the HI-TRAC VW steel structure under the maximum lifted load.

For HI-TRAC VW Version P body, the same approach used to evaluate HI-TRAC VW body is also used. Since the weight of HI-TRAC VW Version P is lighter than HI-TRAC VW and the critical dimensions are identical, the results in Table 3.4.2 for the shear stress in the welds between the top flange and the inner and outer shells, the primary membrane stress in the inner and outer shells, and the primary bending stress in the bottom lid are also bounding for HI-TRAC VW Version P. The bottom lid bolt arrangement is different for HI-TRAC VW Version P and HI-TRAC VW. The detailed calculation for bottom lid bolts is documented in [3.4.13]. Table 3.4.18 summarizes the stress analysis results for the HI-TRAC VW Version P bottom lid bolts.

Case (iii): Stress Analysis of HI-TRAC VW Version P Lifting Trunnions

For the analysis of the trunnion, an accepted conservative technique for computing the bending stress is to assume that the lifting force is applied at the tip of the trunnion "cantilever" and that the stress state is fully developed at the base of the cantilever. This conservative technique, recommended in NUREG-1536, is applied to the VW Version P lifting trunnions.

The lifting trunnions on the HI-TRAC VW Version P are shown on the licensing drawing in Section 1.5. The two lifting trunnions are spaced at 180 degrees. The trunnions are designed for a two-point lift in accordance with the aforementioned NUREG-0612 criteria. The lifting analysis demonstrates that the stresses in the trunnions, computed using the conservative methodology described previously, comply with NUREG-0612 provisions. The results are summarized in Table 3.4.17.

c. HI-STORM FW Overpack Related Lifts

Two related lift conditions are:

i. HI-STORM FW loaded with the heaviest MPC and closure lid installed being lifted (heaviest weight configuration).

ii. HI-STORM FW lid being lifted (heaviest weight configuration)

Case (i): HI-STORM FW Lift Using Anchor Block Connections

Calculations to establish the margin of safety in the TALs and the HI-STORM FW overpack's steel structure are summarized below.

Per Table 3.2.8, the maximum weight of a loaded HI-STORM FW is

D = 425,700 lb

Per the above, the apparent dead load of the HI-STORM FW during handling operations is

D* = 1.15 x D = 489,555 lb

The HI-STORM FW overpack has 4 TALs as shown on the drawing in Section 1.5. Therefore, the lifted load per TAL is equal to

$$\frac{D^*}{4} = 122{,}389 lb$$

Per Machinery's Handbook [3.4.12], the shear area of the internal threads (3 1/4" - 4UNC x 3 1/4" min length.) at each TAL is

A = 24.1 in^2

Finally, the shear stress on the TALs is computed as follows

$$\tau = \frac{D^*}{4A} = 5{,}072 psi$$

The HI-STORM FW anchor blocks are made from SA-350 LF2 material, whose mechanical properties are listed in Table 3.3.3. Based on the design temperature listed in Table 2.2.3, and assuming the yield strength in shear to be 60% of the corresponding tensile yield strength, the allowable stress in the threads is determined as follows

$$Sa = 0.6 \times \frac{Sy}{3} = 6{,}260\,psi$$

Therefore, the safety factor against shear failure of the TALs in the HI-STORM FW overpack is

$$SF = \frac{Sa}{\tau} = 1.234$$

The stress analysis of the overpack body under normal handling conditions is performed using ANSYS [3.4.1]. The finite element model, which is shown in Figure 3.4.3, is ¼-symmetric, and it represents the maximum height HI-STORM FW as defined by Tables 3.2.1 and 3.2.2. The concrete density is also maximized (Table 3.2.5) in the ANSYS model. The key attributes of the ANSYS finite element model of the HI-STORM FW overpack are described in Subsection 3.1.3.1.

The self-weight of the overpack is simulated by applying a constant acceleration of 1.15g in the vertical direction. The apparent dead weight of the fully loaded MPC (which includes a 15% dynamic amplifier) is accounted for by applying a uniformly distributed pressure of 23.8 on the top surface of the HI-STORM FW baseplate. Finally, the model is constrained by fixing four nodes on the top surface of the HI-STORM FW, which coincide with the TALs. Symmetric boundary conditions are applied to the two vertical symmetry planes. The boundary conditions and the applied loads are graphically depicted in Figure 3.4.26.

The resulting stress distribution in the overpack under the applied handling loads is shown in Figure 3.4.4. The maximum primary stresses in the HI-STORM overpack body are compared with the applicable stress limits from Subsection NF of the ASME Code [3.4.2]. The allowable stresses for the load-bearing members are taken at 350°F, which exceeds the maximum operating temperature for the overpack under normal operating conditions (Table 4.4.3 and 4.4.14). The maximum stresses and the corresponding safety factors are summarized in Table 3.4.3.

Case (ii): Lid Lift Analysis

The weight of the HI-STORM FW standard lid is dependent on the shielding concrete's density. The maximum possible weight of the lid is provided in Table 3.2.5. The HI-STORM FW standard lid is lifted using the four equally spaced TALs on the lid top surface, which are shown on the licensing drawing in Section 1.5. Calculations to establish the margin of safety in the TALs and the standard lid's steel structure are summarized below.

Per Table 3.2.5, the maximum weight of the HI-STORM FW lid is

D = 23,300 lb

Per the above, the apparent dead load of the HI-STORM FW lid during handling operations is

$D^* = 1.15 \times D = 26{,}795$ lb

The HI-STORM FW lid has 4 TALs as shown on the drawing in Section 1.5. Therefore, the lifted load per TAL is equal to

$$\frac{D^*}{4} = 6{,}699\text{lb}$$

Per Machinery's Handbook [3.4.12], the shear area of the internal threads (1 1/2" - 6UNC x 1" min length.) at each TAL is

$A = 3.567\ \text{in}^2$

Finally, the shear stress on the TALs is computed as follows

$$\tau = \frac{D^*}{4A} = 1878 psi$$

The HI-STORM FW lid anchor blocks are made from carbon steel material, whose yield and ultimate strengths at the design temperature per Table 2.2.3 are conservatively input as 15,000 psi and 40,000 psi, respectively. Assuming the yield and ultimate strengths in shear to be 60% of the corresponding tensile strengths, the allowable stress in the threads is determined as follows

$$\text{Sa} = 0.6 \times \min\left(\frac{\text{Sy}}{3}, \frac{\text{Su}}{10}\right) = 2{,}400\text{psi}$$

Therefore, the safety factor against shear failure of the TALs in the HI-STORM FW lid is

$$SF = \frac{Sa}{\tau} = 1.278$$

The HI-STORM FW XL lid and domed lid are lifted using the four lifting holes on the lid central ribs. Calculations to establish the margin of safety for tearout, bearing and tension are performed using the bounding weights given in Table 3.2.5. The resulting tear out shear stress, bearing stress, and tensile stress on the lifting hole are compared against the maximum allowables per Regulatory Guide 3.61 and NUREG-0612and the safety factors are shown to be above 1.0.

The global stress analysis of the overpack lid under normal handling conditions is performed using ANSYS 11 [3.4.1] for the standard lid, ANSYS 14 [3.4.25] for Version XL lid, and ANSYS 17.1 [3.4.26] for the domed lid. Figures 3.4.5A and 3.4.5B show the finite element model of the standard lid and Version XL lid, which incorporates the maximum concrete density (Table 3.2.5). Figure 3.4.5C shows the finite element model of the domed lid. The key attributes of the ANSYS

finite element model of the HI-STORM FW lid are described in Subsection 3.1.3.1.

The self-weight of the overpack lid is simulated by applying a constant acceleration of 1.15g in the vertical direction. The standard lid model is constrained by fixing four nodes on the top surface of the HI-STORM FW standard lid, which coincide with the TALs. The XL lid model is constrained by fixing four lifting holes on the HI-STORM FW XL lid ribs. The domed lid model is constrained by fixing a remote point above the lid that is connected to each of the four lifting holes.

The resulting stress distribution in the steel structure of the overpack lid under the applied handling load is shown in Figure 3.4.6A (for standard lid) and Figure 3.4.6B (for Version XL lid). The maximum stresses and the corresponding safety factors for standard lid and Version XL lid are summarized in Table 3.4.4, while the results for the domed lid are provided in Table 3.4.4.A. For conservatism, the maximum calculated stress at any point on the standard and Version XL lids, including secondary stress contributions, are compared against the primary membrane and primary bending stress limits per Subsection NF of the ASME Code for Level A conditions. The allowable stresses for the standard lid are taken at 300°F, which exceeds the maximum operating temperature for the overpack top lid under normal operating conditions. The allowable stresses for the XL lid are taken at 400°F, which bounds the maximum operating temperatures for the Version XL lid under normal operating conditions. The allowable stresses for the domed lid are taken using the temperature limits given in Table 2.2.3.

3.4.3.3 Safety Evaluation of Lifting Scenarios

As can be seen from the above, the computed factors of safety have a large margin over the allowable (of 1.0) in every case. In the actual fabricated hardware, the factors of safety will likely be much greater because of the fact that the actual material strength properties are generally substantially greater than the Code minimums. Minor variations in manufacturing, on the other hand, may result in a small subtraction from the above computed factors of safety. A part 72.48 safety evaluation will be required if the cumulative effect of manufacturing deviation and use of the CMTR (or CoC) material strength in a manufactured hardware renders a factor of safety to fall below the above computed value. Otherwise, a part 72.48 evaluation is not necessary. The above criterion applies to all lift calculations covered in this FSAR.

3.4.4 Heat

The thermal evaluation of the HI-STORM FW system is reported in Chapter 4.

a. Summary of Pressures and Temperatures

Design pressures and design temperatures for all conditions of storage are listed in Tables 2.2.1 and 2.2.3, respectively.

Differential Thermal Expansion

The effect of differential thermal expansion among the constituent components in the HI-STORM FW system is considered in Chapter 4 wherein the temperatures necessary to perform the differential thermal expansion analyses for the MPC in the HI-STORM FW and HI-TRAC VW casks are computed. The material presented in Section 4.4 demonstrates that a constraint to free expansion due to differential growth between discrete components of the HI-STORM FW system (e.g., storage overpack and enclosure vessel) will not develop under any operating condition.

i. Normal Hot Environment

Results presented in Section 4.4 demonstrate that initial gaps between the HI-STORM FW storage overpack or the HI-TRAC VW transfer cask and the MPC canister, and between the MPC canister and the fuel basket, will not close due to thermal expansion of the system components normal operating conditions.

The clearances between the MPC basket and canister structure, as well as between the MPC shell and storage overpack or HI-TRAC VW inside surface, are shown in Section 4.4 to be sufficient to preclude a temperature induced interference from differential thermal expansions under normal operating conditions.

ii. Fire Accident

It is shown in Chapter 4 that the fire accident has a small effect on the MPC temperatures because of the short duration of the fire accidents and the large thermal inertia of the storage overpack. Therefore, a structural evaluation of the MPC under the postulated fire event is not required. The conclusions reached in item (i) above are also appropriate for the fire accident with the MPC housed in the storage overpack. Analysis of fire accident temperatures of the MPC housed within the HI-TRAC VW for thermal expansion is unnecessary, as the HI-TRAC VW, directly exposed to the fire, expands to increase the gap between the HI-TRAC VW and MPC.

As expected, the external surfaces of the HI-STORM FW storage overpack that are directly exposed to the fire event experience maximum rise in temperature. The outer shell and top plate in the top lid are the external surfaces that are in direct contact with heated air from fire. Table 4.6.2 provides the maximum temperatures attained at the key locations in HI-STORM FW storage overpack under the postulated fire event.

The following conclusions are evident from the above table.

- The maximum metal temperature of the carbon steel shell most directly exposed to the combustion air is well below the applicable short-term temperature limit per Table 2.2.3. 700°F is the permissible temperature limit in the ASME Code for the outer shell material.

- The local concrete temperature is below its short term temperature limit specified in Table 2.2.3.

- The metal temperature of the inner shell does not exceed 300°F at any location, which is well below the accident condition temperature specified in Table 2.2.3 for the inner shell.

- The presence of a vented space at the top of the overpack body ensures that there will be no pressure buildup in the concrete annulus due to the evaporation of vapor and gaseous matter from the shielding concrete.

Thus, it is concluded that the postulated fire event will not jeopardize the structural integrity of the HI-STORM FW overpack or significantly diminish its shielding effectiveness.

The above conclusions, as relevant, also apply to the HI-TRAC VW fire considered in Chapter 4. Water jacket over-pressurization is prevented by the pressure relief devices. The non-structural effects of loss of water have been evaluated in Chapter 5 and shown to meet regulatory limits. Therefore, it is concluded that the postulated fire event will not cause a state of non-compliance with the regulations to materialize.

3.4.4.1 Safety Analysis

Calculations of the stresses and displacements in the different components of the HI-STORM FW system from the effects of mechanical load case assembled in Table 3.1.1 for the MPC, the HI-STORM FW storage overpack and the HI-TRAC VW transfer cask are presented in the following. The purpose of the analyses summarized herein is to provide the necessary assurance that there will be no unacceptable risk of criticality, unacceptable release of radioactive material, unacceptable radiation levels, or impairment of ready retrievability of fuel from the MPC (for normal and off-normal conditions of storage) and the MPC from the HI-STORM FW storage overpack or from the HI-TRAC VW transfer cask.

Because many of the analyses must be performed for a particular ISFSI to demonstrate the acceptability of site-specific loads under the provisions of 10CFR72.212, the analyses presented here also set down the acceptable methodologies. Accordingly, the analysis methodologies are configured to exaggerate the severity of response. Also, because the weight and height of all three components (overpack, MPC, and HI-TRAC VW) can vary between specified ranges (see tables in Section 3.2), each analysis is carried out for the dimensional and weight condition of the component that maximizes response. Thus, for example, the seismic stability analysis of the loaded HI-STORM FW (Load Case 2 in Table 3.1.1) is performed for the case of maximum height, but the stability under the impact of a large tornado missile (Load Case 3) is analyzed assuming maximum height and minimum loaded weight (Per Table 3.2.8).

Each load case in Table 3.1.1 is considered sequentially and all affected components are analyzed to determine the factors of safety.

All factors of safety reported in this FSAR utilize nominal dimensions and minimum material strengths. Actual factors of safety in the manufactured hardware are apt to be considerably larger

than those reported herein chiefly because of the actual material strengths being much greater than the values used in the safety analyses. A part 72.48 safety assessment will be required if the combined effect of the actual material strength and manufacturing deviation produces a lower safety factor for a design basis loading than that referenced in the safety evaluation in this FSAR.

3.4.4.1.1 Load Case 1: Moving Floodwater

The object of the analysis is to determine the maximum floodwater velocity that a loaded HI-STORM FW on the ISFSI pad can withstand before tipping over or sliding. The flood data for the ISFSI shall be based on a 40-year (minimum) return flood. The kinematic stability analysis consists of writing static equilibrium equations for tipping and sliding.

The flood condition subjects the HI-STORM FW system to external pressure, together with a horizontal load due to water velocity. Because the HI-STORM FW storage overpack is equipped with ventilation openings, the hydrostatic pressure from flood submergence acts only on the MPC. As stated in Subsection 2.2.3, the design external pressure for the MPC bounds the hydrostatic pressure from flood submergence.

The water velocity associated with flood produces a horizontal drag force, which may act to cause sliding or tip-over. In accordance with the provisions of ANSI/ANS 57.9, the acceptable upper bound flood velocity, V, must provide a minimum factor of safety of 1.1 against overturning and sliding.

The overturning horizontal force, F, due to hydraulic drag, is given by the classical formula:

$$F = Cd\ A\ V^{*} \qquad \text{[Equation 1]}$$

where:

V^{*} = velocity head = $\frac{\rho V^2}{2g}$ (ρ is water weight density, and g is acceleration due to gravity).

A = projected area of the HI-STORM FW cylinder perpendicular to the fluid velocity vector, equal to D times h, where h is the height of the floodwater.

Cd = drag coefficient

The value of Cd for flow past a cylinder at Reynolds number above 5E+05 is given as 0.5 in the literature (viz. Hoerner, Fluid Dynamics, 1965).

The drag force tending to cause HI-STORM FW's sliding is opposed by the friction force, which is given by

$$F_f = \mu W^* \qquad \text{[Equation 2]}$$

where:

μ = limiting value of the friction coefficient at the HI-STORM FW/ISFSI pad interface is assumed to be equal to 0.53 (the NRC-approved value in Docket No. 72-1014).

W* = apparent (buoyant) weight of HI-STORM FW with an empty MPC.

i. Sliding Factor of Safety

The factor of safety against sliding, β_1, is given by

$$\beta_1 = \frac{F_f}{F} = \frac{\mu W^*}{Cd\ A\ V^*} = \frac{2g\mu W^*}{Cd(Dh)\rho V^2} \qquad \text{[Equation 3]}$$

The factor of safety, β_1, must be greater than 1.1. For $g = 32.2$ ft/sec^2, $Cd = 0.5$, and $\rho = 62.4$ lbf/ft^3, the maximum value of V as a function of the floodwater height h is given by

$$V = \sqrt{\frac{1.876\mu W^*}{Dh}} \qquad \text{[Equation 4]}$$

ii. Overturning Factor of Safety

For determining the margin of safety against overturning, β_2, the cask is assumed to pivot about a fixed point located at the outer edge of the contact circle at the interface between HI-STORM FW and the ISFSI. The overturning moment due to the hydraulic force F_T is balanced by a restoring moment from the buoyant weight acting at radius D/2.

Overturning moment, $M_o = Fh/2$ where F is given by Equation 1 above.

Restoring moment, $M_r = W^* D/2$ [Equation 5]

For stability against tipping $M_o \leq M_r$

or $Fh \leq W^*D$

Hence the factor of safety against overturning is

$$\beta_2 = \frac{W^* D}{F h} = \frac{W^* D}{Cd\, A\, V^* h} = \frac{2gW^*}{Cdh^2 \rho V^2} \qquad \text{[Equation 6]}$$

β_2 must be greater than 1.1. For g = 32.2 ft/sec^2, Cd = 0.5, and ρ = 62.4 lbf/ft^3, the maximum value of V as a function of the floodwater height h is given by

$$V = \frac{\sqrt{1.876 W^*}}{h} \qquad \text{[Equation 7]}$$

The smaller of the value of V from Equations 4 and 7 defines the maximum permissible flood velocity for the site. For the HI-STORM FW system, Equation 4 governs since the coefficient of friction (μ) is less than the smallest value of D/h for the limiting overpack geometry (maximum height). The numerical value of V is computed as follows:

From Tables 3.2.1 and 3.2.2 and the drawings in Section 1.5, the diameter and maximum height of the overpack are

D = 139 in = 11.6 ft

h = 240 in = 20.0 ft

From Tables 3.2.3 and 3.2.5, the minimum weight of the HI-STORM FW overpack with an empty MPC (based on Ref. PWR fuel length and 150 pcf concrete density) is

W = 254,600 lbf

Finally, assuming that W* = 0.87W, the acceptable upper bound flood velocity is determined from Equation 4 as

$$V = \sqrt{\frac{1.876(0.53)(0.87 \times 254{,}600)}{(11.6)(20.0)}} = 30.8 \text{ft/sec}$$

3.4.4.1.2 Load Case 2: Design Basis Earthquake

In Subsection 2.2.3 (g), the combination of vertical and horizontal ZPA of the earthquake that would cause incipient loss of kinematic stability is derived using static equilibrium. The resulting inequality defines the threshold of the so-called low intensity earthquake for which the HI-STORM FW system is qualified without a dynamic analysis. However, an earthquake is a cyclic loading event which would produce rattling of the MPC inside the overpack and possibly large strains in the Confinement

Boundary at the location of rattling impact between the MPC and the overpack guide tubes.

For earthquakes stronger than that defined by the inequalities in Subsection 2.2.3(g), it is necessary to perform a dynamic analysis. The dynamic stability analysis may be performed using either one of the following two approaches:

i. Using the nomographs developed in NUREG/CR-6865 [3.4.7] to predict the cask rotation and sliding.

ii. Performing a time history analysis for the cask modeled with 6 degrees-of-freedom and subjected to 3-dimensional seismic accelerations.

The first approach, although limited in its applications, is simple and conservative for the seismic stability evaluation of the HI-STORM FW storage cask as explained below. The nomograph developed in NUREG/CR-6865 [3.4.7] for cylindrical casks are based on extensive parametric study of the seismic response of HI-STORM 100 with a series of seismic inputs fitting three different spectral shapes. The seismic response is predicted through transient finite element analyses where the cask is supported on a flexible concrete pad founded on three substrates ranging from soft soil to rock. The NUREG study offers two sets of nomographs depending on the match of the site-specific free field horizontal spectrum with the three spectral shapes utilized in the study (after normalization to the Peak (Zero Period) Ground Acceleration (PGA)). The power law for the HI-STORM 100 response "y" (either peak cask top displacement or peak cask rotation) in terms of the ground motion parameter "x" at confidence band "m" standard deviations above the median response is:

$$y = A x^{B} \exp\left(m S_{Y|x}\right)$$

In the above equation, "A" and "B" are the nomograph curve fitting parameters, and "S" is the conditional standard deviation of the result data after undergoing a logarithmic transformation. The value for "m" is 0 (for the median curve), +1 (for the 84% confidence level) and –1 (for the 16% confidence level). The units of "A" are meters (for displacement) and degrees (for rotation). The values for the coefficients are given below, as reproduced from [3.4.7]. The nomograph parameters are affected by the cask/pad coefficient of friction, but are independent of substrate stiffness.

Curve Fitting Parameters for Cylindrical Cask, NUREG/CR-0098 Earthquakes, PGA

	A (disp.)	B (disp.)	$S_{Y\|x}$ (disp.)	A (rot.)	B (rot.)	$S_{Y\|x}$ (rot.)
μ=0.2	0.216	2.60	0.409	0.0217	0.689	0.718
μ=0.55	0.911	4.06	0.814	6.70	3.94	0.794
μ=0.8	1.150	4.16	0.796	9.01	4.09	0.765

Curve Fitting Parameters for Cylindrical Cask, Regulatory Guide 1.60 Earthquakes, PGA

	A (disp.)	B (disp.)	S_{Yx} (disp.)	A (rot.)	B (rot.)	S_{Yx} (rot.)
μ=0.2	0.837	2.52	0.465	0.0733	1.71	0.785
μ=0.55	8.96	4.80	1.03	62.5	4.71	0.956
μ=0.8	15.4	5.04	1.13	114	4.94	1.12

Curve Fitting Parameters for Cylindrical Cask, NUREG/CR-6728 Earthquakes, PGA

	A (disp.)	B (disp.)	S_{Yx} (disp.)	A (rot.)	B (rot.)	S_{Yx} (rot.)
μ=0.2	0.0897	1.88	0.377	0.0456	1.17	0.777
μ=0.55	0.219	2.63	0.543	1.64	2.53	0.583
μ=0.8	0.253	2.71	0.631	2.11	2.68	0.606

Curve Fitting Parameters for Cylindrical Cask, All Spectral Shapes, 1 Hz PSA

	A (disp.)	B (disp.)	S_{Yx} (disp.)	A (rot.)	B (rot.)	S_{Yx} (rot.)
μ=0.2	0.271	2.15	0.532	0.0335	0.769	0.91
μ=0.55	0.979	3.20	1.07	7.07	3.10	1.04
μ=0.8	1.29	3.31	1.11	10.1	3.25	1.09

The use of the above nomographs for HI-STORM FW seismic stability analysis is conservative, as long as the h/r ratio (h = height to cask centroid, r = radius of the cask at interface with the pad) of HI-STORM FW is smaller than that of HI-STORM 100 cask, which is true in most cases. The nomographs should not be used when the substrate characteristics indicate that liquefaction will occur under a seismic event [3.4.7]. The basic analysis procedure is as follows:

i. Demonstrate that the cask h/r ratio is less than that of HI-STORM 100 cask. If this condition is not satisfied, this approach cannot be used for the seismic stability analysis.

ii. Evaluate the site-specific substrate data to ensure that the site-specific substrate is within the range considered in the NUREG and that there is no potential for soil liquefaction under a seismic event.

iii. Compare the site-specific horizontal free-field response spectrum for 5% damping with those employed in the NUREG (after normalizing the site-specific data to 1g).

   a. If the site-specific spectrum is a good match with one of the spectrums employed, then use the nomograph appropriate to the matched spectrum and site-specific input at the ZPA to predict cask displacement and rotation.

   b. If the site-specific spectrum is not a good match with any of the spectra, then use the nomograph developed for all spectra with site-specific input at 1 Hz and 5% damping to predict cask displacement and rotation.

If the previously described NUREG/CR-6865 approach is not appropriate to use for a specific ISFSI site, the second approach should be used to perform the seismic stability evaluation for HI-STORM

FW casks. The time history analysis approach, which is free of the limitations associated with NUREG/CR-6865, was used and approved by the USNRC to demonstrate the seismic stability of HI-STORM 100 casks at the Private Fuel Storage ISFSI. The input seismic acceleration time histories shall meet the relevant requirements specified in the SRP 3.7.1 [3.4.8] and shall be baseline corrected.

Finally, a small clearance between the MPC and the MPC guide tubes may lead to a high localized strain in the region of the shell where impacts from rattling of the canister under a seismic event occur. The extent of local strain from impact is minimized by locating the guide tube in the vertical direction such that its impact footprint is aligned with the surface of the closure lid which has been shimmed to close the crevice between the lid and the shell. Thus the impact between the guide tubes and the MPC lid will occur at a location where the maximum damage to the MPC shell will be local denting in the region where it is buttressed by the edge of a (thick) MPC lid. Therefore, a through-wall damage of the MPC shell is not credible. Furthermore, the force of impact will evidently be greater in the non-mechanistic tip-over case. Therefore, the seismic impact case is designated as non-governing for the guide tube/MPC impact scenario.

Stability Assured Installation

During an earthquake event the safety related functions of the cask are ensured by satisfying the requirements of static equilibrium per Section 2.2.3 (g) or, if necessary, the dynamic stability requirements discussed above. For sites that require a dynamic analysis, the ISFSI owner may elect to limit or entirely eliminate the motion of the cask during the earthquake event by implementing the optional Stability Assured Installation (SAI). The SAI option is available to any site where recourse to a dynamic analysis is required (e.g. due to a missile strike exceeding the Design Basis Missile).

The SAI consists of three primary component types: the Radial Plates, the Connector Blocks, and the Anchor Bolts. The Radial Plates are radial plate-type connectors located between the HI-STORM's inner and outer shell, near the bottom of the cask, and act as a buttress for the Connector Blocks. The Connector Blocks are a set of attachments to the external surface of the cask's outer shell that are used to connect the cask to the ISFSI pad. The Anchor Bolts pass through axial thru- holes in the Connector Blocks and thread into a fastener connection located in the ISFSI pad. The Connector Blocks are sufficiently long to impute a limited axial flexibility to the Anchor Bolts allowing the cask to undergo a very small elastic rotation under large lateral loads, and insuring that the SAI attachments are sufficiently forgiving of such loads. The Anchor Bolts are designed to resist tensile forces only. Shear forces acting at the ISFSI pad/cask interface are reacted by Anti-Sliding Blocks, which are an integral part of the ISFSI Pad for the SAI option.

The SAI does not perform a safety related function and may only be implemented where the analysis of the freestanding cask does not indicate tip over. Since seismic stability of the freestanding vertical cask is a prerequisite for the SAI, the ISFSI pad remains classified as a Not Important-to-Safety (NITS) structure even in the restrained HI-STORM configuration.

The sizing and quantity of the SAI components may vary based on site-specific requirements provided that the following criteria are met:

a) The maximum tensile stress in the fasteners at all instants is below the Level D ASME Code limit for Section III, Subsection NF, linear structures.
b) The total shear stress in the weld group joining the Connector Block to HI-STORM shell is below the applicable "NF" limit.
c) The maximum stress in the Connector Block is below the corresponding "NF" limit.

The analysis summarized below seeks to determine the maximum simultaneous horizontal and vertical inertial accelerations that the anchoring system can withstand while meeting stress limits for ASME Section III Subsection NF structures under Level D service conditions.

It is evident from the geometry of the SAI that the use of the long fasteners provides a limited flexibility to an otherwise rigid HI-STORM restraint system. Therefore, it is reasonable to simulate the restrained HI-STORM structure as a 6 degree-of-freedom system with the axial fasteners behaving as flexible linear springs. Other simplifying assumptions, intended to make the seismic analysis overtly conservative, are:

1. The maximum center of gravity (CG) height and weight of the loaded HI-STORM is considered because the overturning moment is directly proportional to the CG height and mass of the cask.
2. The axial fasteners, as shown in Figure 3.4.42B, are located slightly outboard of the outer edge of the cask's Baseplate. For conservatism, the restraining force applied by them is assumed to be acting at the outer edge of the Cask's Baseplate, thus reducing the lever arm of the bolt's restoring force.
3. The seismic inertia force equal to a_h times the mass of the system may act in the direction that leads to the maximum axial load in the worst loaded bolt; a_h is the vector sum of the two horizontal ZPAs.
4. The vertical seismic load equal to a_v times the mass of the cask is assumed to be acting upwards to reduce the apparent weight of the system concurrently with the horizontal inertia load. a_v is the ZPA of the DBE in the vertical direction. Assuming the vertical ZPA to be acting in opposition to the cask's weight helps maximize the tensile force in the fasteners. The quantity a_v can be greater than 1.

The above simplifying assumptions define the pivot point of the cask (if it were to rotate) as the edge of the cask's Baseplate in the plane of action of the horizontal seismic moment (see Figure 3.4.43).

Referring to Figure 3.4.43, the locations of the fasteners are indicated by 1, 2, 3, and 4, situated on two orthogonal planes. The horizontal seismic force, which induces an overturning moment, is assumed to act in a vertical plane oriented at an angle θ from the plane of fasteners 1 and 3 (Figure 3.4.43).

The following symbols are used in the derivation:

a_h : Horizontal ZPA of the Design Basis Earthquake (DBE)

A : Root area of each fastener bolt

F_i : Tensile force in the i'th bolt (i = 1, 2, 3, 4)

h : Height of the C.G of a loaded system

r : Outer radius of the overpack's baseplate

a_v : Vertical ZPA of the DBE

W : Mass of the loaded system

θ : Angle between the plane of one set of fasteners and the plane of action of the horizontal ZPA

σ : Allowable bolt tensile stress under Level D conditions

As shown in Figure 3.4.43, the cask will tend to pivot about the point, P, if the overturning moment acting on the cask is sufficiently high. The overturning moment is given by:

$$M = Wha_h - W(1 - a_v)r \quad (1)$$

where the vertical ZPA is conservatively assumed to act to reduce the apparent weight of the cask.

Based on the assumption of rigid cask behavior, the tensile force in the bolt at location i, F_i, is given by the x-distance from the pivot point, x_i:

$$\begin{aligned} x_1 &= r(1 - \cos(\theta)) \\ x_2 &= r(1 + \sin(\theta)) \\ x_3 &= r(1 + \cos(\theta)) \\ x_4 &= r(1 - \sin(\theta)) \end{aligned} \quad (2)$$

The bolt forces are proportional to the moment arm, i.e., the distance from each bolt to the pivot axis. The forces are given by:

$$F_i = ax_i$$

where α is the proportionality factor. The resisting moment due to the bolt forces about the pivot point is, therefore:

$$M = ax_1^2 + ax_2^2 + ax_3^2 + ax_4^2 \tag{3}$$

Using equations (1) and (3), and substituting for x_1, x_2, x_3 and x_4 from equation (2), we have, after some simplification:

$$W(a_h - r + a_v r) = 6ar^2 \tag{4}$$

Therefore, the maximum force in the bolt occurs when x_i is maximized, i.e., when $\theta = 0$ or $\pi/2$. The maximum tensile bolt force is:

$$F_{max} = 2ar = \frac{W(a_h h - r + a_v r)}{3r} \tag{5}$$

If σ and A denote the maximum allowable axial stress and the root area of the fasteners, then the limiting values of a_h and a_v are defined by:

$$\sigma A = 2ar = \frac{W(a_h h - r + a_v r)}{3r}$$

$$a_h = \left(\frac{3\sigma A}{W} + 1 - a_v\right)\left(\frac{r}{h}\right) \tag{6}$$

For the general case where $a_v = \zeta\, a_h$, the maximum permitted value of a_h is given by:

$$a_h = \frac{\left(\frac{3\sigma A}{W} + 1\right)\left(\frac{r}{h}\right)}{\left(1 + \zeta\frac{r}{h}\right)} \tag{7}$$

The above equation provides an initial estimate of the capacity of the SAI, in terms of the maximum allowable horizontal ZPA, for a HI-STORM FW system of a given size and mass. If the estimated capacity exceeds the seismic demands for the candidate site, then a final dynamic analysis, separate from the free standing analysis, should be performed using similar methodology to the provisions of §72.212 required by the CoC.

A reference SAI design is shown in Figures 3.4.42B and 3.4.42C. The Connector Block welds shown in the reference figure have been sized to withstand the shear and bending loads associated with the maximum allowable tensile load in the reference Anchor Bolt. The results are summarized in the following table.

Item	Calculated Value (ksi)	Allowable Limit (ksi)	Factor of safety
Weld primary shear stress due to fastener maximum allowable tensile load	17.26	-	-
Weld secondary shear stress due to bending moment from fastener tensile load	18.55	-	-
Total weld shear (vector sum of primary and secondary stresses)	25.34	34.33	1.355

3.4.4.1.3 Load Case 3: Tornado-Borne Projectiles

During a tornado event, the HI-STORM FW overpack and the HI-TRAC VW are assumed to be subjected to a constant wind force. They are also subject to impacts by postulated missiles. The maximum wind speed is specified in Table 2.2.4, and the three missiles, designated as large, intermediate, and small, are described in Table 2.2.5.

a. Large Missile

Overturning Analysis

The large tornado missile acting at the top region of the cask (HI-STORM FW or HI-TRAC VW) to produce maximum overturning effect (Table 3.1.1) is analyzed to determine whether the cask will remain stable. Because the site-specific large missile is apt to be different from the one analyzed herein, the method of analysis presented here will provide the means for the site-specific safety evaluation pursuant to 10CFR72.212.

The overturning analysis of the cask under the tornado wind load and large missile impact is performed by solving the 1-DOF equation of motion for the cask angular rotation, which is same methodology used in the HI-STORM 100 FSAR (Docket No. 72-1014). Specifically, the solution of the post-impact dynamics problem is obtained by solving the following equation of motion:

$$I_r \alpha = \left(- W_c \frac{a}{2} \right) + F_{max} \left(\frac{L}{2} \right)$$

where:

I_r = cask moment of inertia about the pivot point
α = angular acceleration of the cask
W_c = lower bound weight of the cask
a = diameter of cask at its base (see Figure 3.4.7)
F_{max} = force on the cask due to tornado wind/instantaneous pressure drop
L = height of the cask (see Figure 3.4.7)

The impacting missile enters into the above through the post-strike angular velocity of the cask, which is the relevant initial condition for the cask equation of motion. The solution gives the post-impact position of the cask centroid as a function of time, which indicates whether the cask remains stable.

The following assumptions are made in the analysis:

i. The cask is assumed to be a rigid solid cylinder, with uniform mass distribution. This assumption implies that the cask sustains no plastic deformation (i.e. no absorption of energy through plastic deformation of the cask occurs).

ii. The angle of incidence of the missile is assumed to be such that its overturning effect on the cask is maximized (see Figure 3.4.7).

iii. The analysis considers the maximum height cask per Tables 3.2.1 and 3.2.2. The missile is assumed to strike at the highest point of the cask (see Figure 3.4.7), again maximizing the overturning effect.

iv. The cask is assumed to pivot about a point at the bottom of the base plate opposite the location of missile impact and the application of wind force in order to conservatively maximize the propensity for overturning (see Figure 3.4.7).

v. Inelastic impact is assumed, with the missile velocity reduced to zero after impact. This assumption conservatively lets the missile impart the maximum amount of angular momentum to the cask, and it is in agreement with missile impact tests conducted by EPRI [3.4.14].

vi. The analysis is performed using the minimum loaded HI-STORM FW weight per Table 3.2.8. A lighter cask will tend to rotate further after the missile strike. The weight of the missile is not included in the total post-impact weight.

vii. Planar motion of the cask is assumed; any loads from out-of-plane wind forces are neglected.

viii. The drag coefficient for a cylinder in turbulent cross flow is used.

ix. The missile and wind loads are assumed to be perfectly aligned in direction.

The results for the post-impact response of the HI-STORM FW overpack and the HI-TRAC VW transfer cask are summarized in Table 3.4.5. The table shows that both casks remain in a vertical upright position (i.e., no overturning) in the aftermath of a large missile impact. The complete details of the tornado wind and large missile impact analyses for the HI-STORM FW overpack and the HI-TRAC VW transfer cask are provided in Appendix 3.A.

Sliding Analysis

A conservative calculation of the extent of sliding of the HI-STORM FW overpack and the HI-TRAC VW cask due to the impact of a large missile (Table 2.2.5) and tornado wind (Table 2.2.4) is obtained using a common formulation as explained below. A more realistic impact simulation using LS-DYNA, with less bounding assumptions, has been used in Subsection 3.4.4.1.4 to qualify the HI-STORM overpack for a non-mechanistic tip over event. While it is not necessary for demonstrating adequate safety margins for this problem, an LS-DYNA analysis could also be used to calculate the sliding potential of the HI-STORM FW and HI-TRAC VW for a large missile impact. In what follows, both HI-STORM FW and HI-TRAC VW are identified by the generic term "cask".

The principal assumptions that render these calculations for sliding conservative are:

i. The weight of the cask used in the analysis is assumed to be the lowest per Table 3.2.8.

ii. The cask is assumed to absorb the energy of impact purely by sliding. In other words, none of the impact energy is dissipated by the noise from the impact, from local plastic deformation in the cask at the location of impact, or from the potential tipping action of the cask.

iii. The missile impact and high wind, which applies a steady drag force on the cask, are assumed to act synergistically to maximize the movement of the cask.

iv. The cask is assumed to be freestanding on a concrete surface. The interface friction coefficient is assumed to be equal to that endorsed in the HI-STORM 100 FSAR (USNRC Docket No. 72-1014) and adopted here in the HI-STORM FW FSAR.

v. The dynamic effect of the impact is represented by the force-time curve developed in the Bechtel topical report "Design of Structures for Missile Impact" [3.4.9], previously used to qualify the HI-STORM 100 System (USNCR Docket No. 72-1014).

The analysis for sliding under the above assumptions reduces to solving Newton's equation of motion of the form:

$$m\frac{d^2x}{dt^2} = F(t) + F_{dp} - \mu mg$$

where

m: mass of the cask,

t: time coordinate with its origin set at the instant when the sum of the missile impact force and wind drag force overcomes the static friction force,

x: displacement as a function of time coordinate t,

$F(t)$: missile impact force as a function of time (from [3.4.9]),

F_{dp}: drag force from high wind,

μ: interface friction set as 0.53 for freestanding cask on a reinforced concrete pad in Docket No. 72-1014,

g: acceleration due to gravity.

The above second-order differential equation is solved numerically in [3.4.15] for the HI-STORM FW overpack and the HI-TRAC VW transfer cask, and the calculated sliding displacements are summarized in Table 3.4.16.

Referring to the spacing dimensions for HI-STORM FW arrays in Table 1.4.1, the minimum space between HI-STORM FW overpacks and the minimum distance of the overpack to the edge of the pad are calculated. The above table demonstrates the HI-STORM FW overpack will not collide with another overpack, and the overpack will not slide off the pad due to the combined effects of a large tornado missile impact and high wind.

No generic limits for sliding are established for the HI-TRAC VW. Therefore, the sliding result for the HI-TRAC VW transfer cask in Table 3.4.16 is strictly informational.

b. Small and Intermediate Missiles

The small and intermediate missiles (Table 2.2.5) are analyzed to determine the extent to which they will penetrate the HI-STORM FW overpack or the HI-TRAC VW and cause potential damage to the MPC Enclosure Vessel. Classical energy balance methods are used to compute the depth of penetration at the following impact locations:

- on the HI-STORM FW outer shell (with concrete backing)
- on the HI-STORM FW lid top plate (with concrete backing)
- on the HI-TRAC VW outer shell (with lead backing)
- on the top surface of the MPC upper lid

The MPC upper lid is analyzed for a direct missile impact because, when the MPC is placed inside the HI-TRAC VW, the MPC lid is theoretically accessible to a vertically downward directed small or intermediate missile.

The following assumptions are made in the analysis:

i. The intermediate missile and the small missile are assumed to be unyielding, and hence the entire initial kinetic energy is assumed to be absorbed by local yielding and denting of the cask surface.

ii. No credit is taken for the missile resistance offered by the HI-TRAC VW water jacket shell. It is assumed a priori that the small and intermediate missiles will penetrate the water jacket shell (with no energy loss). Therefore, in the analysis 100% of the missile impact energy is applied directly to the HI-TRAC VW outer shell.

iii. For missile strikes on the side and top lid of the overpack, the analysis credits the structural resistance in compression offered by the concrete material that backs the outer shell and the lid.

iv. The resistance from the concrete is conservatively assumed to act over an area equal to the target area of impact. In other words, no diffusion of the load is assumed to occur through the concrete.

The analyses documented in Appendix 3.B show that the depth of penetration of the small missile is less than the thinnest section of material on the exterior surface of the HI-STORM FW or the HI-TRAC VW. Therefore, the small missile will dent, but not penetrate, the cask. The 1-inch missile can enter the air inlet/outlet vents in the HI-STORM FW overpack, but geometry prevents a direct impact with the MPC.

For the intermediate missile, the analyses documented in Appendix 3.B show that there will be no penetration through the concrete surrounding the inner shell of the storage overpack or penetration of the top lid. Likewise, the intermediate missile will not penetrate the lead surrounding the HI-TRAC VW inner shell. Therefore, there will be no impairment to the Confinement Boundary due to tornado-borne missile strikes. Furthermore, since the HI-STORM FW and HI-TRAC VW inner shells are not compromised by the missile strike, there will be no permanent deformation of the inner shells and ready retrievability of the MPC will be assured.

The penetration results for the small and intermediate missile are summarized in Table 3.4.6.

3.4.4.1.4 Load Case 4: Non-Mechanistic Tipover

The non-mechanistic tipover event, as described in Subsection 2.2.3(b), is site-dependent only to the extent that the stiffness of the target (ISFSI pad) affects the severity of the impact impulse. To bound

the majority of ISFSI pad sites, the tipover analyses are performed using a stiff target foundation, which is defined in Table 2.2.9. The results presented in the main body of this subsection, including referenced Figures, were obtained using a foundation concrete strength of 6000 psi. Tipover analyses have also been performed using the bounding target foundation concrete strength in Table 2.2.9. The results of these analyses are summarized at the end of this subsection.

The objectives of the analyses are to demonstrate that the plastic deformation in the fuel basket is sufficiently limited to permit the stored SNF to be retrieved by normal means and that there is no significant loss of radiation shielding in the storage system. Furthermore, the maximum lateral deflection of the lateral surface of the fuel basket is within the limit assumed in the criticality analyses (Chapter 6), and therefore, the lateral deflection does not have an adverse effect on criticality safety.

The tipover event is an artificial construct wherein the HI-STORM FW overpack is assumed to be perched on its edge with its C.G. directly over the pivot point A (Figure 3.4.8). In this orientation, the overpack begins its downward rotation with zero initial velocity. Towards the end of the tip-over, the overpack is horizontal with its downward velocity ranging from zero at the pivot point (point A) to a maximum at the farthest point of impact. The angular velocity at the instant of impact defines the downward velocity distribution along the contact line.

In the following, an explicit expression for calculating the angular velocity of the cask at the instant when it impacts on the ISFSI pad is derived. Referring to Figure 3.4.8, let r be the length AC where C is the cask centroid. Therefore,

$$r = \left(\frac{d^2}{4} + h^2 \right)^{1/2}$$

The mass moment of inertia of the HI-STORM FW system, considered as a rigid body, can be written about an axis through point A, as

$$I_A = I_c + \frac{W}{g} r^2$$

where I_c is the mass moment of inertia about a parallel axis through the cask centroid C, and W is the weight of the cask (W = Mg).

Let $\theta_1(t)$ be the rotation angle between a vertical line and the line AC. The equation of motion for rotation of the cask around point A, during the time interval prior to contact with the ISFSI pad, is

$$I_A \frac{d^2 \theta_1}{dt^2} = Mgr \sin \theta_1$$

This equation can be rewritten in the form

$$\frac{I_A}{2} \frac{d(\dot{\theta}_1)^2}{d\theta_1} = Mgr \sin \theta_1$$

which can be integrated over the limits $\theta_1 = 0$ to $\theta_1 = \theta_{2f}$ (Figure 3.4.8). The final angular velocity θ_1 at the time instant just prior to contact with the ISFSI pad is given by the expression

$$\dot{\theta}_1(t_B) = \sqrt{\frac{2\,Mgr}{I_A}(1 - \cos\theta_{2f})}$$

where, from Figure 3.4.8,

$$\theta_{2f} = \cos^{-1}\left(\frac{d}{2r}\right)$$

This equation establishes the initial conditions for the final phase of the tip-over analysis; namely, the portion of the motion when the cask is decelerated by the resistive force at the ISFSI pad interface. Using the data germane to HI-STORM FW (Table 3.4.11) and the above equations, the angular velocity of impact is calculated as

$$\dot{\theta}_1(t_B) = 1.45 \text{ rad/sec}$$

The LS-DYNA analysis to characterize the response of the HI-STORM FW system under the non-mechanistic tipover event is focused on two principal demonstrations, namely:

(i) The lateral deformation of the basket panels in the active fuel region is less than the limiting value in Table 2.2.11.

(ii) The impact between the MPC guide tubes and the MPC does not cause a thru-wall penetration of the MPC shell.

Two LS-DYNA finite element models are developed to simulate the postulated tipover event of HI-STORM FW storage cask with loaded MPC-37 and MPC-89, respectively. The two LS-DYNA models are constructed according to the dimensions specified in the licensing drawings included in Section 1.5; the tallest configuration for each MPC type is considered to ensure a bounding tipover analysis. Because of geometric and loading symmetries, a half model of the loaded cask and impact target (i.e., the ISFSI pad) is considered in the analysis. The LS-DYNA models of the HI-STORM FW overpack and the MPC are described in Subsections 3.1.3.1 and 3.1.3.2, respectively.

The ISFSI pad LS-DYNA model, which consists of a 320"×100"×36" concrete pad and the underlying subgrade (800"×275"×470" in size) with non-reflective lateral and bottom surface boundaries, is identical to that used in the HI-STORM 100 tipover analysis documented in the HI-STORM 100 FSAR [3.1.4]. All structural members of the loaded cask are explicitly modeled so that any violation of the acceptance criteria can be found by examining the LS-DYNA simulation results (note: the fuel assembly, which is not expected to fail in a tipover event, is modeled as an elastic rectangular body). This is an improvement compared with the approach taken in the HI-STORM 100 tipover analysis, where the loaded MPC was modeled as a cylinder and therefore the structural integrity of the MPC and fuel basket had to be analyzed separately based on the rigid body deceleration result of the cask. Except for the fuel basket, which is divided into four parts based on the temperature distribution of the basket, each structural member of the cask is modeled as an independent part in the LS-DYNA model. Note that the critical weld connection between the MPC shell and the MPC lid is treated as a separate part and modeled with solid elements. Each of the two LS-DYNA models consists of forty-two parts, which are discretized with sufficiently high mesh density; very fine grids are used in modeling the MPC enclosure vessel, especially in the areas where high stress gradients are expected (e.g., initial impact location with the overpack). To ensure numerical accuracy, full integration thin shell and thick shell elements with 10 though-thickness integration points or multi-layer solid elements are used. The LS-DYNA tipover model consists of over 470,000 nodes and 255,000 elements for HI-STORM FW with loaded MPC-37, and the model for the cask with loaded MPC-89 consists of over 689,000 nodes and 350,000 elements.

The same ISFSI concrete pad material model used for the HI-STORM 100 tipover analysis reported in [3.1.4] is repeated for the HI-STORM FW tipover analysis. Specifically, the concrete pad behavior is characterized using the same LS-DYNA material model (i.e., MAT_PSEUDO_TENSOR or MAT_016) as for the end drop and tipover analyses of the HI-STORM 100 storage cask (the only difference between the HI-STORM FW reference ISFSI concrete pad model and the model of the HI-STORM 100 Set B ISFSI concrete pad is thickness). Moreover, the subgrade is also conservatively modeled as an elastic material as before. Note that this ISFSI pad material modeling approach was originally taken in the USNRC approved storage cask tipover and end drop LS-DYNA analyses [3.4.5] where a good correlation was obtained between the analysis results and the test results.

To assess the potential damage of the cask caused by the tipover accident, an LS-DYNA nonlinear material model with strain rate effect is used to model the responses of all HI-STORM FW cask structural members based on the true stress-strain curves of the corresponding materials. Note that the strain rate effect for the fuel basket material, i.e., Metamic HT, is not considered for conservatism.

Figures 3.4.9 to 3.4.14 depict the two finite-element tipover analysis models developed for the bounding HI-STORM FW cask configurations with loaded MPC-37 and MPC-89, respectively.

As shown in Figure 3.4.15, the fuel basket does not experience significant plastic deformation in the active fuel region to exceed the acceptable limits; plastic deformation is essentially limited locally in cells near the top of the basket beyond the active fuel region for both MPC-37 and MPC-89 baskets. Note that the basket corner welds are not considered in the tip-over analysis for conservatism.. The fuel basket is considered to be structurally safe since it can continue maintaining appropriate spacing between fuel assemblies after the tipover event. The MPC enclosure vessel experiences minor plastic deformation at the impact locations with the overpack guide tubes; the maximum local plastic strain (9.9%, see Figure 3.4.16) is well below the failure strain of the material and smaller than the plastic strain limit (i.e., at least 0.2 for stainless steel) recommended by [3.4.6] for ASME NB components. Similarly, local plastic deformation occurs in the overpack shear ring near the cask-to-pad impact location as shown in Figure 3.4.17. However, the shielding capacity of overpack will not be compromised by the tipover accident and there is no gross plastic deformation in the overpack inner shell to affect the retrievablilty of the MPC. In addition, the cask closure lid bolts are demonstrated to be structurally safe after the tipover event, only a negligibly small plastic strain is observed in the bolt near the impact location (see Figure 3.4.18). Therefore, the cask lid will not dislodge after the tipover event. Finally, Figures 3.4.19 and 3.4.20 present the deceleration time history results of the cask lid predicted by LS-DYNA. The peak rigid body decelerations, measured for the HI-STORM FW lid concrete, are shown to be 61.75 g's in the vertical direction and 16.71 g's in the horizontal direction, respectively. Note that the deceleration time histories are filtered using the LS-DYNA built-in Butterworth filter with a cut-off frequency of 350 Hz; the same filter was used for the HI-STORM 100 non-mechanistic tipover analysis [3.1.4].

The structural integrity of the HI-STORM FW lid (standard, Version XL, and domed) cannot be ascertained from the LS-DYNA tipover analyses since some components of the lid, namely the lid outer shell and the lid gussets, are defined as rigid members in order to simplify the modeling effort and maintain proper connectivity. Therefore, a separate tipover analysis has been performed for the HI-STORM FW lid (standard, Version XL, and domed) using ANSYS, wherein a bounding peak rigid body deceleration established based on LS-DYNA tipover analysis results is statically applied to the lid. The finite element model is identical to the one used in Subsection 3.4.3 to simulate a vertical lift of the HI-STORM FW lid (Figures 3.4.5A, 3.4.5B, and 3.4.5C), except that the eight circumferential gussets are conservatively neglected (i.e., deleted from the finite element model for the standard lid).

The resulting stress distributions in the HI-STORM FW lids (standard and Version XL) are shown in Figures 3.4.21A and 3.4.21B. Per Subsection 2.2.3, the HI-STORM FW lid should not suffer any gross loss of shielding as a result of the non-mechanistic tipover event. To satisfy this criterion, the primary membrane stresses in the lid components are compared against the material yield strength. The most heavily loaded component in the standard lid is the upper shim plate closest to the point of impact (Figure 3.4.21A). In order to determine the primary membrane stress in the upper shim plate, the stresses are linearized along a path that follows the outside vertical edge of the upper shim plate

(see Figure 3.4.21A for path definition). Figure 3.4.22A shows the linearized stress results. Since the membrane stress is less than the yield strength of the material at 300°F (Table 3.3.6), it is concluded that the standard lid will not suffer any gross loss of shielding as a result of the non-mechanistic tipover event. The most heavily loaded component in the Version XL lid is the base plate ligament closest to the point of impact (Figure 3.4.21B). In order to determine the primary membrane stresses in the base plate, the stresses are linearized along a path that follows the middle plane of the ligament (see Figure 3.4.21C for path definition). Figure 3.4.22B shows the linearized stress results. Since the membrane stress is less than the material primary membrane stress for accident conditions at 400°F (Table 3.1.6), it is concluded that the Version XL lid will not suffer any gross loss of shielding as a result of the non-mechanistic tipover event. Similar to the XL lid, the domed lid bolt holes are enlarged and a shear ring is welded to the underside of the lid ribs. Therefore, the lid studs only encounter axial (tensile) loads. The in-plane load is resisted by the shear ring as it bears against the overpack body top plate. Using strength of materials calculation, the lid components which are in the load path are evaluated with the bounding acceleration at the top of the lid due to tip-over event and the resulting stresses are compared with the corresponding allowables in Level D conditions. The studs connecting the lid to the body are evaluated for pure axial load due to axial acceleration and it is shown that the bolts are structurally adequate. The complete details of the lid tipover analysis are provided in [3.4.13].

Finally, to evaluate the potential for crack propagation and growth for the MPC fuel baskets under the non-mechanistic tipover event, a conservative crack propagation analysis is carried out for both MPC-37 and MPC-89 fuel baskets using the same methodology utilized in Attachment D of [1.2.6] to evaluate the HI-STAR 180 F-37 fuel basket in support of the HI-STAR 180 SAR [3.1.10]. The crack propagation analysis is bounding since the maximum tensile strength of the basket material (28.2 ksi) documented in Table 1.2.8 is conservatively considered as the maximum tensile stress experienced by the Metamic fuel baskets in the tip-over accident and used as input to the following crack propagation analysis.

Per [1.2.6] the critical stress intensity factor of Metamic-HT panels is estimated to be

$$K_{IC} = 30ksi\sqrt{in}$$

based on Charpy V-notch absorbed energy (CVE) correlations for steels. The estimated value is consistent with the range for aluminum alloys, which is 20 to 50 $MPa\sqrt{m}$ or 18.2 to 45 $ksi\sqrt{in}$ per Table 3 of [3.4.19]. Next the minimum crack size, a_{min}, for crack propagation to occur is calculated below using the formula for a through-thickness edge crack given in [3.1.5]. Although the formula is derived for a straight-edge specimen, the use of the maximum tensile strength of the fuel basket material as the maximum tensile stress experienced by the basket well compensates for the geometric difference between the basket panel and the specimen. Moreover, the maximum size of a pre-existing crack (1/16") in the fuel basket panel is less than 1/9th of the basket panel thickness (0.59"). Thus, the assumption of a through-thickness edge crack is very conservative. The result is

$$a_{\min} = \frac{\left(\frac{K_{IC}}{1.12\sigma_{\max}}\right)^2}{\pi} = \frac{\left[\frac{30ksi\sqrt{in}}{1.12(28.2ksi)}\right]^2}{\pi} = 0.287in$$

And the safety factor against crack propagation (based on a 1/16" minimum detectable flaw size) is

$$SF = \frac{a_{\min}}{a_{\det}} = \frac{0.287in}{0.0625in} = 4.595$$

The calculated minimum crack size is about 4.6 times the maximum possible pre-existing crack size in the fuel basket (based on 100% surface inspection of each panel). The large safety factor ensures that crack propagation in the HI-STORM FW fuel baskets will not occur due to the non-mechanistic tipover event.

Non-Mechanistic Tipover Using Bounding Concrete Pad Compressive Strength

A non-mechanistic tipover analysis is performed using the bounding concrete compressive strength specified in Table 2.2.9. The methodology, acceptance criteria, assumptions, and input data are the same as those delineated in the discussion above. Two limiting cases are considered:

- Case 1: HI-STORM FW loaded with MPC 37 fuel basket, without corner welds, all basket panels have matching tabs and notches for interlocking perpendicular panels at the basket corners.
- Case 2: HI-STORM FW loaded with MPC 37 fuel basket, without corner welds, basket panels are made with straight edges so a flat contact interface is formed between any two perpendicular panels meeting at the basket corner.

As shown in the tipover analysis [3.4.11], the fuel basket does not experience significant plastic deformation in the active fuel region to exceed the acceptable limits. The maximum panel displacement due to the tip-over event is located beyond the active fuel region for both MPC-37 and MPC-89 baskets (tipover of MPC-89 is not analyzed here but the results are bounded by MPC-37), which is considered to be acceptable from the perspectives of shielding and criticality. Note that the basket corner welds are not considered in the tip-over analysis for conservatism. The fuel baskets in both Case 1 and Case 2 corner configuration are considered to be structurally safe as they can continue to maintain appropriate spacing between fuel assemblies after the tipover event. The MPC enclosure vessel experiences minor plastic deformation at the impact locations with the overpack guide tubes; the maximum local plastic strain (9.0%, see Figures 3.4.16C & 3.4.16D) is well below the failure strain of the material and smaller than the plastic strain limit (i.e., at least 0.2 for stainless steel) recommended by [3.4.6] for ASME NB components. Similarly, local plastic deformation occurs in the overpack shear ring near the cask-to-pad impact location as shown in Figure 3.4.17C & 3.4.17D. However, the shielding capacity of overpack will not be compromised by the tipover accident and there is no gross plastic deformation in the overpack inner shell to affect the

retrievablilty of the MPC. In addition, the cask closure lid bolts are demonstrated to be structurally safe after the tipover event, only a small plastic strain is observed in the bolt near the impact location (see Figures 3.4.18C & 3.4.18D). Therefore, the cask lid will not dislodge after the tipover event. Finally, the peak rigid body decelerations, measured for the HI-STORM FW lid concrete, are shown to be 60.91 g's for Case 1 and 62.82 g's for Case 2 in the vertical direction (see Figures 3.4.19C & 3.4.19D) and 17.80 g's for Case 1 and 17.75 g's for Case 2 in the horizontal direction (see Figures 3.4.20C & 3.4.20D). Note that the deceleration time histories are filtered using the LS-DYNA built-in Butterworth filter with a cut-off frequency of 350 Hz; the same filter was used for the HI-STORM 100 non-mechanistic tipover analysis.

The tipover analysis for the HI-STORM FW lid [3.4.13] is performed using a bounding peak rigid body deceleration; therefore, the results are applicable to the non-mechanistic tipover event with target foundation concrete strength specified in Table 2.2.9. It is concluded that the lid will not suffer any gross loss of shielding.

3.4.4.1.5 Load Case 5: Design, Short-Term Normal and Off-Normal MPC Internal Pressure

The MPC Enclosure Vessel, which is designed to meet the stress intensity limits of ASME Subsection NB [3.4.4], is analyzed for a bounding normal (design, long-term and short-term) internal pressure (Table 2.2.1) of 120 psig using the ANSYS finite element code [3.4.1]. Except for the applied loads and the boundary conditions, the finite element model of the MPC Enclosure Vessel used for this load case is identical to the model described in Subsections 3.1.3.2 and 3.4.3.2 for the MPC lifting analysis.

The only load applied to the finite element model for this load case is the bounding MPC design internal pressure for normal conditions (Table 2.2.1). All internal surfaces of the MPC storage cavity are subjected to the design pressure. The center node on the top surface of the MPC upper lid is fixed against translation in all directions. Symmetric boundary conditions are applied to the two vertical symmetry planes. This set of boundary conditions allows the MPC Enclosure Vessel to deform freely under the applied pressure load. Figure 3.4.31 graphically depicts the applied pressure load and the boundary conditions for Load Case 5.

The stress intensity distribution in the MPC Enclosure Vessel under design internal pressure is shown in Figure 3.4.23. Figures 3.4.32 and 3.4.33 plot the thru-thickness variation of the stress intensity at the baseplate center and at the baseplate-to-shell juncture, respectively. The maximum primary stress intensities in the MPC Enclosure Vessel are compared with the applicable stress intensity limits from Subsection NB of the ASME Code (Fig. NB-3221-1). The allowable stress intensities are obtained at design temperature limits in Table 2.2.3 (600°F for the shell and lid, 400°F for the baseplate, and 600°F at the baseplate-to-shell juncture). The maximum calculated stress intensities in the MPC Enclosure Vessel, and their corresponding allowable limits, are summarized in Table 3.4.7 for Load Case 5.

Similar evaluations are performed for the MPC Enclosure Vessel under short-term normal (Level A) and off-normal (Level B) conditions. The applied loads are bounding internal pressure (120 psig) from Table 2.2.1 and conservatively bounding temperature contours based on thermal evaluations in Sections 4.5 and 4.6 for short-term normal and off-normal conditions, respectively. The maximum primary and secondary stress intensities in the MPC Enclosure Vessel are compared with the applicable stress intensity limits from Subsection NB of the ASME Code (Fig. NB-3222-1 and Subsection NB-3223 for Level A and Level B, respectively). The allowable stress intensities are obtained at bounding bulk temperatures [3.4.13] from thermal evaluations. The maximum calculated stress intensities in the MPC Enclosure Vessel and their corresponding allowable limits, are summarized in Tables 3.4.7A and 3.4.7B for Level A and Level B, respectively.

3.4.4.1.6 Load Case 6: Maximum MPC Internal Pressure Under Accident Conditions

The maximum pressure in the MPC Enclosure Vessel under accident conditions is specified in Table 2.2.1. The stress analysis under this pressure condition uses the same model as the one described in the preceding subsection for design internal pressure. The only change is the magnitude of the applied pressure. Figure 3.4.34 graphically depicts the applied pressure load and the boundary conditions for Load Case 6.

The stress intensity distribution in the MPC Enclosure Vessel under accident internal pressure is shown in Figure 3.4.24. The maximum primary stress intensities in the MPC Enclosure Vessel are compared with the applicable stress intensity limits from Subsection NB of the ASME Code [3.4.4]. The allowable stress intensities are taken at 800°F for shell, lid, baseplate, and baseplate-to-shell juncture. These temperatures are obtained from Table 2.2.3 for accident conditions and bound the calculated temperatures under normal operating conditions for the respective MPC components based on the thermal evaluations in Chapter 4. The allowable stress intensities are determined based on normal operating temperatures since the MPC accident internal pressure is dictated by the 100% fuel rod rupture accident, which does not cause any significant rise in MPC temperatures. In fact, the temperatures inside the MPC tend to decrease as a result of the 100% fuel rod rupture accident due to the increase in the density and internal pressure of the circulating gas. The maximum calculated stress intensities in the MPC Enclosure Vessel, and their corresponding allowable limits, are summarized in Table 3.4.8 for Load Case 6.

3.4.4.1.7 Load Case 7: Accident External Pressure

The only affected component for this load case is the MPC Enclosure Vessel. The accident external pressure (Table 2.2.1) is selected sufficiently high to envelop hydraulic-pressure in the case of flood or explosion-induced pressure at all ISFSI Sites.

The main effect of an external pressure on the MPC is to cause compressive stress in the MPC shell. Therefore, the potential of buckling must be investigated. The methodology used for this investigation is from ASME Code Case N-284-2 (Metal Containment Shell Buckling Design

Methods, Section III, Division 1, Class MC (1/07)). This Code Case has been previously used by Holtec in [3.1.4] and accepted by the NRC as a valid method for evaluation of stability in vessels.

The detailed evaluation of the MPC shell under accident external pressure is provided in Appendix 3.C. It is concluded that positive safety margins exist so that elastic or plastic instability of the maximum height MPC shell does not occur under the applied pressure.

3.4.4.1.8 Load Case 8: Non-Mechanistic Heat-Up of the HI-TRAC VW Water Jacket

Even though the analyses presented in Chapter 4 indicate that the temperature of water in the water jacket shall not reach boiling and the rupture disks will not open, it is (non-mechanistically) assumed that the hydraulic pressure in the water jacket reaches the relief devices' set point. The object of this analysis is to demonstrate that the stresses in the water jacket and its welds shall be below the limits set down in an appropriate reference ASME Boiler and Pressure Vessel Code (Section II Class 3) for the Level D service condition. The accident pressure inside the water jacket is given in Table 2.2.1.

The HI-TRAC VW water jacket is analyzed using classical strength-of-materials. Specifically, the unsupported span of the water jacket shell between radial ribs is treated as a curved beam, with clamped ends, under a uniformly distributed radial pressure. The force and moment reactions at the ends of the curved beam for this type of loading are calculated using the formula for Case 5j of Table 18 in [3.4.16]. The primary membrane plus bending stress is then calculated using the formula for Case 1 of Table 16 in [3.4.16]. Figure 3.4.35 depicts the curved beam model that is used to analyze the water jacket shell and defines the key input variables. The input values that are used in the calculations are provided in Table 3.4.12.

The bottom flange, which serves as the base of the water jacket, is conservatively analyzed as an annular plate clamped at the water jacket inside diameter and simply supported at the water jacket outside diameter. The maximum bending stress in the bottom flange is calculated using the following formula from [3.4.18, Art. 23]:

$$\sigma_{max} = k\frac{q \cdot a^2}{h^2}$$

where q is the internal pressure inside the water jacket (= 73.65 psi), a is the outside radius of the water jacket (= 47.5 in), and h is the thickness of the bottom flange (= 2.0 in). The analyzed pressure accounts for the accident internal pressure inside the water jacket (Table 2.2.1) plus the hydrostatic pressure at the base of the water jacket. The value of k is dependent on the diameter ratio of the annular plate and the boundary conditions. Per Table 5 of [3.4.18], k is equal to 0.122 for a bounding diameter ratio of 1.25 and simply supported-clamped boundary conditions (Case 4). Therefore, the maximum bending stress in the bottom flange is:

$$\sigma_{max} = 5{,}068 \text{ psi}$$

Per Table 3.1.6, the allowable primary membrane plus bending stress intensity for SA-516 Gr. 70 material at the design temperature listed in Table 2.2.3 leads to a factor of safety greater than 10.0.

The maximum stresses in the various water jacket components, including the connecting welds, are summarized in Table 3.4.9.

3.4.4.1.9 Load Case 9: Handling of Components

The stress analyses of the MPC, the HI-STORM FW overpack, and the HI-TRAC VW transfer cask under normal handling conditions are presented in Subsection 3.4.3.

3.4.4.1.10 Load Case 10: Snow Load

In accordance with Table 3.1.1, the HI-STORM FW lid is analyzed using ANSYS to demonstrate that the design basis snow load (Table 2.2.8) does not cause stress levels in the overpack lid to exceed ASME Subsection NF stress limits for Level A. The finite element model is identical to the one used in Subsection 3.4.3 to simulate a vertical lift of the HI-STORM FW lid (see Figures 3.4.5A and 3.4.5B). For conservatism, a pressure load of 10 psig is used in the finite element analysis. The stress distribution in the lid under the bounding snow load is shown in Figure 3.4.25A for the standard lid and Figure 3.4.25B for the Version XL lid. The maximum stress results are summarized in Table 3.4.10. For conservatism, the maximum calculated stress at any point on the lid, including secondary stress contributions, is compared against the primary membrane and primary bending stress limits per ASME Subsection NF. Since the domed lid has similar configuration but is much thicker compared to the XL lid, the results from XL lid are bounding for domed lid.

3.4.4.1.11 Load Case 11: MPC Reflood Event

During a MPC reflood event, water is introduced to the MPC cavity through the lid drain line to cooldown the MPC internals and support fuel unloading. This quenching operation induces thermal stresses and strains in the fuel rod cladding, which are maximum at the boundary interface between the rising water and the dry (gaseous) cavity. The following analysis demonstrates that the maximum total strain in the fuel cladding due to the reflood event is well below the failure strain limit of the material. Thus, the fuel rod cladding will not be breached due to the MPC reflood event.

The analysis is carried out using the finite element code ANSYS [3.4.1]. The model, which is shown in Figure 3.4.37, is constructed using 4-node plastic large strain elements (SHELL43) based on the cladding dimensions of the PWR reference fuel type. The overall length of the model is equal to 30 times the outside diameter of the fuel cladding. As seen in Figure 3.4.37, the mesh size is reduced at the boundary between the wetted fuel rod and the dry fuel rod, where the highest stresses and strains occur. To account for the gas pressure inside the fuel rod, the top end of the fuel rod is fixed in the vertical direction, and an equivalent axial force is applied at the bottom end. A radial pressure is also applied to the inside surface of the fuel cladding (see Figure 3.4.38). The fuel cladding material is modeled as a bi-linear isotropic hardening material with temperature dependent properties. The key input data used to develop the finite element model are summarized in Table 3.4.14.

The MPC reflood pressure, which is restricted to below the normal condition pressure limit, is too low to have an adverse effect on the fuel cladding, the reflood water pressure acts to produce compressive hoop stresses which help reduce the tensile hoop stress (albeit by a small amount) from the internal gas pressure in the rods. Therefore, the MPC flooding pressure has no harmful consequence to the fuel cladding and is neglected in the analysis.

At t = 0 sec, the uniform temperature throughout the entire fuel rod is set at 752°F (400°C), which equals the fuel cladding temperature limit under normal operating conditions. At t = 0.1 sec, the temperature assigned to the lower half of the fuel rod model is suddenly reduced to 80°F to simulate the water quenching (see Figure 3.4.39). The resulting stress and strain distributions in the fuel rod are shown in Figures 3.4.40 and 3.4.41, respectively. The maximum stress and strain values are summarized in Table 3.4.15. The maximum total strain in the fuel rod is well below the failure strain limit of 1.7% for the cladding material per [3.4.20]. In fact, the maximum stress and strain in the fuel rod remain in the elastic range.

The analysis described above makes a number of assumptions that significantly overstate the computed thru-wall strain in the fuel cladding. The major assumptions are:

1. Even though the peak cladding temperature occurs at a localized location, the fuel rod is modeled as a pressurized tube with closed ends at a uniform temperature that is greater than the maximum peak cladding temperature value reported in Chapter 4 when the MPC is in the HI-TRAC under the Design Basis heat load condition.
2. The rapid thermal straining of the pressurized tube (fuel rod) due to the quenching effect of water is simulated as a step transient wherein the temperature of the quenched portion of the tube is assumed to drop down to the injected water temperature (assumed to be 80°F) causing a step change in the cladding wall temperature in the longitudinal direction at its interface with the "dry" portion of the tube. This assumption is extremely conservative because in actuality the immersed portion of the fuel rod is blanketed by vapor which acts to retard the severity of the thermal transient.
3. Even though, as the rod is gradually immersed in water, the axial heat conduction will tend to cool the un-immersed portion of the tube thus reducing the ΔT at the quenched/dry interface, no credit for axial conduction is taken.
4. The cooling of the fuel rod by gradual immersion in the water has the beneficial effect of reducing the internal pressure (per the ideal gas law) and thus the magnitude of pressure induced stress in the fuel cladding. As the peak cladding temperature in the MPC is reached in the upper half of the fuel rods (see Chapter 4), a substantial amount of rod is cooled by water (as its level gradually rises inside the MPC) before the vulnerable zone (where the peak cladding temperature exists) is subjected to the thermal transient from quenching. No credit for this amelioration of the pressure stresses due to the gradual cooling of the rod is taken in the analysis.

In summary, even though the analysis presented above is highly conservative, the maximum stress and strain in the fuel rod remain elastic. Moreover, the maximum strain is less than the failure strain limit by a factor of 6. Thus, the MPC reflood event will not cause a breach of the fuel rod cladding.

3.4.5 Cold

A discussion of the resistance to failure due to brittle fracture is provided in Subsection 3.1.2.

The value of the ambient temperature has two principal effects on the HI-STORM FW system, namely:

i. The steady-state temperature of all material points in the cask system will go up or down by the amount of change in the ambient temperature.

ii. As the ambient temperature drops, the absolute temperature of the contained helium will drop accordingly, producing a proportional reduction in the internal pressure in accordance with the Ideal Gas Law.

In other words, the temperature gradients in the system under steady-state conditions will remain the same regardless of the value of the ambient temperature. The internal pressure, on the other hand, will decline with the lowering of the ambient temperature. Since the stresses under normal storage condition arise principally from pressure and thermal gradients, it follows that the stress field in the MPC under –40 degree F ambient would be smaller than the "heat" condition of storage, treated in the preceding subsection. Additionally, the allowable stress limits tend to increase as the component temperatures decrease.

Therefore, the stress margins computed in Subsection 3.4.4 can be conservatively assumed to apply to the "cold" condition as well.

Finally, it can be readily shown that the HI-STORM FW system is engineered to withstand “cold” temperatures (-40 degrees F) without impairment of its storage function.

Unlike the MPC, the HI-STORM FW storage overpack is an open structure; it contains no pressure. Its stress field is unaffected by the ambient temperature, unless low temperatures produce brittle fracture due to the small stresses which develop from self-weight of the structure and from the minute difference in the thermal expansion coefficients in the constituent parts of the equipment (steel and concrete). To prevent brittle fracture, all steel material in HI-STORM FW is qualified by impact testing pursuant to the ASME Code (Table 3.1.9).

The structural material used in the MPC (Alloy X) is recognized to be completely immune from brittle fracture in the ASME Codes.

As no liquids are included in the HI-STORM FW storage overpack design, loads due to expansion of freezing liquids are not considered. The HI-TRAC VW transfer cask utilizes demineralized water in

the water jacket. However, the specified lowest service temperature for the HI-TRAC VW is 0 degrees F and a 25% ethylene glycol solution is required for the temperatures from 0 degrees F to 32 degrees F. Therefore, loads due to expansion of freezing liquids are not considered.

There is one condition, however, that does require examination to ensure ready retrievability of the fuel. Under a postulated loading of an MPC from a HI-TRAC VW transfer cask into a cold HI-STORM FW storage overpack, it must be demonstrated that sufficient clearances are available to preclude interference when the "hot" MPC is inserted into a "cold" storage overpack. To this end, a bounding analysis for free thermal expansions has been performed in Subsection 4.4.6, wherein the MPC shell is postulated at its maximum design basis temperature and the thermal expansion of the overpack is ignored. The results from the evaluation of free thermal expansion are summarized in Table 4.4.6. The final radial clearance is sufficient to preclude jamming of the MPC upon insertion into a cold HI-STORM FW storage overpack.

3.4.6 Miscellaneous Evaluations

3.4.6.1 Structural Integrity of Damaged Fuel Containers (DFCs)

The Damaged Fuel Container (DFC) is used to store fuel that is physically impaired such that it cannot be handled by normal means. The DFC, as shown in the licensing drawings, is equipped with a handle welded to a square cellular box with a perforated baseplate structurally capable of supporting the weight of the fuel while permitting water (but not particulates) to pass through. All load bearing members of the DFC are designed to meet Level A service limit when holding a spent fuel assembly.

Because the DFC is always handled under water, there are no radiation release-related issues associated with it.

3.4.7 Service Life of HI-STORM FW and HI-TRAC VW

The term of the 10CFR72, Subpart L C of C, granted by the NRC is 20 years; therefore, the License Life (see Glossary) of all components is 20 years. Nonetheless, the HI-STORM FW storage overpack and the HI-TRAC VW transfer cask are engineered for 60 years of design life, while satisfying the conservative design requirements defined in Chapter 2, including the regulatory requirements of 10CFR72. In addition, the storage overpack and HI-TRAC VW are designed, fabricated, and inspected under the comprehensive Quality Assurance Program approved by the USNRC and in accordance with the applicable requirements of the ACI and ASME Codes. This assures high design margins, high quality fabrication, and verification of compliance through rigorous inspection and testing, as described in Chapter 10 and the licensing drawings in Section 1.5. Technical Specifications defined in Chapter 13 assure that the integrity of the cask and the contained MPC are maintained throughout the components' design life. The design life of a component, as defined in the Glossary, is the minimum duration for which the equipment or system is engineered to perform its intended function if operated and maintained in accordance with the FSAR. The design life is essentially the lower bound value of the service life, which is the expected functioning life of the

component or system. Therefore, component longevity should be: licensed life < design life < service life. (The licensed life, enunciated by the USNRC, is the most pessimistic estimate of a component's life span). For purposes of further discussion, we principally focus on the service life of the HI-STORM FW system components that, as stated earlier, is the reasonable expectation of equipment's functioning life span.

The service life of the storage overpack and HI-TRAC VW transfer cask is further discussed in the following.

3.4.7.1 Storage Overpack

The principal design considerations that bear on the adequacy of the storage overpack for the service life are addressed as follows:

Exposure to Environmental Effects

All exposed surfaces of the HI-STORM FW overpack are made from ferritic steels that are readily painted. Concrete, which serves strictly as a shielding material, is completely encased in steel. Therefore, the potential of environmental vagaries such as spalling of concrete, are ruled out for HI-STORM FW. Under normal storage conditions, the bulk temperature of the HI-STORM FW storage overpack will, because of its large thermal inertia, change very gradually with time. Therefore, material degradation from rapid thermal ramping conditions is not credible for the HI-STORM FW storage overpack. Similarly, corrosion of structural steel embedded in the concrete structures due to salinity in the environment at coastal sites is not a concern for HI-STORM FW because HI-STORM FW does not rely on rebars (indeed, it contains no rebars). As discussed in Appendix 1.D of HI-STORM 100 FSAR, the aggregates, cement and water used in the storage cask concrete are carefully controlled to provide high durability and resistance to temperature effects. The configuration of the storage overpack assures resistance to freeze-thaw degradation. In addition, the storage overpack is specifically designed for a full range of enveloping design basis natural phenomena that could occur over the 60-year design life of the storage overpack as defined in Subsection 2.2.3 and evaluated in Chapter 12. Chapter 8 provides further discussions on chemical and galvanic reactions, material compatibility and operating environments.

Material Degradation

As discussed in Chapter 8, the relatively low neutron flux to which the storage overpack is subjected cannot produce measurable degradation of the cask's material properties and impair its intended safety function. Exposed carbon steel components are coated to prevent corrosion. The controlled environment of the ISFSI storage pad mitigates damage due to direct exposure to corrosive chemicals that may be present in other industrial applications.

Maintenance and Inspection Provisions

The requirements for periodic inspection and maintenance of the storage overpack throughout the 60-year design life are defined in Chapter 10. These requirements include provisions for routine inspection of the storage overpack exterior and periodic visual verification that the ventilation flow paths of the storage overpack are free and clear of debris. ISFSIs located in areas subject to atmospheric conditions that may degrade the storage cask or canister should be evaluated by the licensee on a site-specific basis to determine the frequency for such inspections to assure long-term performance. In addition, the HI-STORM FW system is designed for easy retrieval of the MPC from the storage overpack should it become necessary to perform more detailed inspections and repairs on the storage overpack.

The above findings are consistent with those of the NRC's Waste Confidence Decision Review [3.4.10], which concluded that dry storage systems designed, fabricated, inspected, and operated in accordance with such requirements are adequate for a 100-year service life while satisfying the requirements of 10CFR72.

3.4.7.2 Transfer Cask

The principal design considerations that bear on the adequacy of the HI-TRAC VW transfer cask for the service life are addressed as follows:

Exposure to Environmental Effects

All transfer cask materials that come in contact with the spent fuel pool are coated to facilitate decontamination. The HI-TRAC VW is designed for repeated normal condition handling operations with high factor of safety to assure structural integrity. The resulting cyclic loading produces stresses that are well below the endurance limit of the cask's materials, and therefore, will not lead to a fatigue failure in the transfer cask. All other off-normal or postulated accident conditions are infrequent or one-time occurrences that do not contribute significantly to fatigue. In addition, the transfer cask utilizes materials that are not susceptible to brittle fracture during the lowest temperature permitted for loading, as discussed in Subsection 8.4.3.

Chapter 8 provides further discussions on chemical and galvanic reactions, material compatibility and operating environments.

Material Degradation

As discussed in Chapter 8, all transfer cask materials that are susceptible to corrosion are coated. The controlled environment in which the HI-TRAC VW is used mitigates damage due to direct exposure to corrosive chemicals that may be present in other industrial applications. The infrequent use and relatively low neutron flux to which the HI-TRAC VW materials are subjected do not result in radiation embrittlement or degradation of the HI-TRAC's shielding materials that could impair the HI-TRAC's intended safety function. The HI-TRAC VW transfer cask materials are selected for

durability and wear resistance for their deployment.

Maintenance and Inspection Provisions

The requirements for periodic inspection and maintenance of the HI-TRAC VW transfer cask throughout the 60-year design life are defined in Chapter 10. These requirements include provisions for routine inspection of the HI-TRAC VW transfer cask for damage prior to each use, including an annual inspection of the lifting attachments. Precautions are taken during lid handling operations to protect the sealing surfaces of the bottom lid. The leak tightness of the liquid neutron shield is verified periodically. The water jacket pressure rupture discs and other fittings used can be easily removed.

3.4.8 MPC Service Life

The term of the 10CFR72, Subpart L C of C, granted by the NRC (i.e., licensed life) is 20 years. Nonetheless, the HI-STORM FW MPCs are designed for 60 years of design life, while satisfying the conservative design requirements defined in Chapter 2, including the regulatory requirements of 10CFR72. Additional assurance of the integrity of the MPC and the contained SNF assemblies throughout the 60-year life of the MPC is provided through the following:

- Design, fabrication, and inspection invoke the pertinent requirements of the ASME Code, as applicable, assures high inherent design margins in operating modes.

- Fabrication and inspection performed in accordance with the comprehensive Quality Assurance program assures competent compliance with the fabrication requirements.

- Use of materials with known characteristics, verified through rigorous inspection and testing, as described in Chapter 10, assures component compliance with design requirements.

- Use of welding procedures in full compliance with Section III of the ASME Code ensures high-quality weld joints.

Technical Specifications, as defined in Chapter 13, have been developed and imposed on the MPC that assure that the integrity of the MPC and the contained SNF assemblies are maintained throughout the 60-year design life of the MPC.

The principal design considerations bearing on the adequacy of the MPC for the service life are summarized below.

Corrosion

All MPC materials are fabricated from corrosion-resistant austenitic stainless steel and passivated aluminum. The corrosion-resistant characteristics of such materials for dry SNF storage canister

applications, as well as the protection offered by these materials against other material degradation effects, are well established in the nuclear industry. The moisture in the MPC is removed to eliminate all oxidizing liquids and gases and the MPC cavity is backfilled with dry inert helium at the time of closure to maintain an atmosphere in the MPC that provides corrosion protection for the SNF cladding throughout the dry storage period. The preservation of this non-corrosive atmosphere is assured by the inherent sealworthiness of the MPC Confinement Boundary integrity (there are no gasketed joints in the MPC).

Structural Fatigue

The passive non-cyclic nature of dry storage conditions does not subject the MPC to conditions that might lead to structural fatigue failure. Ambient temperature and insolation cycling during normal dry storage conditions and the resulting fluctuations in MPC thermal gradients and internal pressure is the only mechanism for fatigue. These low-stress, high-cycle conditions cannot lead to a fatigue failure of the MPC that is made from stainless alloy stock (endurance limit well in excess of 20,000 psi). All other off-normal or postulated accident conditions are infrequent or one-time occurrences, which cannot produce fatigue failures. Finally, the MPC uses materials that are not susceptible to brittle fracture.

Maintenance of Helium Atmosphere

The inert helium atmosphere in the MPC provides a non-oxidizing environment for the SNF cladding to assure its integrity during long-term storage. The preservation of the helium atmosphere in the MPC is assured by the robust design of the MPC Confinement Boundary described in Section 7.1. Maintaining an inert environment in the MPC mitigates conditions that might otherwise lead to SNF cladding failures. The required mass quantity of helium backfilled into the canister at the time of closure and the associated fabrication and closure requirements for the canister are specifically set down to assure that an inert helium atmosphere is maintained in the canister throughout the 60-year design life.

Allowable Fuel Cladding Temperatures

The helium atmosphere in the MPC promotes heat removal and thus reduces SNF cladding temperatures during dry storage. In addition, the SNF decay heat will substantially attenuate over a 60-year dry storage period. Maintaining the fuel cladding temperatures below allowable levels during long-term dry storage mitigates the damage mechanism that might otherwise lead to SNF cladding failures. The allowable long-term SNF cladding temperatures used for thermal acceptance of the MPC design are conservatively determined, as discussed in Section 4.3.

Neutron Absorber Boron Depletion

The effectiveness of the fixed borated neutron absorbing material used in the MPC fuel basket design requires that sufficient concentrations of boron be present to assure criticality safety during worst case design basis conditions over the 60-year design life of the MPC. Information on the

characteristics of the borated neutron absorbing material used in the MPC fuel basket is provided in Subsection 1.2.1 and Chapter 8. The relatively low neutron flux, to which this borated material is subjected and will continue to decay over time, does not result in significant depletion of the material's available boron to perform its intended safety function. In addition, the boron content of the material used in the criticality safety analysis is conservatively based on the minimum specified boron areal density (rather than the nominal), which is further reduced by 25% for analysis purposes, as described in Section 6.1. Analysis discussed in Section 6.3 demonstrates that the boron depletion in the neutron absorber material is negligible over a 60-year duration. Thus, sufficient levels of boron are present in the fuel basket neutron absorbing material to maintain criticality safety functions over the 60-year design life of the MPC.

The above findings are consistent with those of the NRC's Waste Confidence Decision Review, which concluded that dry storage systems designed, fabricated, inspected, and operated in the manner of the requirements set down in this document are adequate for a 100-year service life, while satisfying the requirements of 10CFR72.

3.4.9 Design and Service Life

The discussion in the preceding sections seeks to provide the logical underpinnings for setting the design life of the storage overpacks, the HI-TRAC VW transfer cask, and the MPCs as sixty years. Design life, as stated earlier, is a lower bound value for the expected performance life of a component (service life). If operated and maintained in accordance with this Safety Analysis Report, Holtec International expects the service life of HI-STORM FW casks to substantially exceed their design life values.

Table 3.4.1

STRESS INTENSITY RESULTS FOR MPC ENCLOSURE VESSEL – NORMAL HANDLING

Item	Calculated Value (ksi)	Allowable Limit (ksi)	Safety Factor
Lid – Primary Membrane Stress Intensity	9.47	16.5	1.74
Lid – Local Membrane Plus Primary Bending Stress Intensity	15.19	24.75	1.63
Baseplate – Primary Membrane Stress Intensity	11.0	18.05	1.64
Baseplate – Local Membrane Plus Primary Bending Stress Intensity	26.27	27.1	1.03
Shell – Primary Membrane Stress Intensity	15.92	17.5	1.10
Shell – Local Membrane Plus Primary Bending Stress Intensity	23.07	26.3	1.14

Table 3.4.2

STRESS RESULTS FOR HI-TRAC VW – NORMAL HANDLING

Item	Calculated Value (ksi)	Allowable Limit (ksi)	Safety Factor
Top Flange-to-Inner/Outer Shell Weld – Primary Shear Stress	5.75	16.6	2.88
Inner/Outer Shell – Primary Membrane Stress	1.71	18.4	10.75
Bottom Lid Bolts – Tensile Stress	9.33	57.5	6.16
Bottom Lid Bolts – Shear Stress on Bolt Threads	5.22	23.8	4.56
Bottom Lid – Primary Bending Stress	3.81	29.4	7.71
Bottom Lid – Thread Shear Stress	3.81	12.4	3.25

Table 3.4.3

STRESS RESULTS FOR HI-STORM FW – NORMAL HANDLING[NOTE 1]

Item	Calculated Value (ksi)	Allowable Limit (ksi)	Safety Factor
Inner/Outer Shell – Primary Membrane Stress	1.92	20.0	10.4
Inner/Outer Shell – Primary Membrane Plus Bending Stress	3.42	30.0	8.77
Baseplate – Primary Membrane Stress	1.97	20.0	10.2
Baseplate – Primary Membrane Plus Bending Stress	3.42	30.0	8.77
Lifting Rib – Primary Membrane Stress	4.79	20.0	4.18
Lifting Rib – Primary Membrane Plus Bending Stress	6.22	30.0	4.82
Shell-to-Baseplate Weld – Primary Shear Stress	4.56	21.0	4.60

NOTE 1: For users of the HI-STORM FW Version XL with domed lid, a site specific evaluation shall be performed for cask lifting if the bounding weight in Table 3.2.8 is exceeded.

Table 3.4.4

STRESS RESULTS FOR HI-STORM FW LID – NORMAL HANDLING

Item	Calculated Value (ksi)	Allowable Limit (ksi)	Safety Factor
Maximum Primary Membrane Stress			
- Standard lid	1.57	16.6	10.6
- Version XL lid	3.435	20.0	5.822
Maximum Primary Membrane Plus Bending Stress			
- Standard lid	1.57	24.9	15.9
- Version XL lid	3.435	30.0	8.734

Table 3.4.4A

STRESS RESULTS FOR HI-STORM FW DOMED LID – NORMAL HANDLING

Item	Calculated Value (ksi)	Allowable Limit (ksi)	Safety Factor
Lift Lug Tearout	2.356	4.20	1.78
Lift Lug Tension	2.752	7.00	2.54
Maximum Primary Membrane Stress	7.626	19.80	2.6
Maximum Primary Membrane Plus Bending Stress	7.626	29.70	3.89
Lift Lug-to-Base Plate Weld	1.704	7.00	4.11

Table 3.4.5

CASK ROTATIONS DUE TO LARGE MISSILE IMPACT

Event	Calculated Value (deg)	Allowable Limit (deg)	Safety Factor
Missile Impact plus Tornado Wind on HI-STORM FW	3.83	30.3	7.91
Missile Impact plus Pressure Drop on HI-STORM FW	4.37	30.3	6.93
Missile Impact plus Tornado Wind on HI-TRAC VW	14.88	23.6	1.59
Missile Impact plus Pressure Drop on HI-TRAC VW	12.66	23.6	1.86

Table 3.4.6

MISSILE PENETRATION RESULTS –
SMALL AND INTERMEDIATE MISSILE

Missile Type – Impact Location	Calculated Value (in)	Allowable Limit (in)	Safety Factor
Small Missile – All Impact Locations	< 0.4 in	> 0.5 in (MPC shell thickness)[†]	> 1.25
Intermediate Missile – Side Strike on HI-STORM FW Outer Shell (away from Inlet)	8.39	29.00	3.46
Intermediate Missile – Side Strike on HI-STORM FW Outer Shell (at Inlet)	11.69	24.00	2.05
Intermediate Missile – End Strike on HI-STORM FW Lid - Standard version - XL version - Domed lid version	 10.46 10.18 10.46*	 19.25 10.75 18.00	 1.84 1.06 1.72
Intermediate Missile – Side Strike on HI-TRAC VW Outer Shell	0.50	1.50	3.00
Intermediate Missile – End Strike on MPC Closure Lid	0.23	9.00	39.13

* The reported value is conservative because it assumes the same thickness as the standard lid cover plate.

[†] In reality, a maximum velocity impact between the small projectile missile and the MPC shell is not credible due to the geometry of the HI-STORM FW inlet and outlet vents (i.e., no direct line of sight).

Table 3.4.7

STRESS INTENSITY RESULTS FOR MPC ENCLOSURE VESSEL – DESIGN INTERNAL PRESSURE

Item	Calculated Value (ksi)	Allowable Limit (ksi)	Safety Factor
Lid – Primary Membrane Stress Intensity	6.42	16.5	2.57
Lid – Local Membrane Plus Primary Bending Stress Intensity	14.26	24.75	1.74
Baseplate – Primary Membrane Stress Intensity	9.0	18.6	2.07
Baseplate – Local Membrane Plus Primary Bending Stress Intensity	21.97	27.9	1.27
Shell – Primary Membrane Stress Intensity	13.76	16.5	1.20
Shell – Local Membrane Plus Primary Bending Stress Intensity	19.84	24.75	1.25

Table 3.4.7A

STRESS INTENSITY RESULTS FOR MPC ENCLOSURE VESSEL – SHORT-TERM NORMAL INTERNAL PRESSURE

Item	Calculated Value (ksi)	Allowable Limit (ksi)	Safety Factor
Lid – Primary Membrane Stress Intensity	13.10	18.05	1.38
Lid – Local Membrane Plus Primary Bending Stress Intensity	21.56	27.1	1.26
Baseplate – Primary Membrane Stress Intensity	12.40	18.95	1.53
Baseplate – Local Membrane Plus Primary Bending Stress Intensity	28.25	28.425	1.01
Shell – Primary Membrane Stress Intensity	14.07	18.05	1.28
Shell – Local Membrane Plus Primary Bending Stress Intensity	23.12	27.1	1.17
Shell – Local Membrane Plus Primary Bending Plus Secondary Stress Intensity	49.81	56.85	1.14

Table 3.4.7B

STRESS INTENSITY RESULTS FOR MPC ENCLOSURE VESSEL – OFF-NORMAL INTERNAL PRESSURE

Item	Calculated Value (ksi)	Allowable Limit (ksi)	Safety Factor
Lid – Primary Membrane Stress Intensity	12.10	18.15	1.50
Lid – Local Membrane Plus Primary Bending Stress Intensity	16.45	27.225	1.66
Baseplate – Primary Membrane Stress Intensity	9.69	19.25	1.99
Baseplate – Local Membrane Plus Primary Bending Stress Intensity	26.15	28.93	1.11
Shell – Primary Membrane Stress Intensity	15.93	19.25	1.21
Shell – Local Membrane Plus Primary Bending Stress Intensity	26.00	28.93	1.11
Shell – Local Membrane Plus Primary Bending Plus Secondary Stress Intensity	48.92	54.15	1.11

Table 3.4.8

STRESS INTENSITY RESULTS FOR MPC ENCLOSURE VESSEL – ACCIDENT INTERNAL PRESSURE

Item	Calculated Value (ksi)	Allowable Limit (ksi)	Safety Factor
Lid – Primary Membrane Stress Intensity	10.69	35.5	3.32
Lid – Local Membrane Plus Primary Bending Stress Intensity	13.60	53.25	3.92
Baseplate – Primary Membrane Stress Intensity	16.0	35.5	2.20
Baseplate – Local Membrane Plus Primary Bending Stress Intensity	36.61	53.25	1.45
Shell – Primary Membrane Stress Intensity	22.93	35.	1.55

Table 3.4.9

STRESS RESULTS FOR HI-TRAC VW WATER JACKET – ACCIDENT INTERNAL PRESSURE

Item	Calculated Value (ksi)	Allowable Limit (ksi)	Safety Factor
Bottom Flange – Primary Membrane Plus Bending Stress	5.10	55.8	10.95
Water Jacket Shell – Primary Membrane Plus Bending Stress	7.99	55.8	6.98
Water Jacket Rib – Primary Membrane Stress	4.73	37.2	7.86
Water Jacket Shell-to-Bottom Flange Weld – Primary Shear Stress	3.70	29.4	7.94

Table 3.4.10

STRESS RESULTS FOR HI-STORM FW LID – SNOW LOAD

Item	Calculated Value (ksi)	Allowable Limit (ksi)	Safety Factor
Maximum Primary Membrane Stress - Standard Lid - Version XL Lid (bounds Domed lid)	1.81 4.851	16.6 20.0	9.16 4.123
Maximum Primary Membrane Plus Bending Stress - Standard Lid - Version XL Lid (bounds domed lid)	1.81 4.851	24.9 30.0	13.7 6.184

Table 3.4.11

INPUT DATA USED FOR CALCULATING ANGULAR VELOCITY OF OVERPACK DURING NON-MECHANISTIC TIPOVER (LOAD CASE 4)

Item	Value
Maximum weight of loaded HI-STORM FW (W)	426,300 lbf[†]
Mid-height of maximum length HI-STORM FW (h)	119.75 in
Outer diameter of HI-STORM FW (d)	140 in
Distance between cask pivot point and cask center (r)	138.709 in
Mass moment of inertia of loaded HI-STORM FW about cask pivot point (I_A)	1.076×10^{10} lb-in^2

[†] Bounds value in Table 3.2.8.

Table 3.4.12

INPUT VALUES USED FOR CALCULATING STRESS IN WATER JACKET SHELL (LOAD CASE 8)

Item	Value
Mean radius of water jacket shell (R)	47.375 in
Thickness of water jacket shell (d)	0.5 in
Width of beam strip (b)	1 in
Extreme fiber distance of beam cross-section (c)	0.25 in
Unsupported span of water jacket shell (θ)	45 deg
Distributed load on water jacket shell (w)	-75 lbf/in[†]
Span of distributed load on water jacket shell (ϕ)	45 deg

Note: Variables are defined in Figure 3.4.35.

[†] Bounds accident internal pressure in Table 2.2.1 for HI-TRAC water jacket.

Table 3.4.13

Intentionally Deleted

Table 3.4.14

KEY INPUT DATA FOR FUEL ROD INTEGRITY ANALYSIS DURING MPC REFLOOD EVENT (LOAD CASE 11)

Item	Input Value	Source
Cladding Thickness (for reference PWR fuel), in	0.022	SAR Tables 1.0.4 and 2.1.2
Cladding OD (for reference PWR fuel), in	0.377	SAR Tables 1.0.4 and 2.1.2
Fuel Rod Pressure, psi	2,000	Ref. [3.4.24] (upper bound value)
Yield Strength of Zircaloy, psi	100,000 (at 80°F) 50,500 (at 750°F)	Ref. [3.4.21]
Tensile Strength of Zircaloy, psi	112,100 (at 80°F) 68,200 (at 750°F)	Ref. [3.4.21]
Elastic Modulus of Zircaloy, $\times 10^6$ psi	13.42 (at 80°F) 10.4 (at 750°F)	Ref. [3.4.21]
Coefficient of Thermal Expansion of Zircaloy, $\times 10^{-6}$ in/in/°F	3.3 (at 80°F) 4.5 (at 750°F)	Ref. [3.4.22]
Poisson's Ratio of Zircaloy	0.4	Appendix C of Ref. [3.4.23]

Table 3.4.15 MAXIMUM RESULTS FOR FUEL ROD INTEGRITY ANALYSIS DURING MPC REFLOOD EVENT (LOAD CASE 11)	
Result	Value
Maximum Stress in Fuel Rod Cladding	29,995 psi
Maximum Strain in Fuel Rod Cladding	2.66×10^{-3}

Table 3.4.16

CASK SLIDING DISPLACEMENTS DUE LARGE MISSILE IMPACT (LOAD CASE 3)

Cask	Calculated Sliding Displacement (ft)	Allowable Sliding Displacement (ft)	Safety Factor
HI-STORM FW	0.454	3.33 (cask to cask) 6.2 (cask to edge of ISFSI pad)	7.33 13.6
HI-TRAC VW	1.133	None Established	-

Table 3.4.17

STRESS RESULTS FOR HI-TRAC VW VERSION P LIFTING TRUNNIONS

Item	Calculated Value (ksi)	Allowable Limit (ksi)	Safety Factor
Bending Stress in Trunnion	8.465	14.0	1.65
Shear Stress in Trunnion	6.534	8.4	1.29
Bearing Stress in Top Flange	32.55	33.2	1.02*

Note*- the marginal safety factor is based on a conservative bounding weight of 270,000 pounds. The actual weight is expected to be much less and therefore it is acceptable.

Table 3.4.18

STRESS RESULTS FOR HI-TRAC VW VERSION P – NORMAL HANDLING

Item	Calculated Value (ksi)	Allowable Limit (ksi)	Safety Factor
Bottom Lid Bolts – Tensile Stress	12.07	57.5	4.76
Bottom Lid Bolts – Shear Stress on Bolt Threads	4.35	23.8	5.46
Bottom Lid Bolts – Shear Stress on Bolt	12.9	23.8	1.84
Bottom Lid – Internal Thread Shear Stress	3.12	13.2	4.23

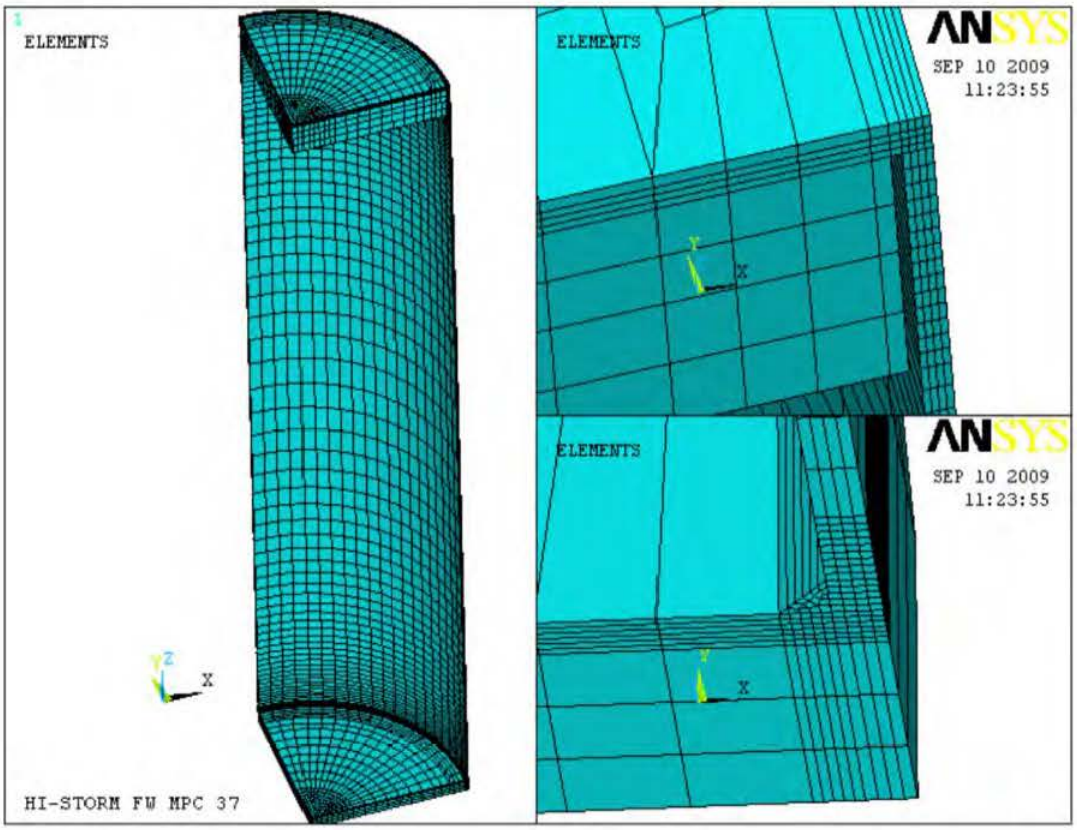

Figure 3.4.1: ANSYS Model of MPC Enclosure Vessel – Normal Handling

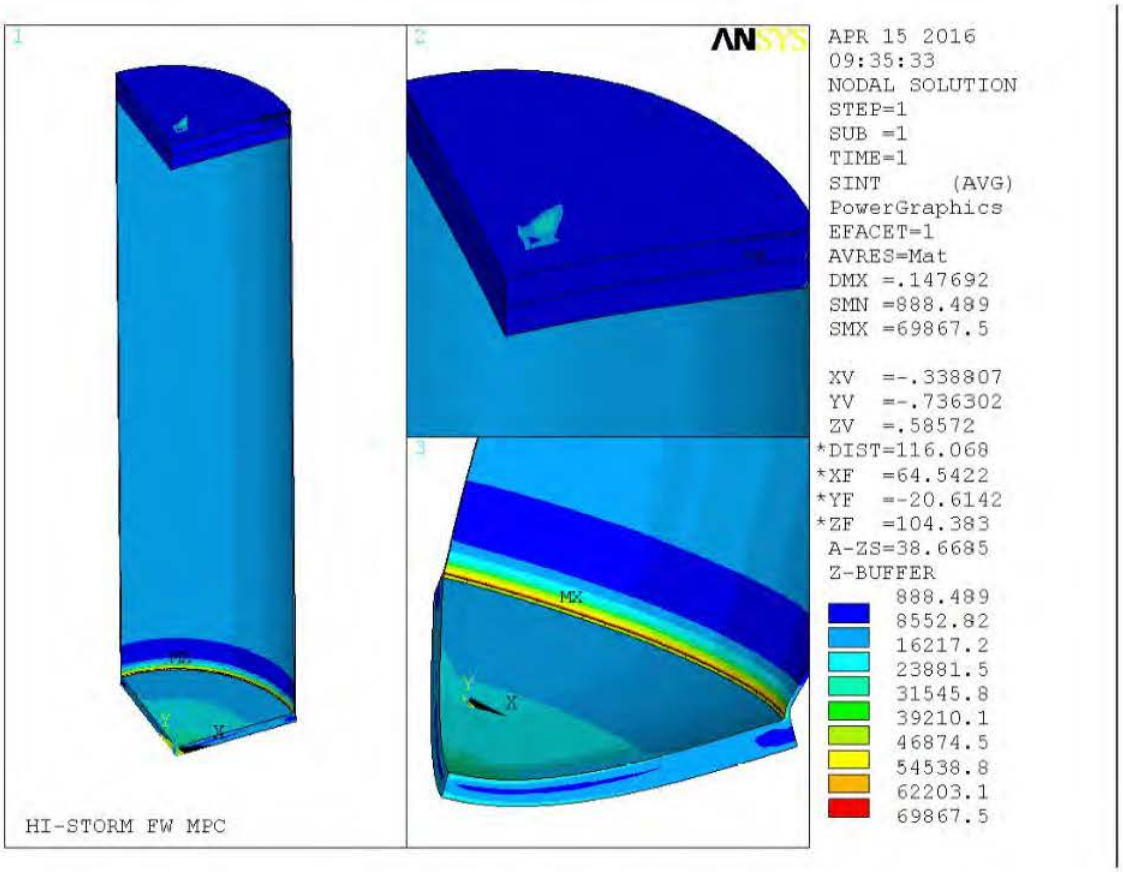

Figure 3.4.2: Stress Intensity Distribution in MPC Enclosure Vessel – Normal Handling

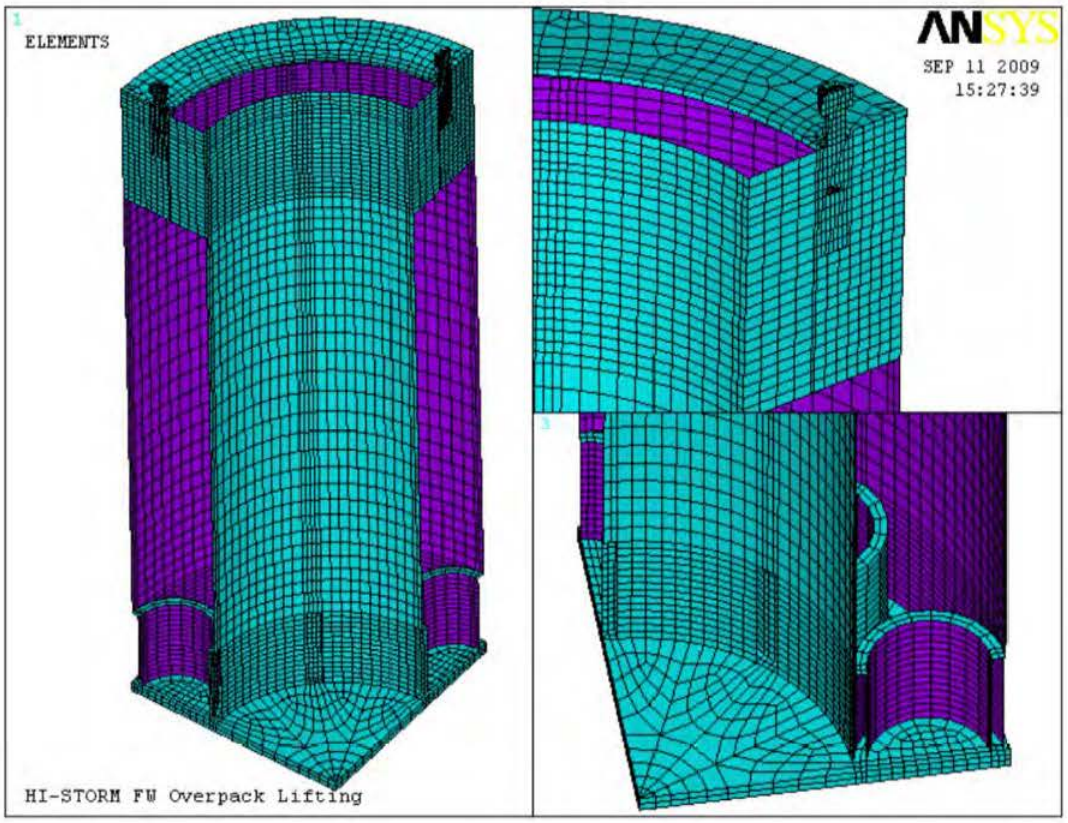

Figure 3.4.3: ANSYS Model of HI-STORM FW Overpack – Normal Handling

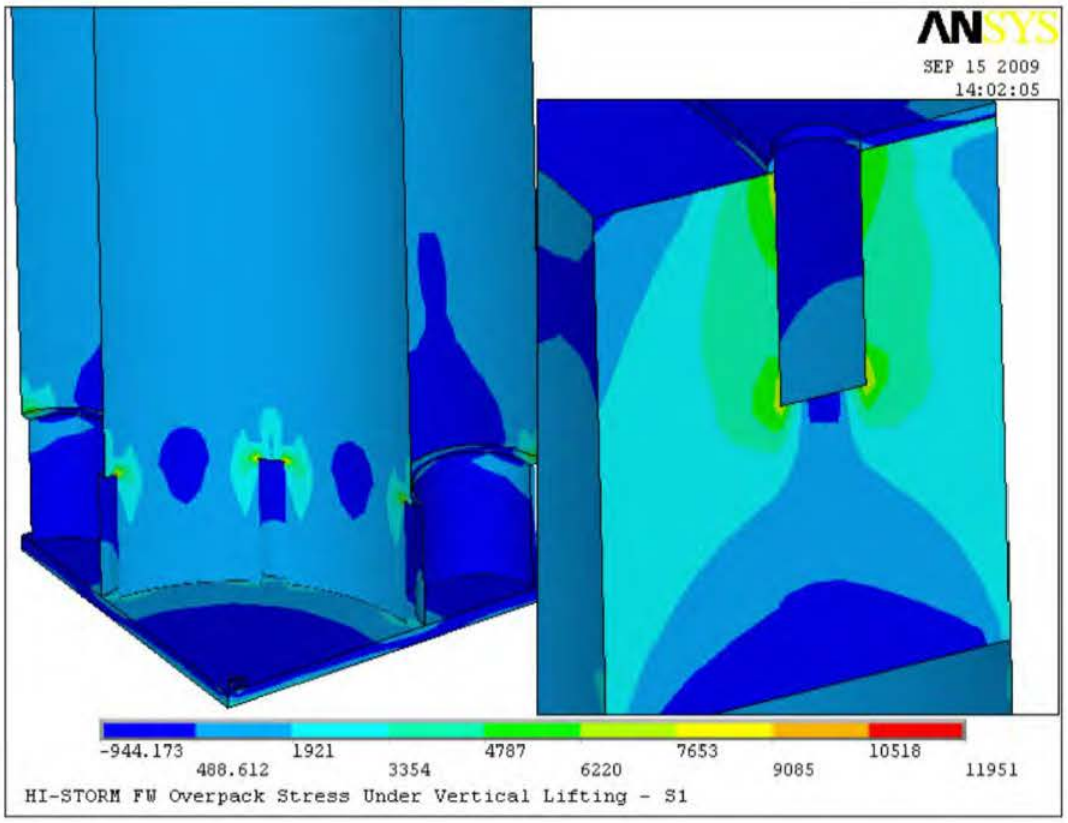

Figure 3.4.4: Stress Distribution in HI-STORM FW Overpack – Normal Handling

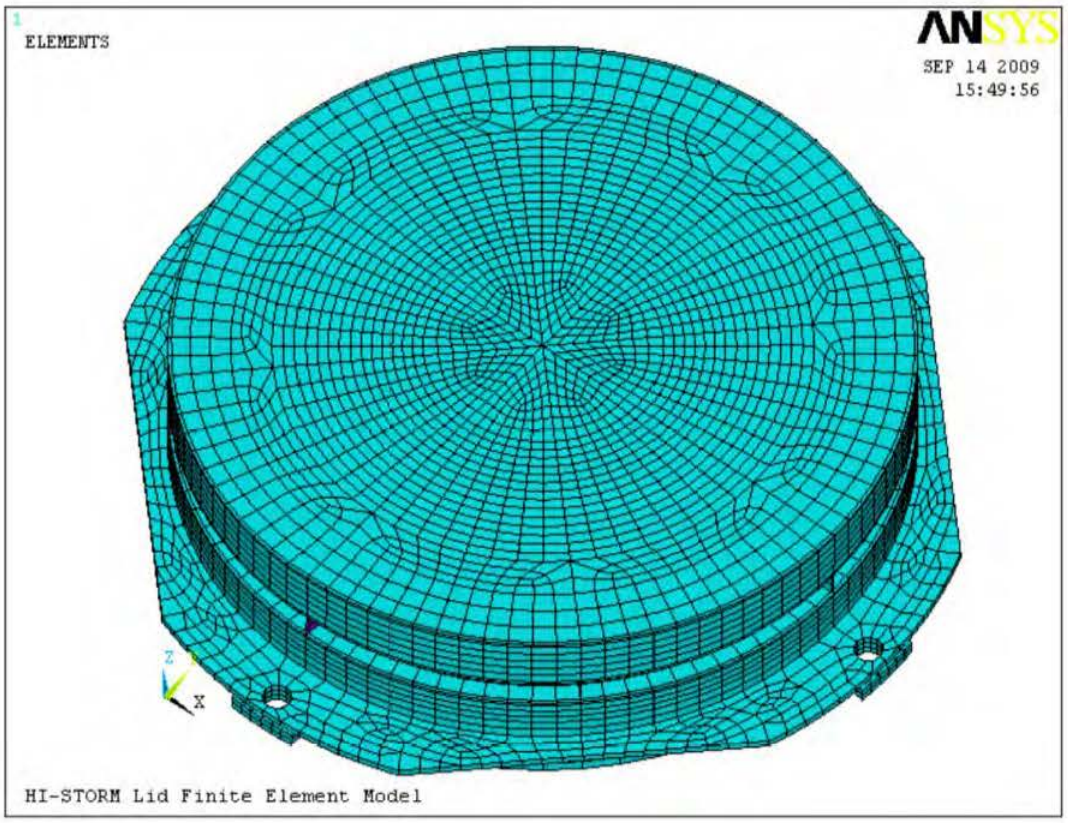

Figure 3.4.5A: ANSYS Model of HI-STORM FW Lid – Normal Handling

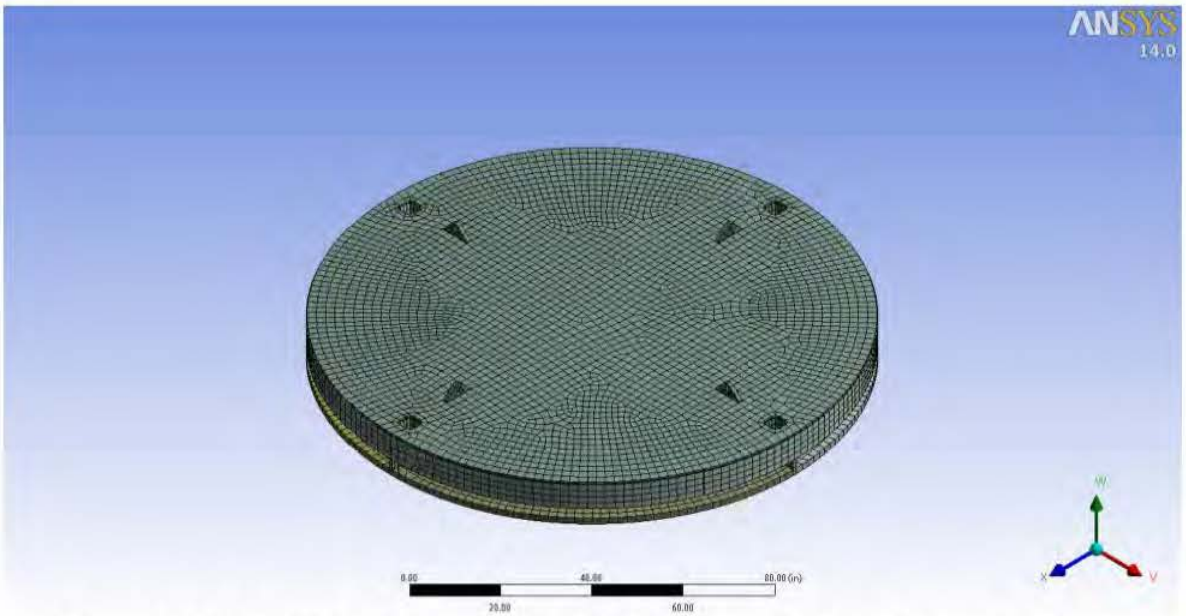

Figure 3.4.5B: ANSYS Model of HI-STORM FW Version XL Lid – Normal Handling

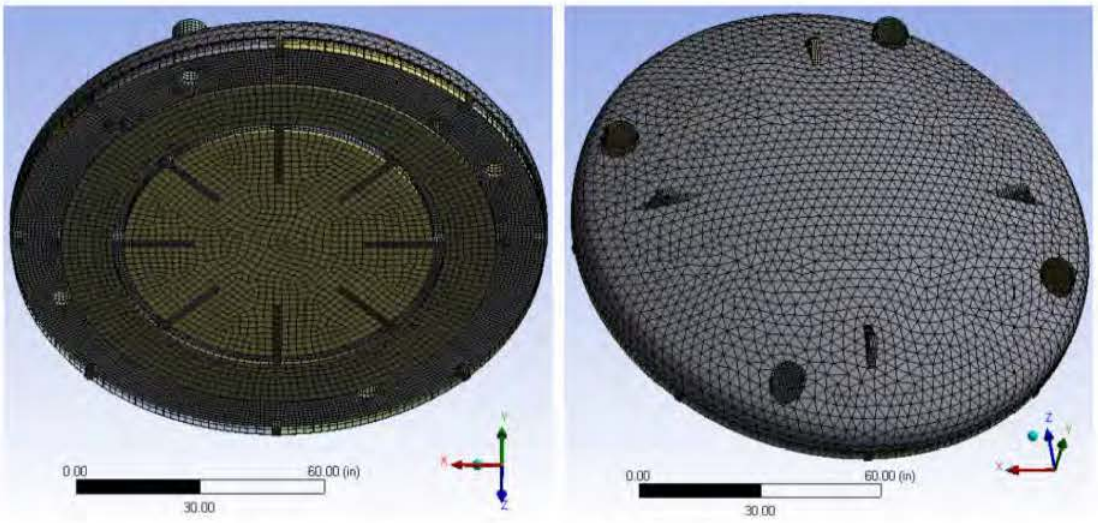

Figure 3.4.5C: ANSYS Model of HI-STORM FW Domed Lid – Normal Handling

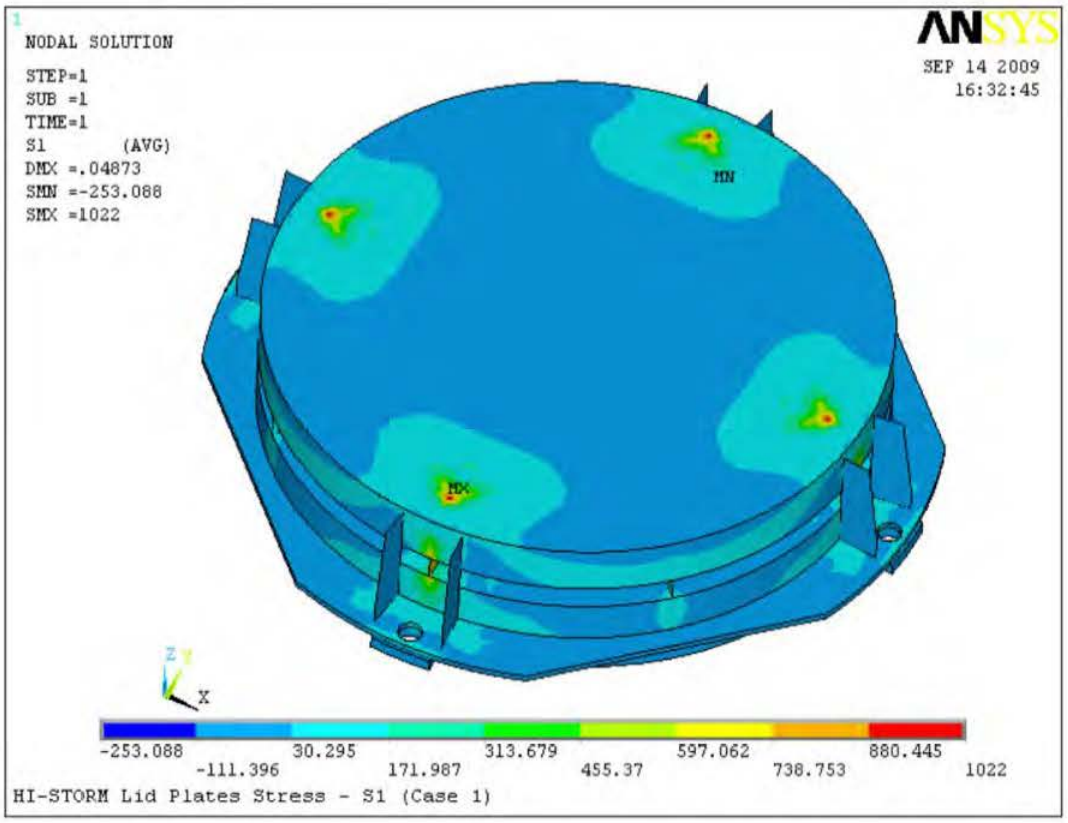

Figure 3.4.6A: Stress Distribution in HI-STORM FW Lid – Normal Handling

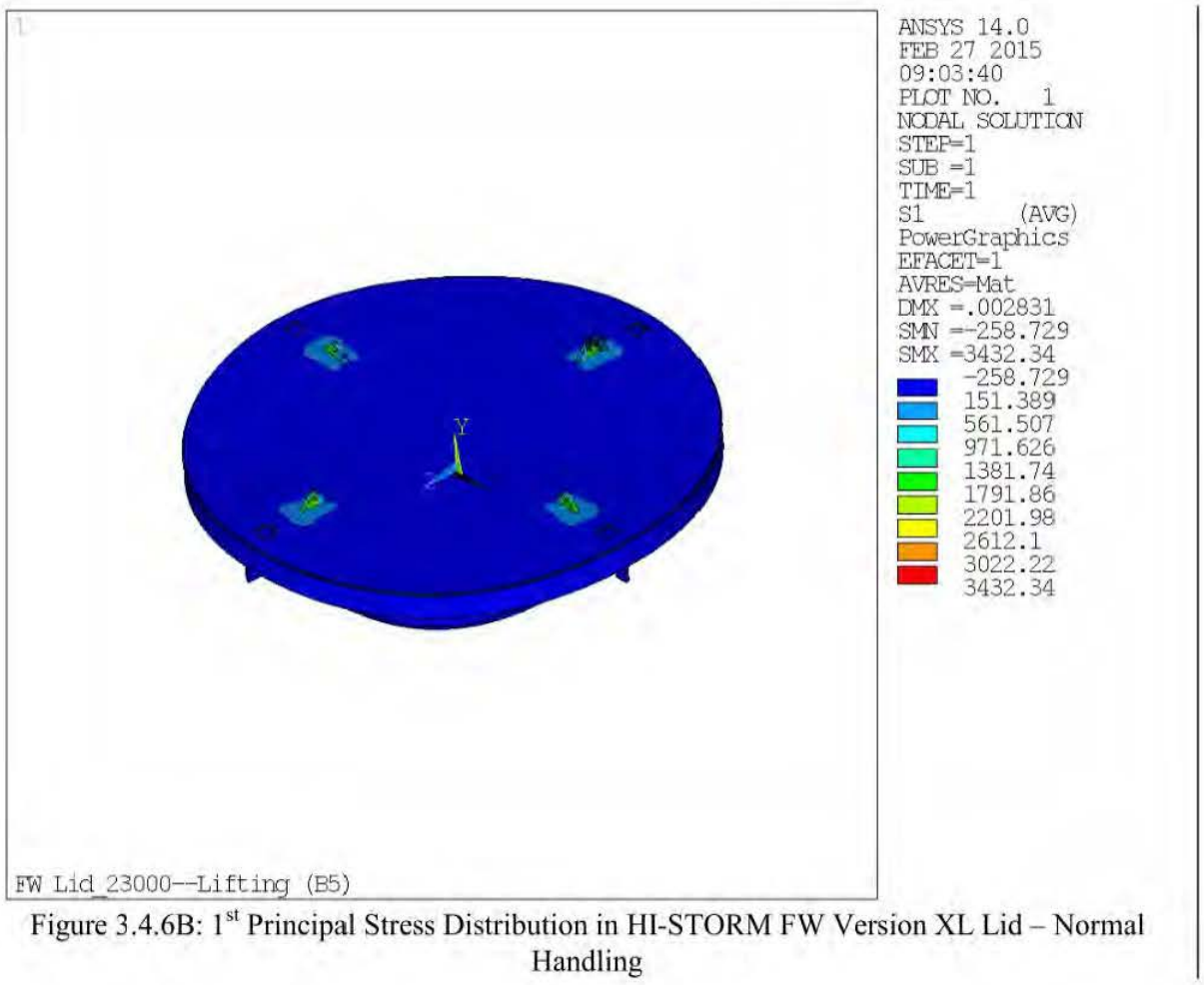

Figure 3.4.6B: 1st Principal Stress Distribution in HI-STORM FW Version XL Lid – Normal Handling

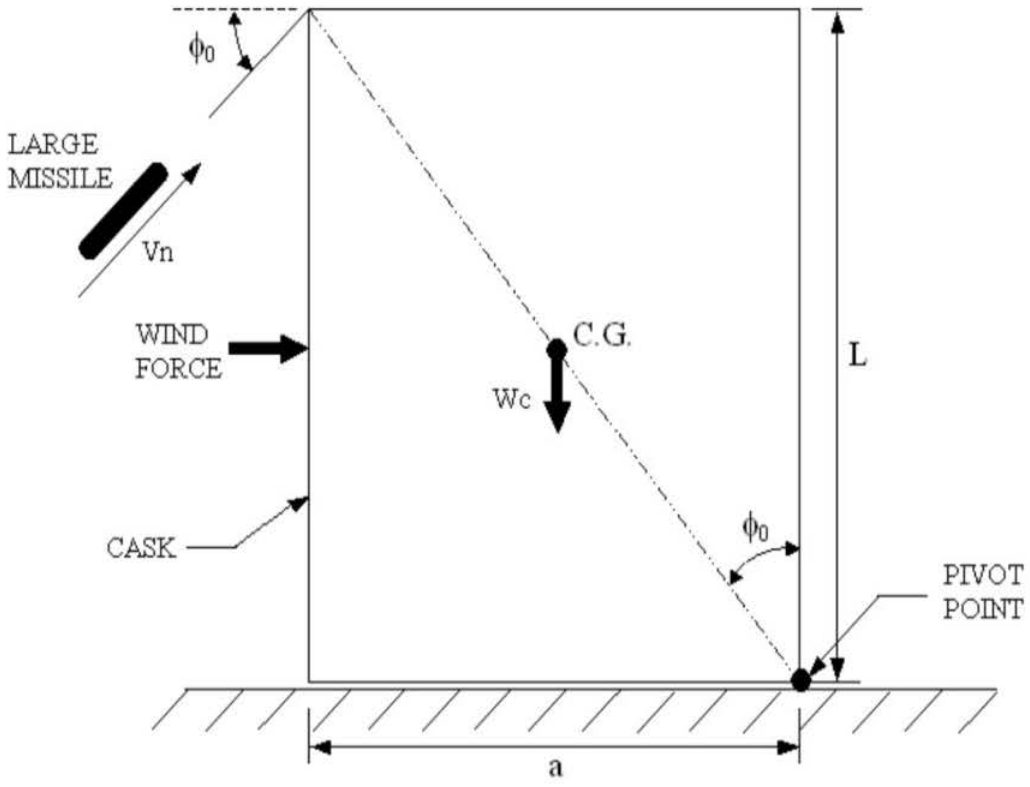

Figure 3.4.7: Free Body Diagram of Cask for Large Missile Strike/Tornado Event

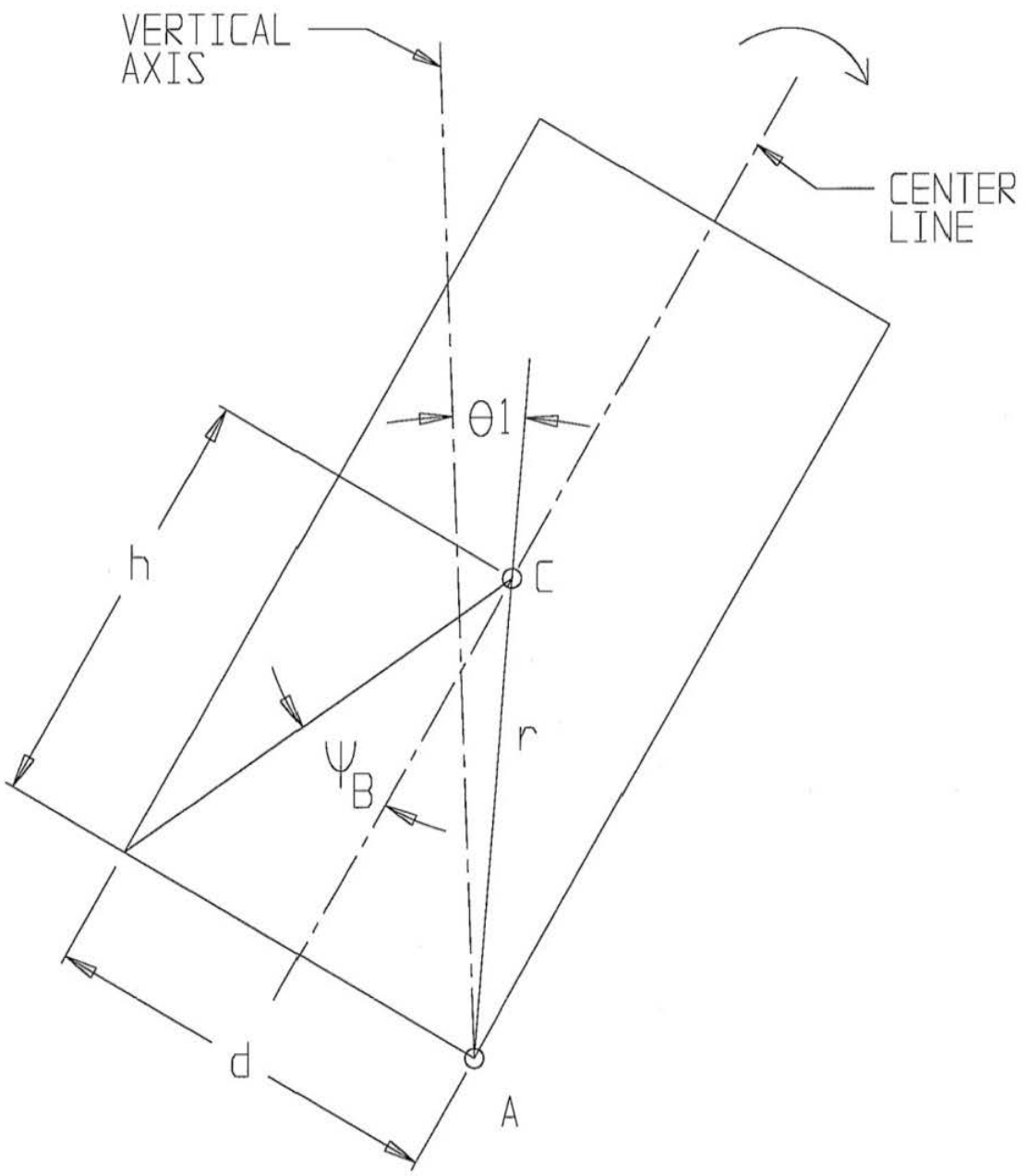

Figure 3.4.8: Cask Configuration at Incipient Tipping

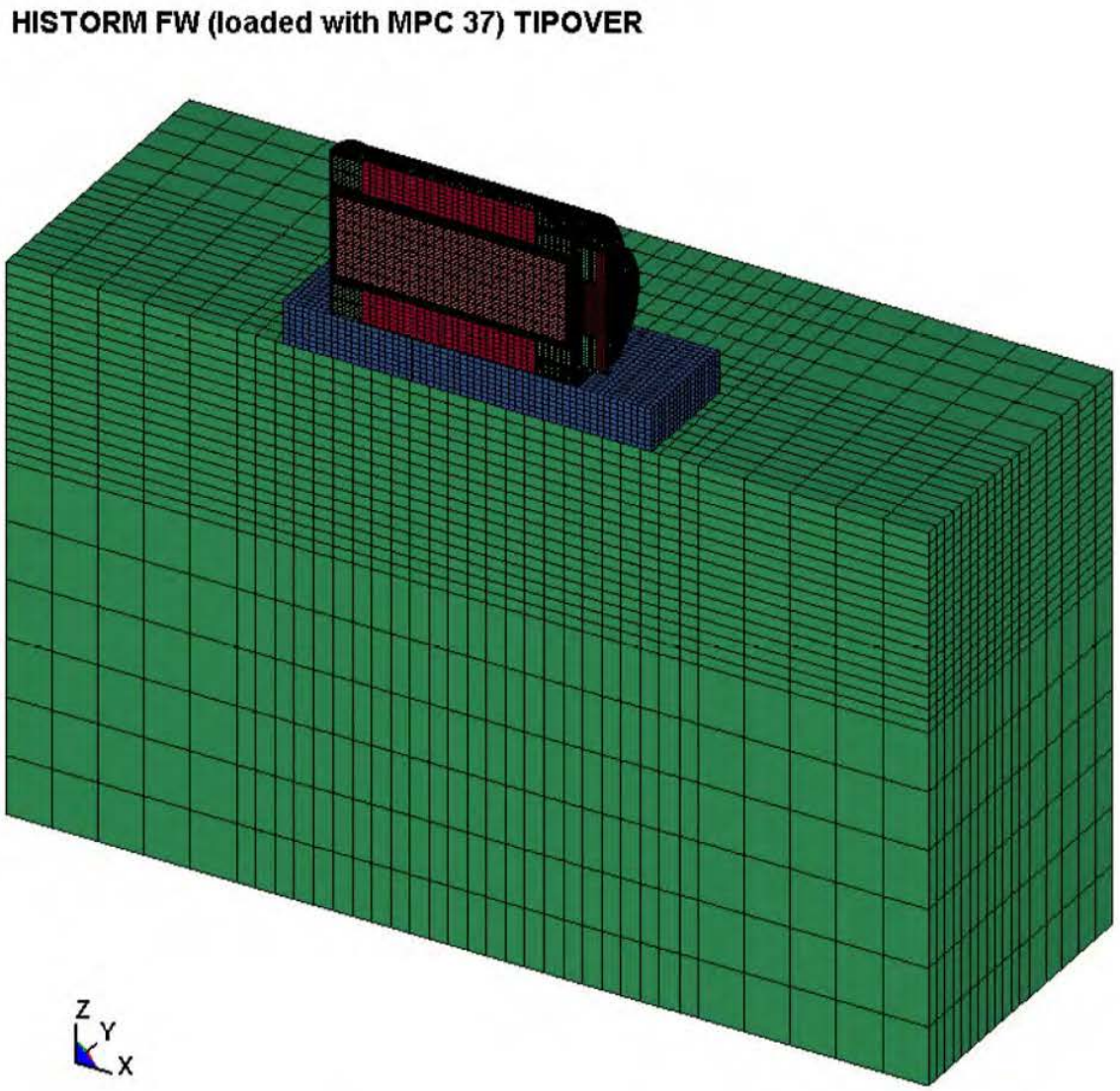

Figure 3.4.9A: LS-DYNA Tipover Model – HI-STORM FW Loaded with MPC-37

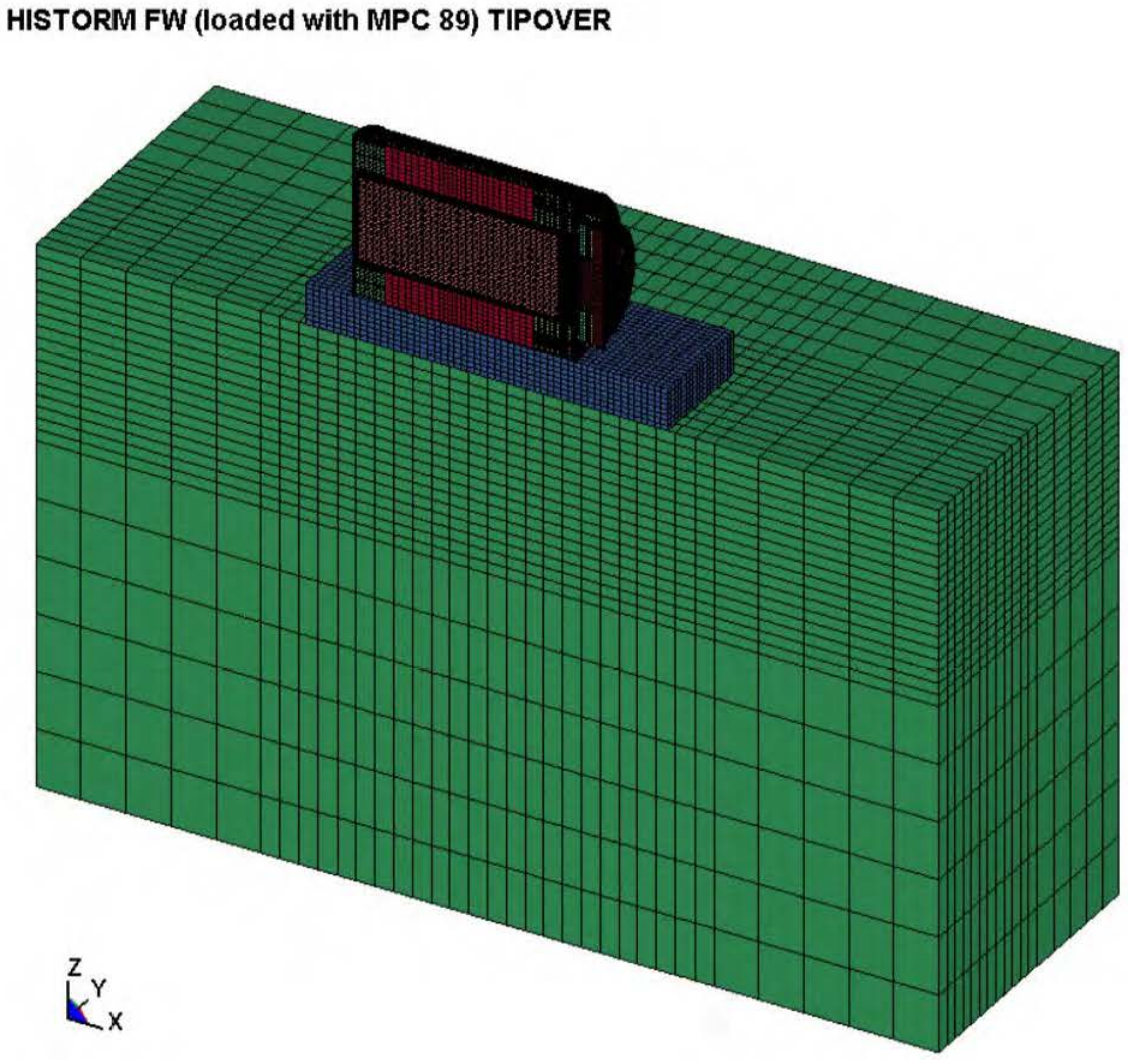

Figure 3.4.9B: LS-DYNA Tipover Model – HI-STORM FW Loaded with MPC-89

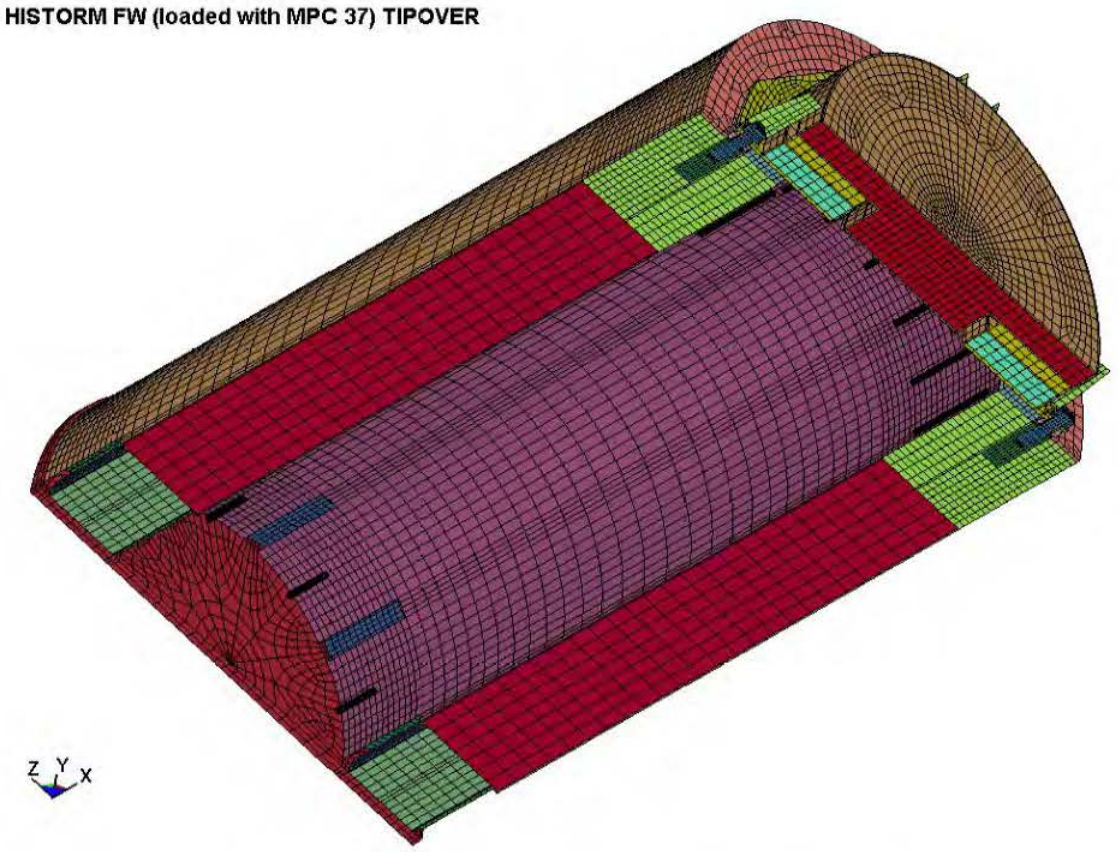

Figure 3.4.10A: LS-DYNA Model – HI-STORM FW for MPC-37

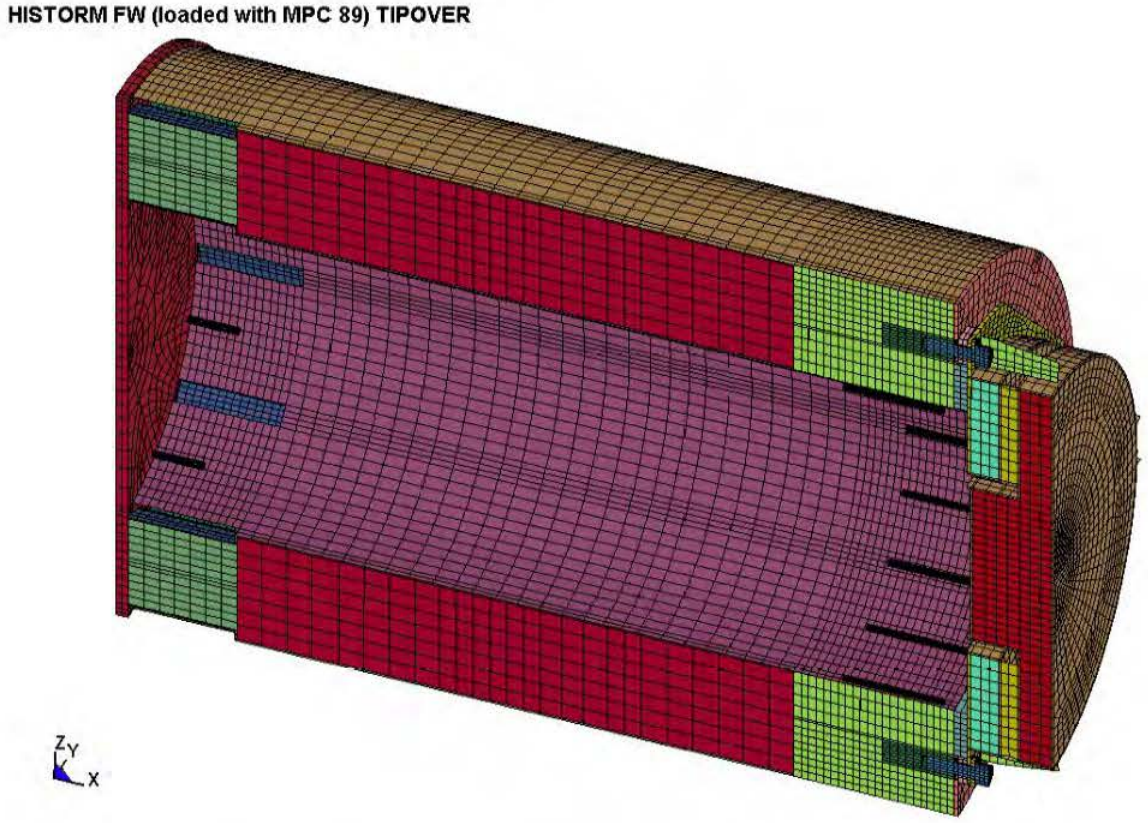

Figure 3.4.10B: LS-DYNA Model – HI-STORM FW for MPC-89

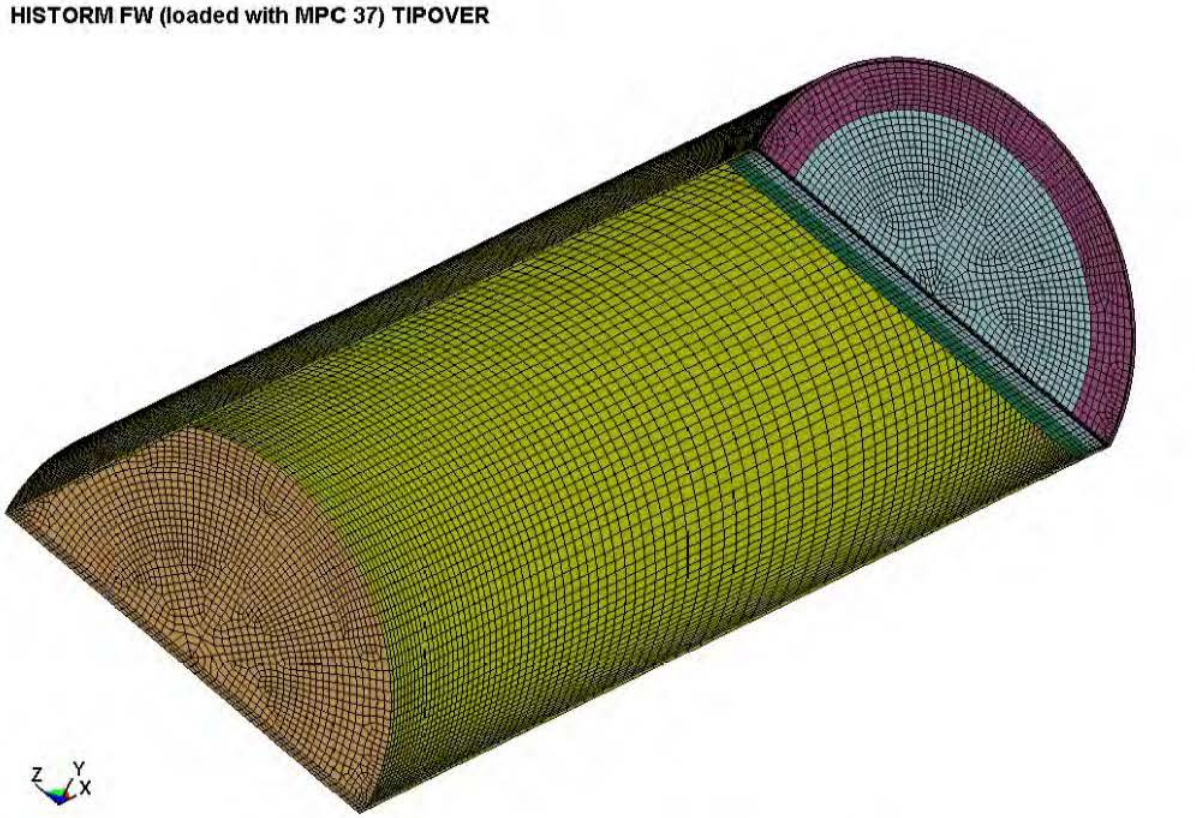

Figure 3.4.11A: LS-DYNA Model – MPC-37 Enclosure Vessel

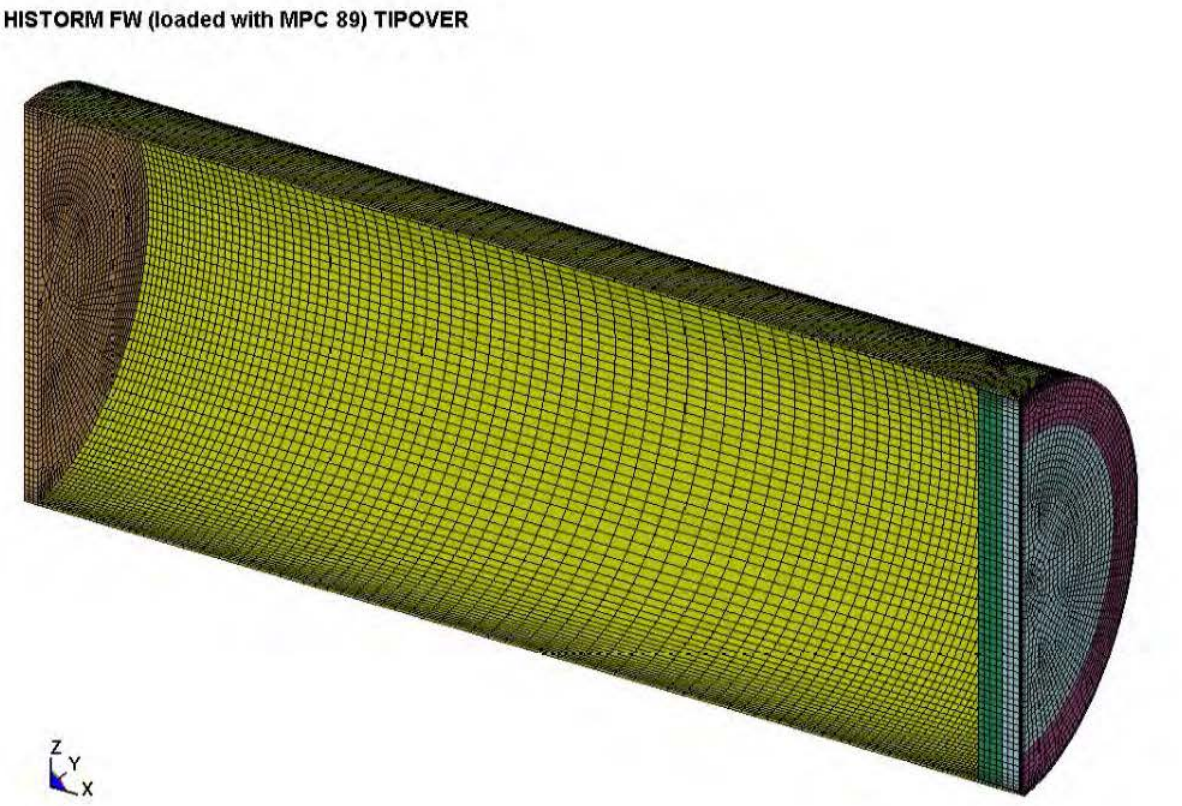

Figure 3.4.11B: LS-DYNA Model – MPC-89 Enclosure Vessel

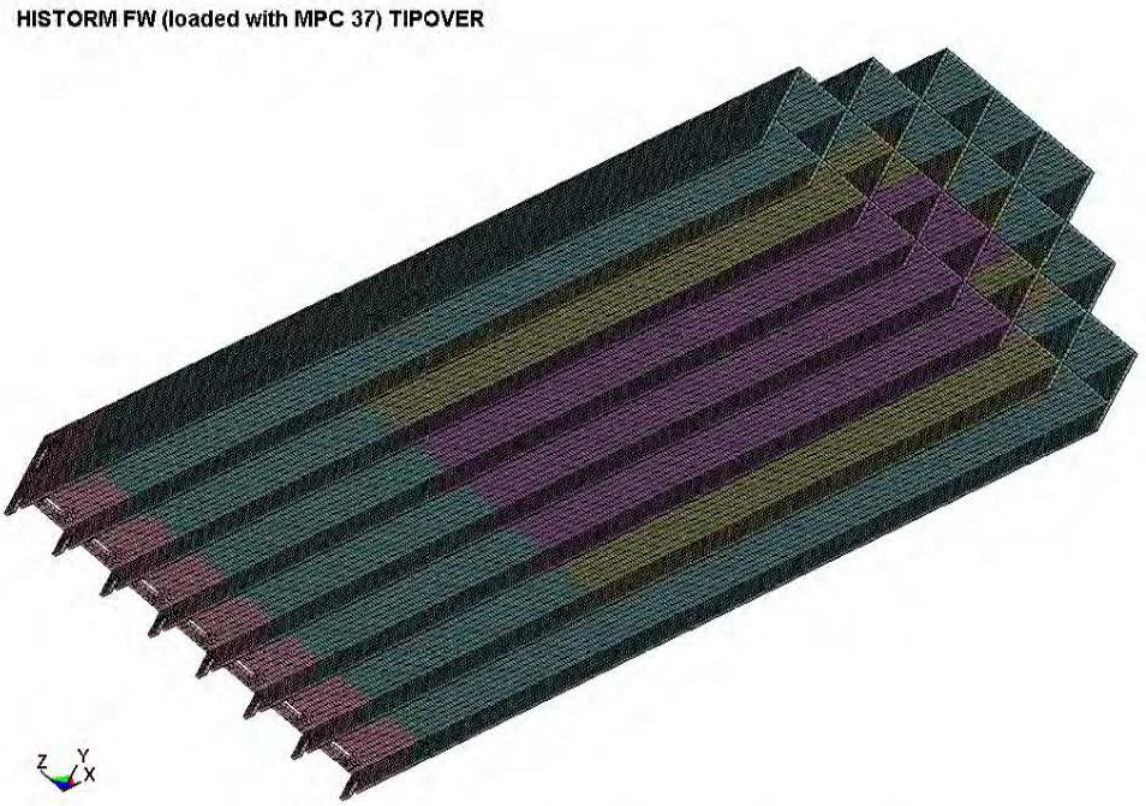

Figure 3.4.12A: LS-DYNA Model – MPC-37 Fuel Basket
(note: the different colors represent regions with bounding temperatures of 340°C, 325°C, 300°C and 250°C, respectively)

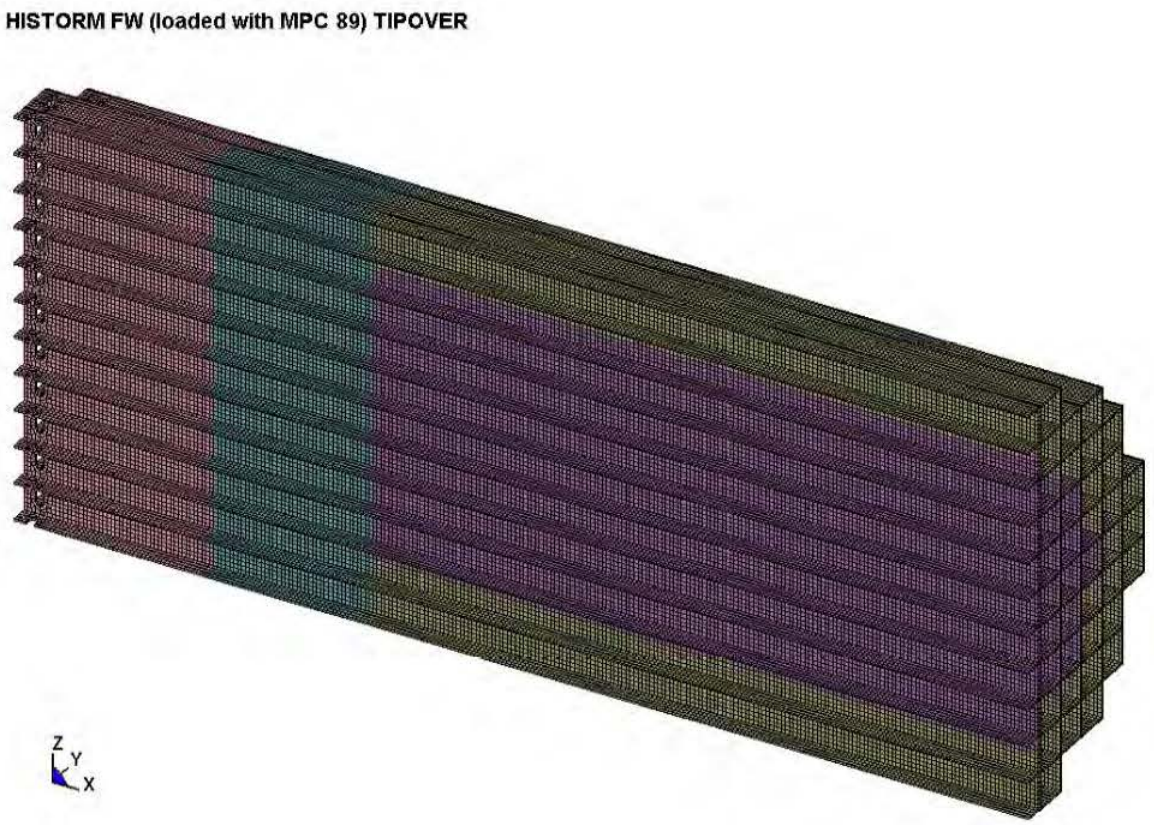

Figure 3.4.12B: LS-DYNA Model – MPC-89 Fuel Basket
(note: the different colors represent regions with bounding temperatures of 325°C, 300°C, 250°C and 200°C, respectively)

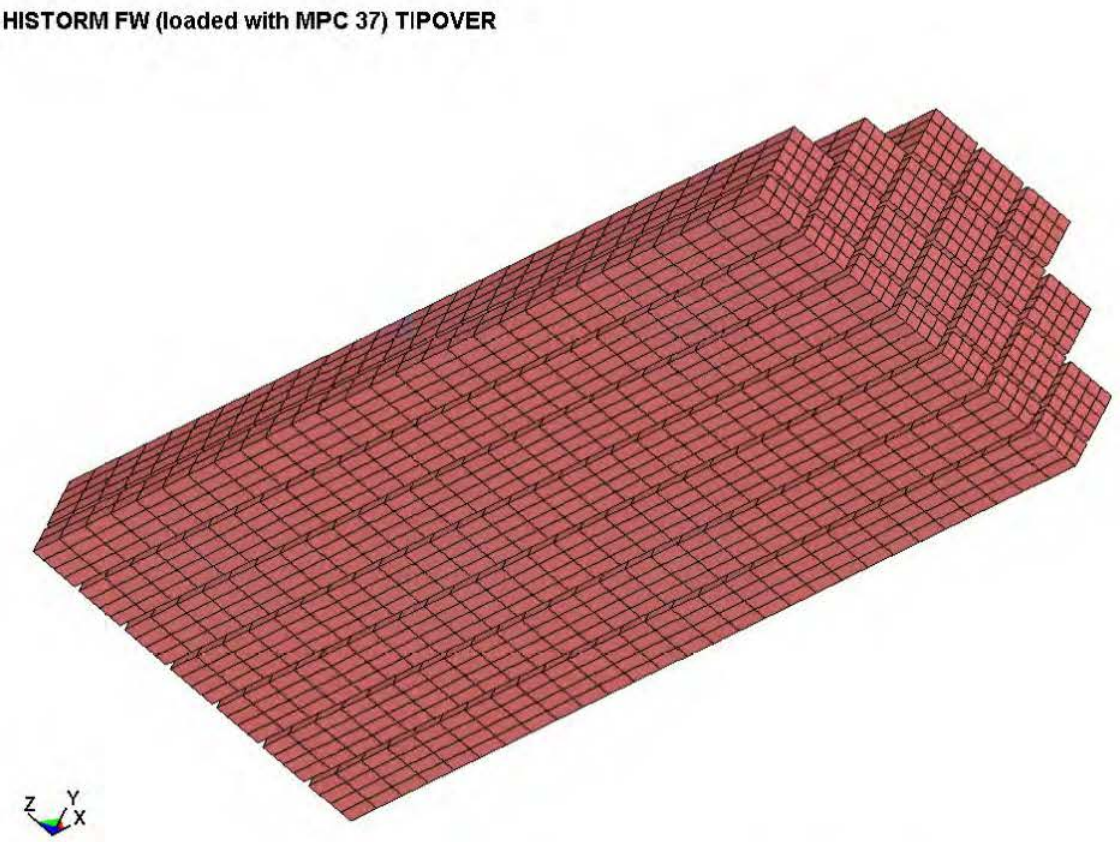

Figure 3.4.13A: LS-DYNA Model – PWR Fuel Assemblies

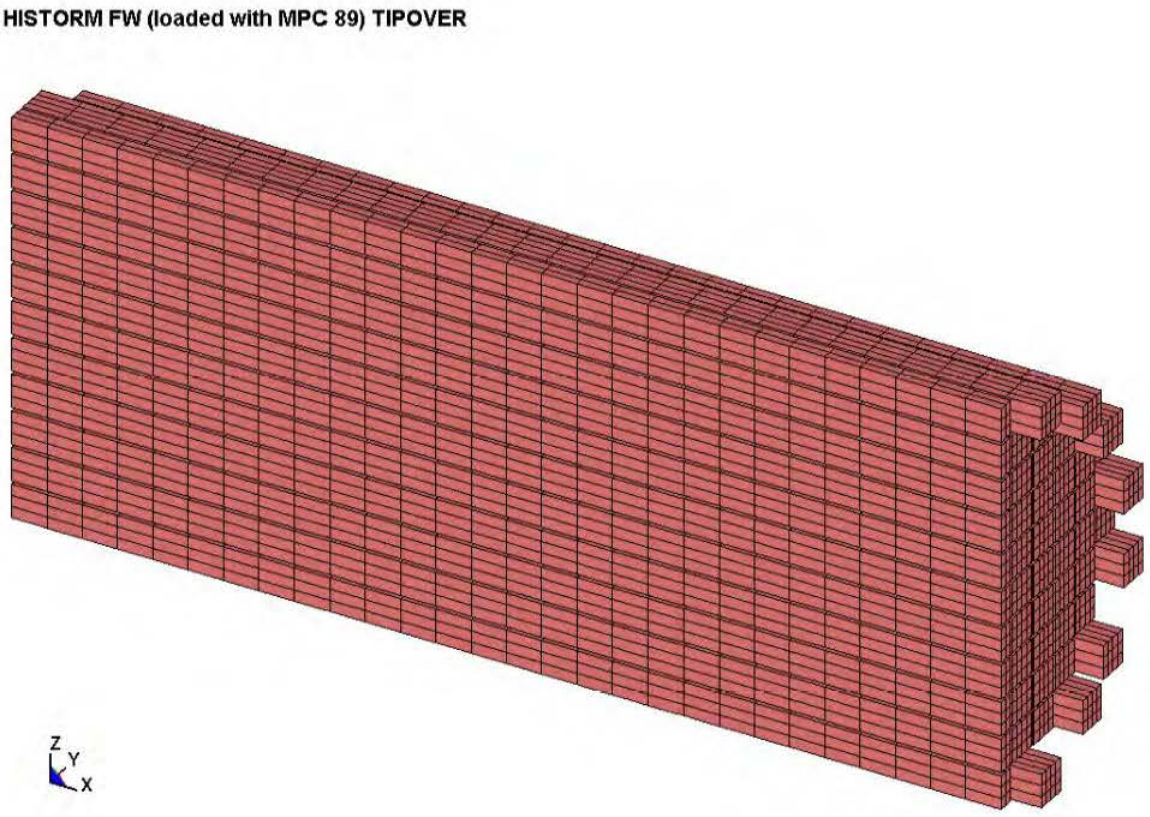

Figure 3.4.13B: LS-DYNA Model – BWR Fuel Assemblies & Damaged Fuel Containers

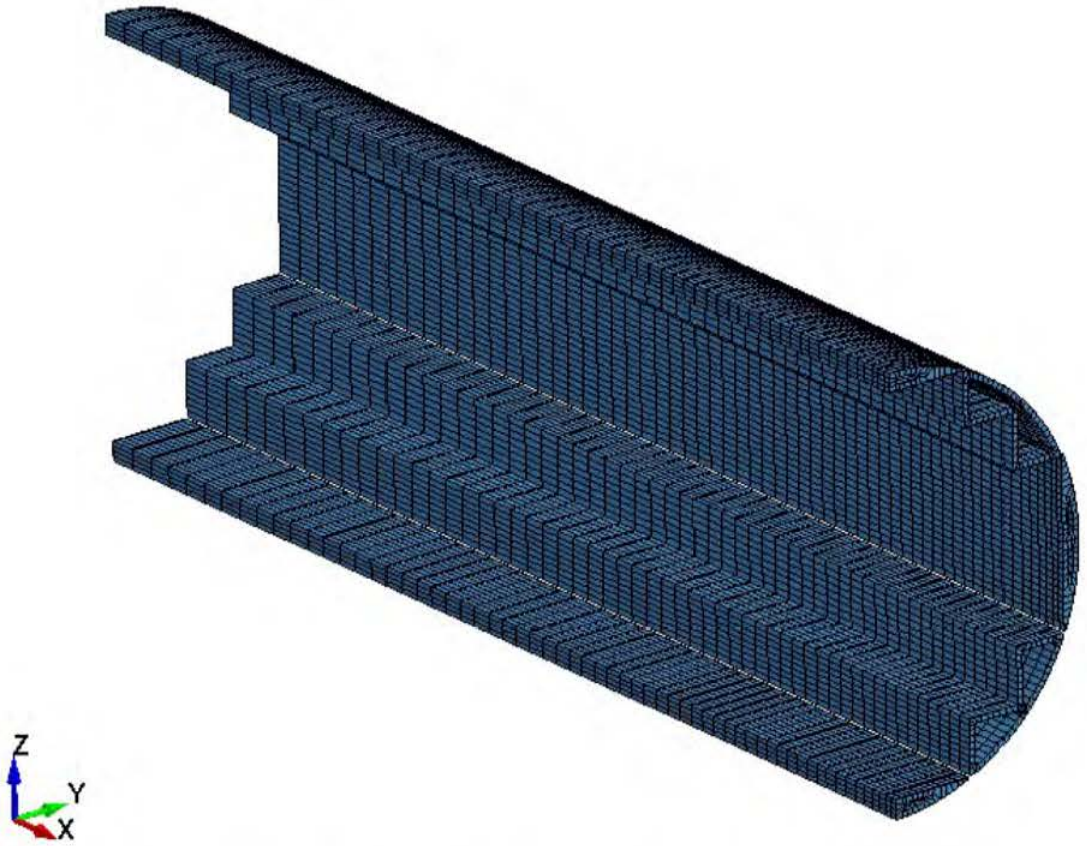

Figure 3.4.14A: LS-DYNA Model – MPC-37 Fuel Basket Shims

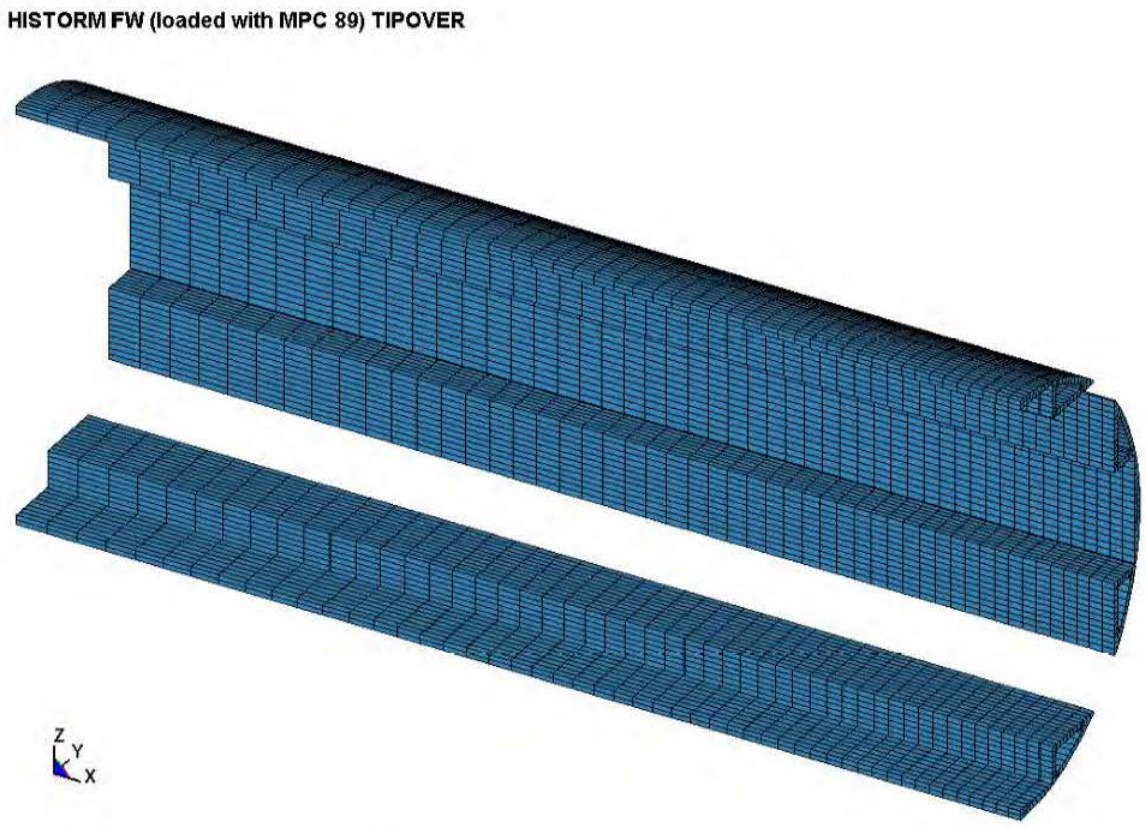

Figure 3.4.14B: LS-DYNA Model – MPC-89 Fuel Basket Shims

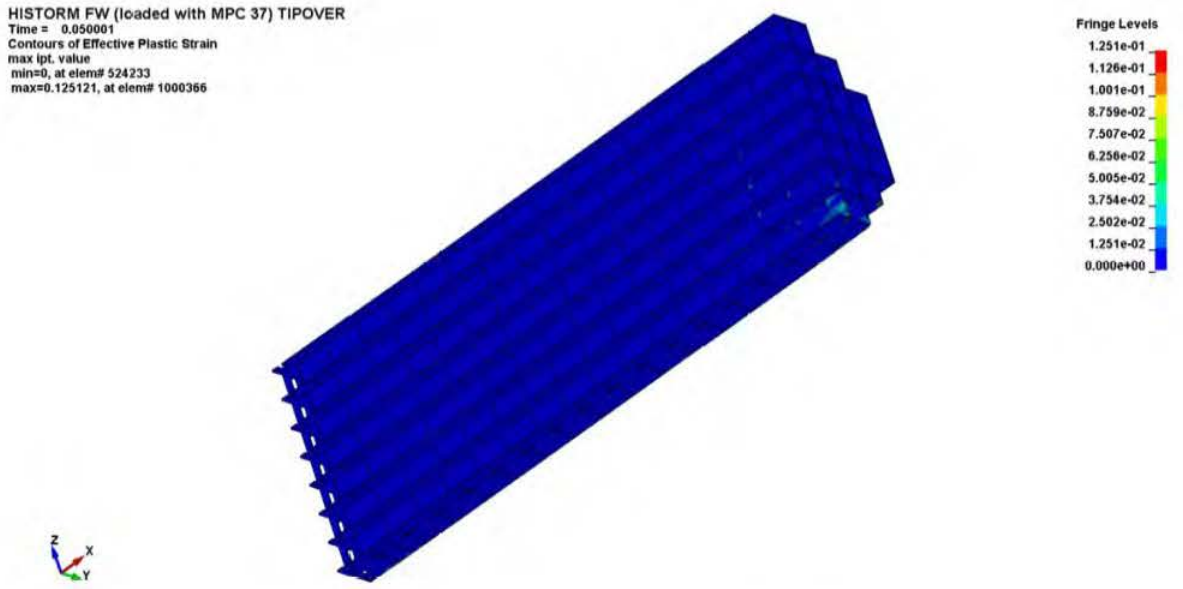

Figure 3.4.15A: Maximum Plastic Strain – MPC-37 Fuel Basket

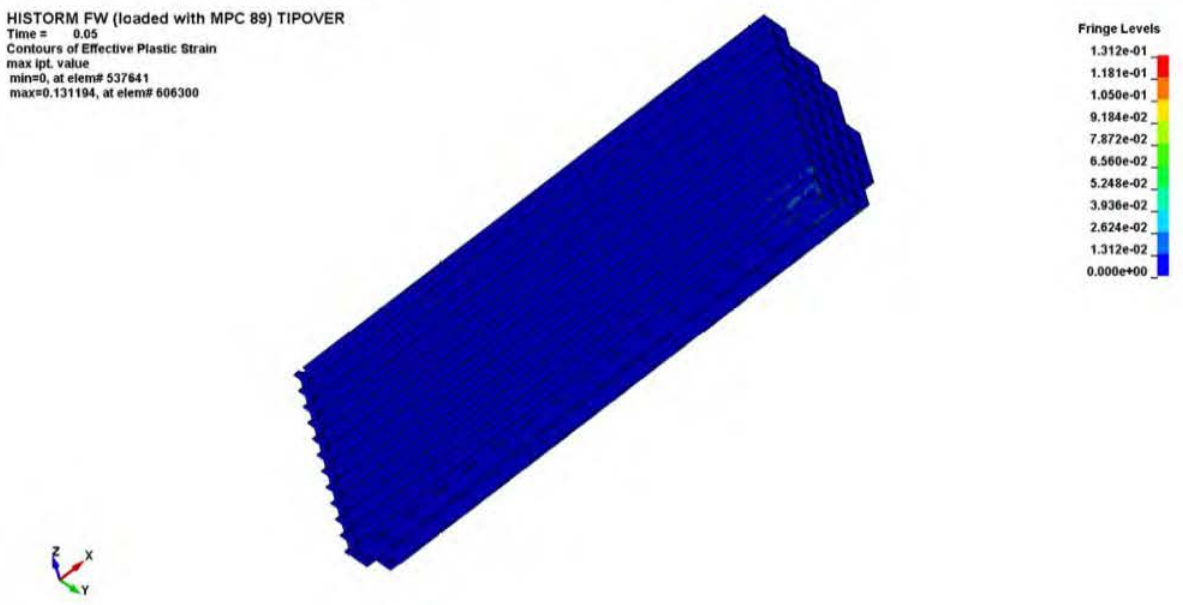

Figure 3.4.15B: Maximum Plastic Strain – MPC-89 Fuel Basket

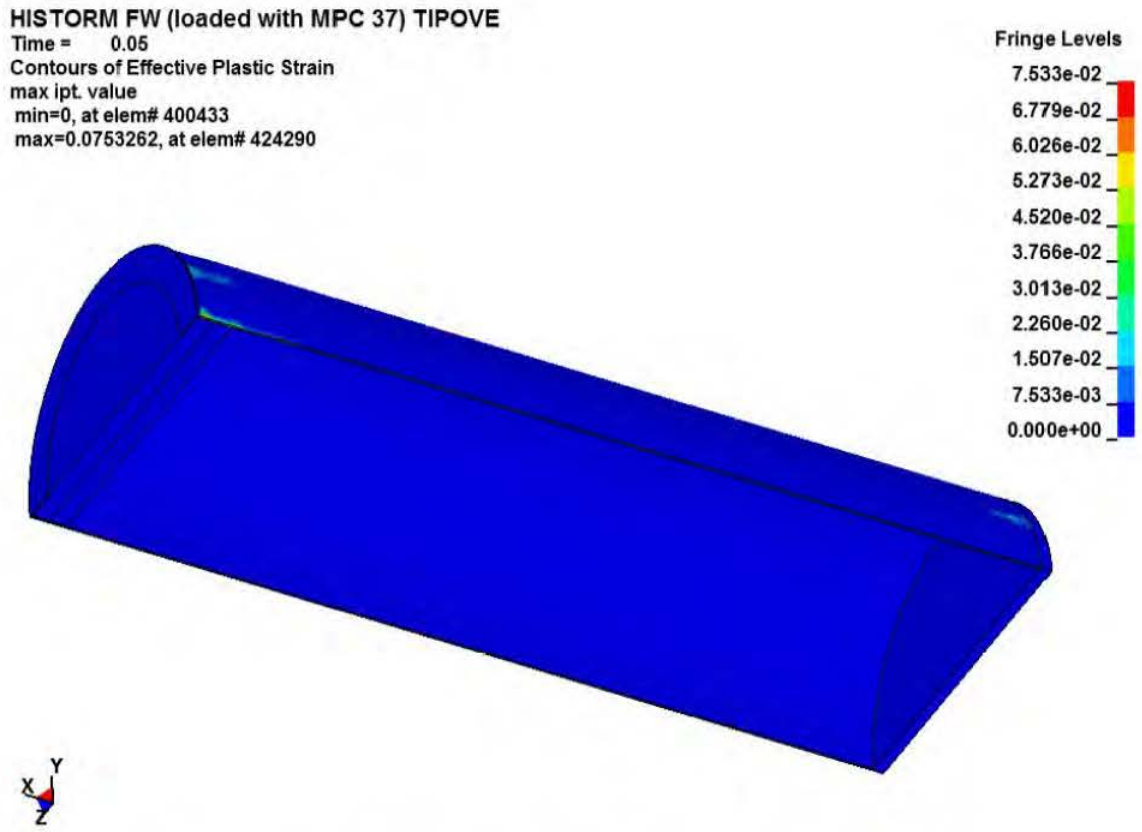

Figure 3.4.16A: Maximum Plastic Strain – MPC-37 Enclosure Vessel

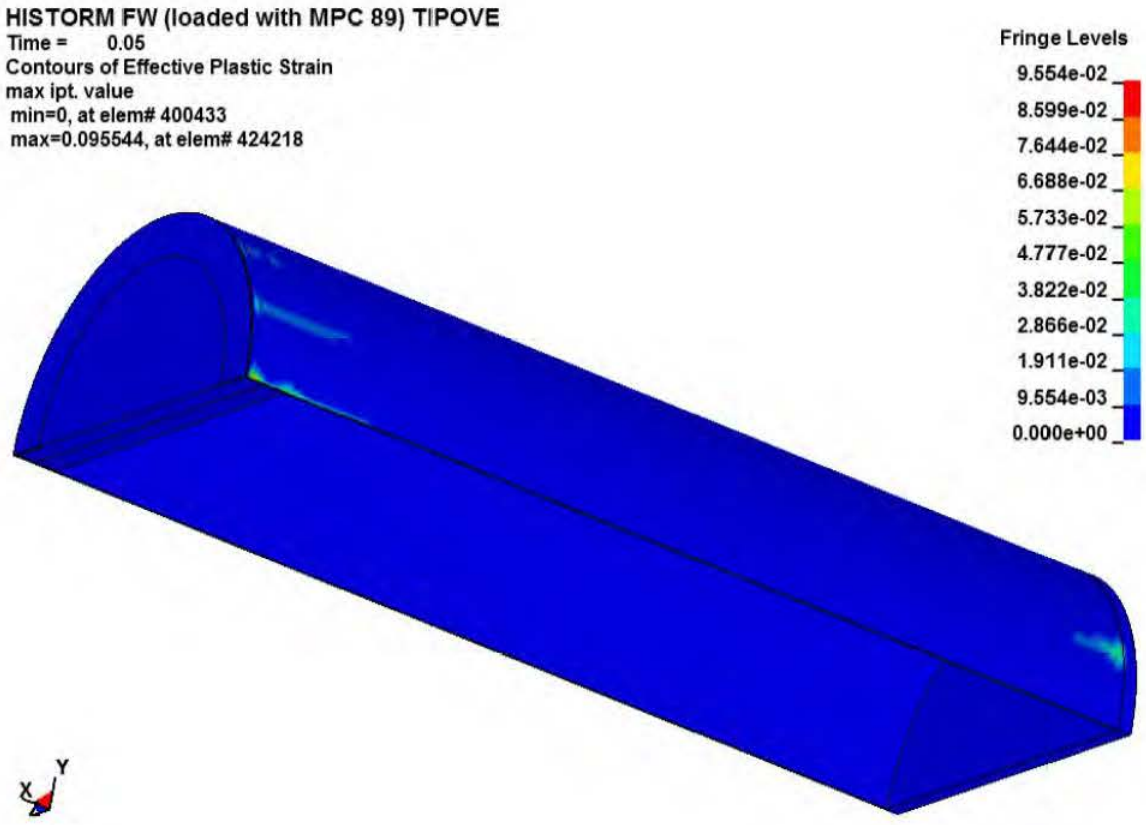

Figure 3.4.16B: Maximum Plastic Strain – MPC-89 Enclosure Vessel

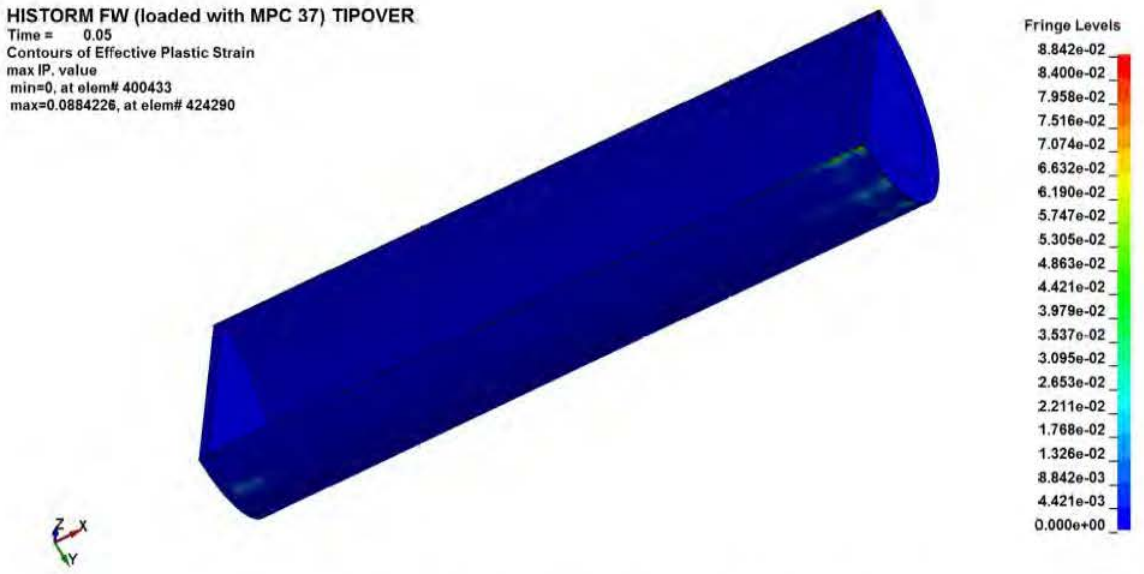

Figure 3.4.16C: Plastic Stain – MPC-37 Enclosure Vessel (Case 1)

Figure 3.4.16D: Plastic Strain – MPC-37 Enclosure Vessel (Case 2)

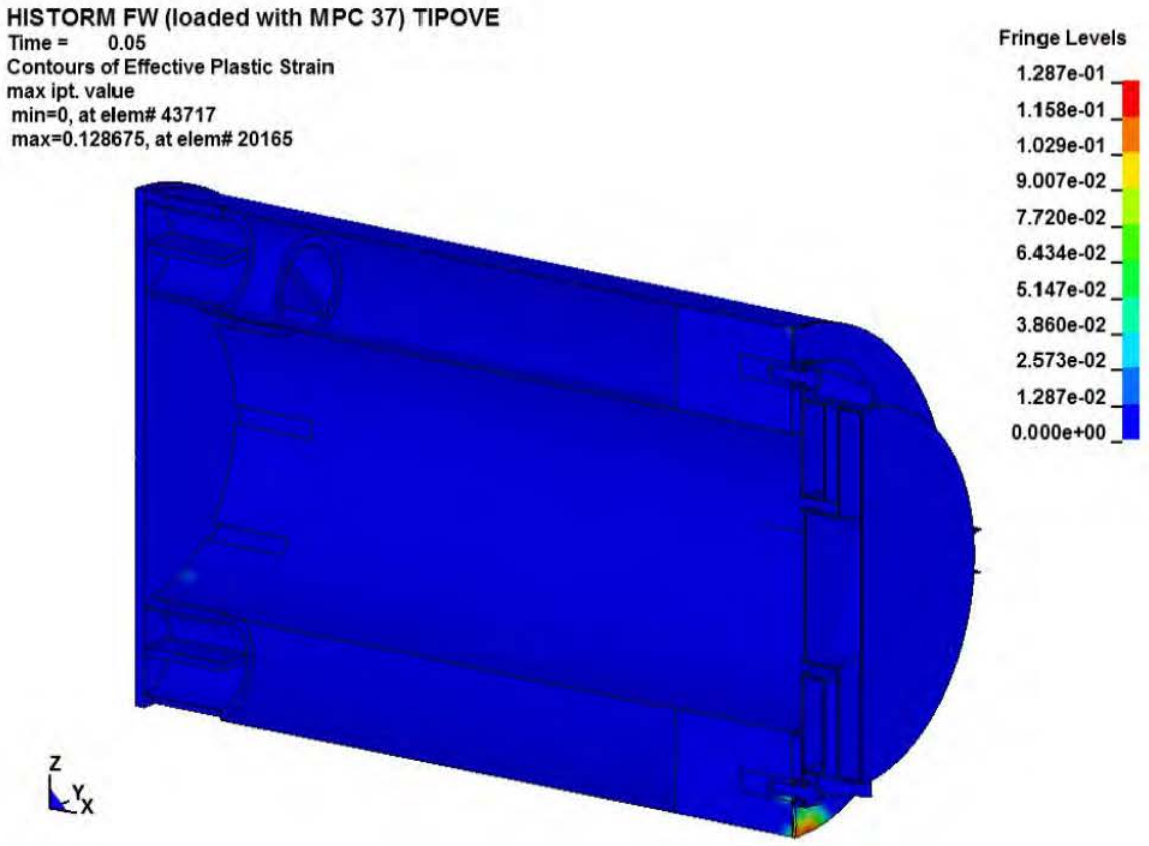

Figure 3.4.17A: Maximum Plastic Strain – HI-STORM FW Overpack
(for MPC-37, Excluding MPC Guide Tubes)

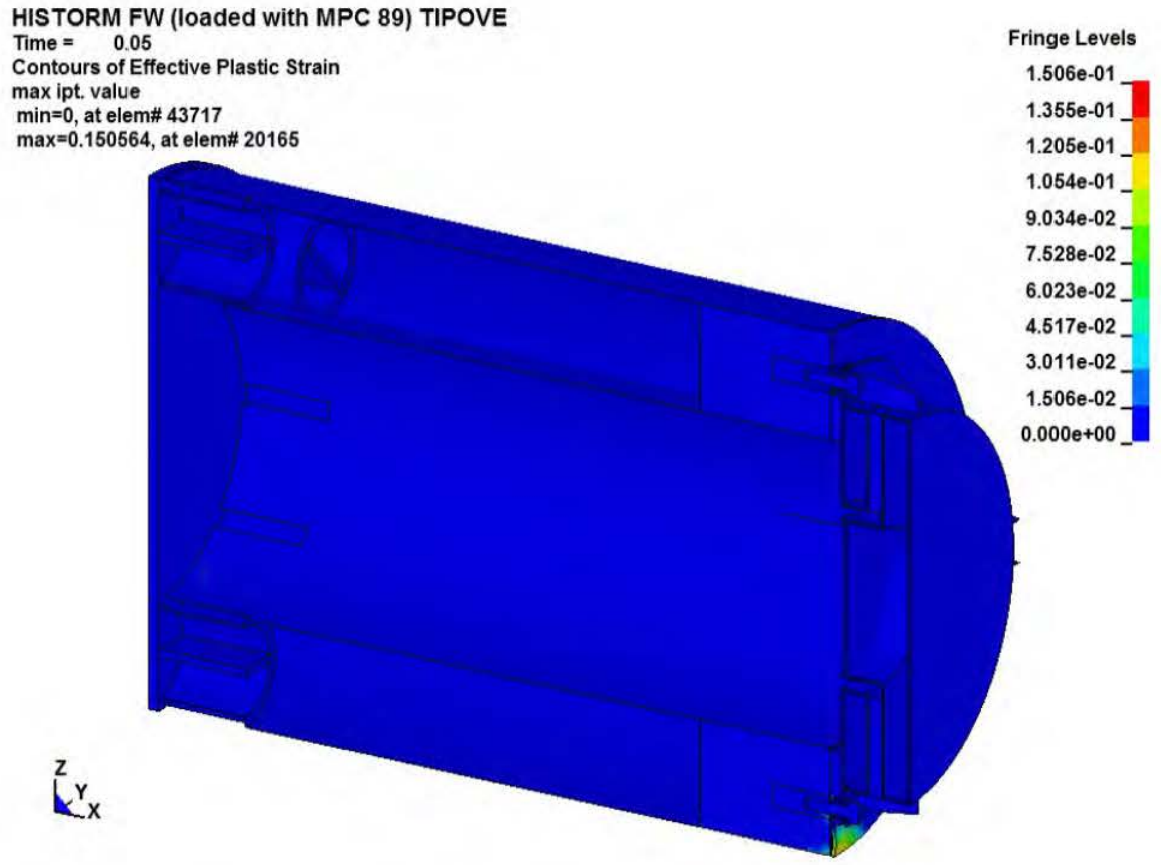

Figure 3.4.17B: Maximum Plastic Strain – HI-STORM FW Overpack
(for MPC-89, Excluding MPC Guide Tubes)

Figure 3.4.17C: Plastic Strain – HI-STORM FW Overpack (Case 1)

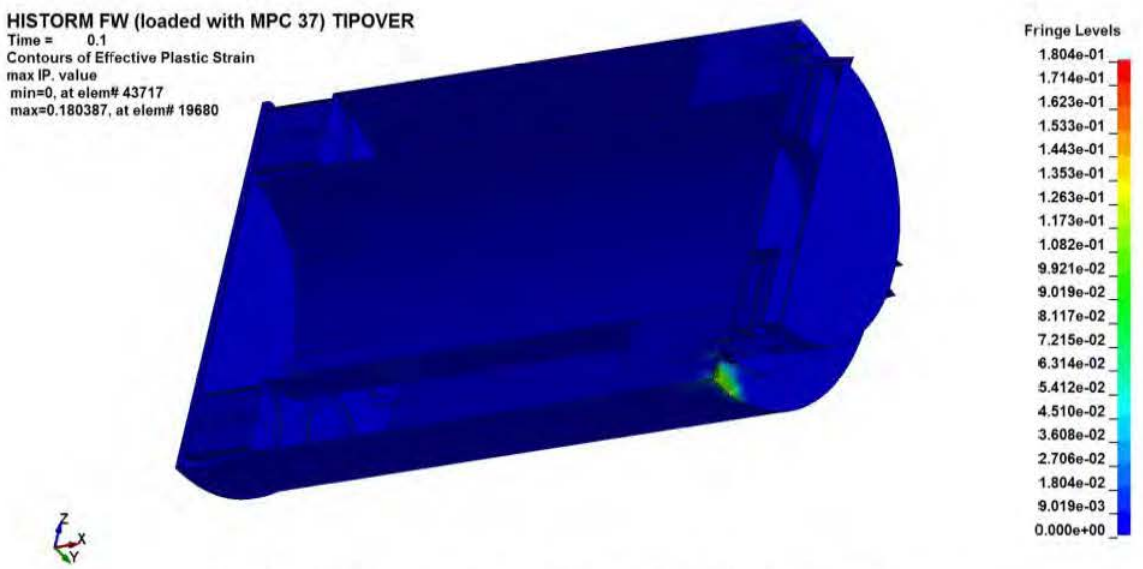

Figure 3.4.17D: Plastic Strain – HI-STORM FW Overpack (Case 2)

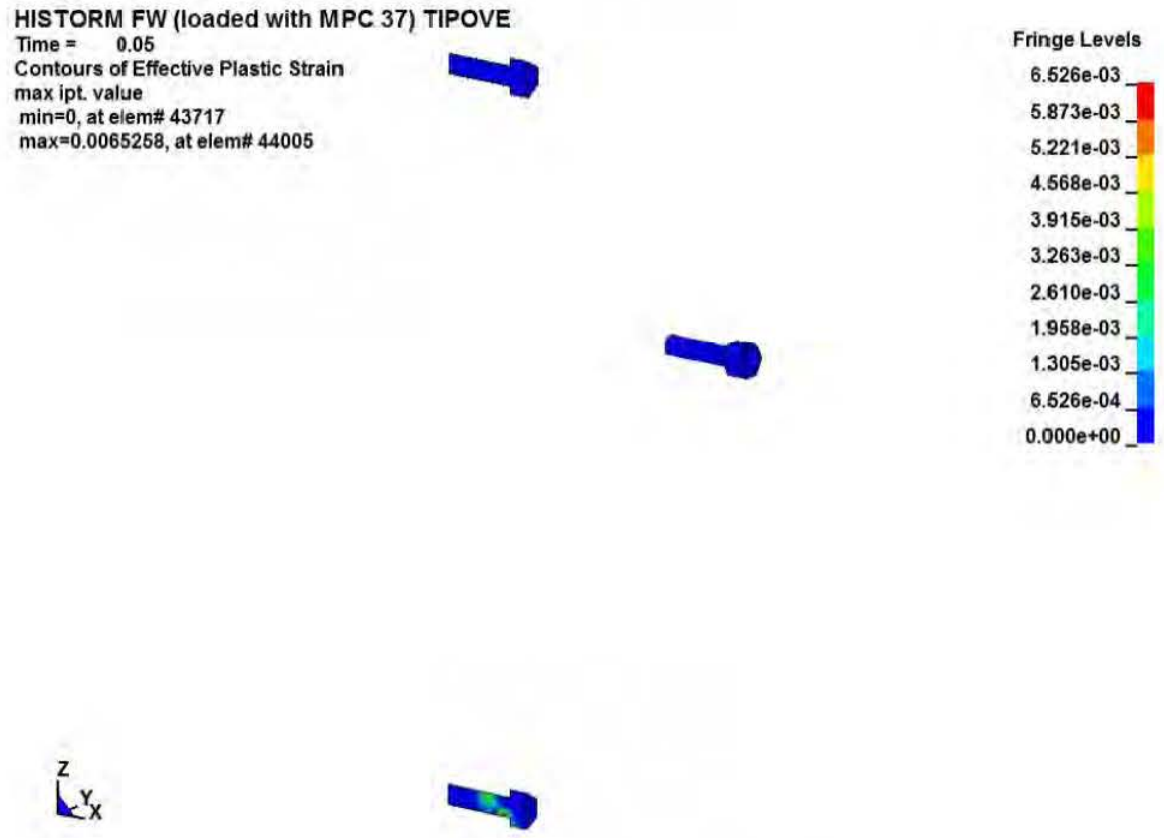

Figure 3.4.18A: Maximum Plastic Strain –
HI-STORM FW Overpack (for MPC-37) Closure Lid Bolts

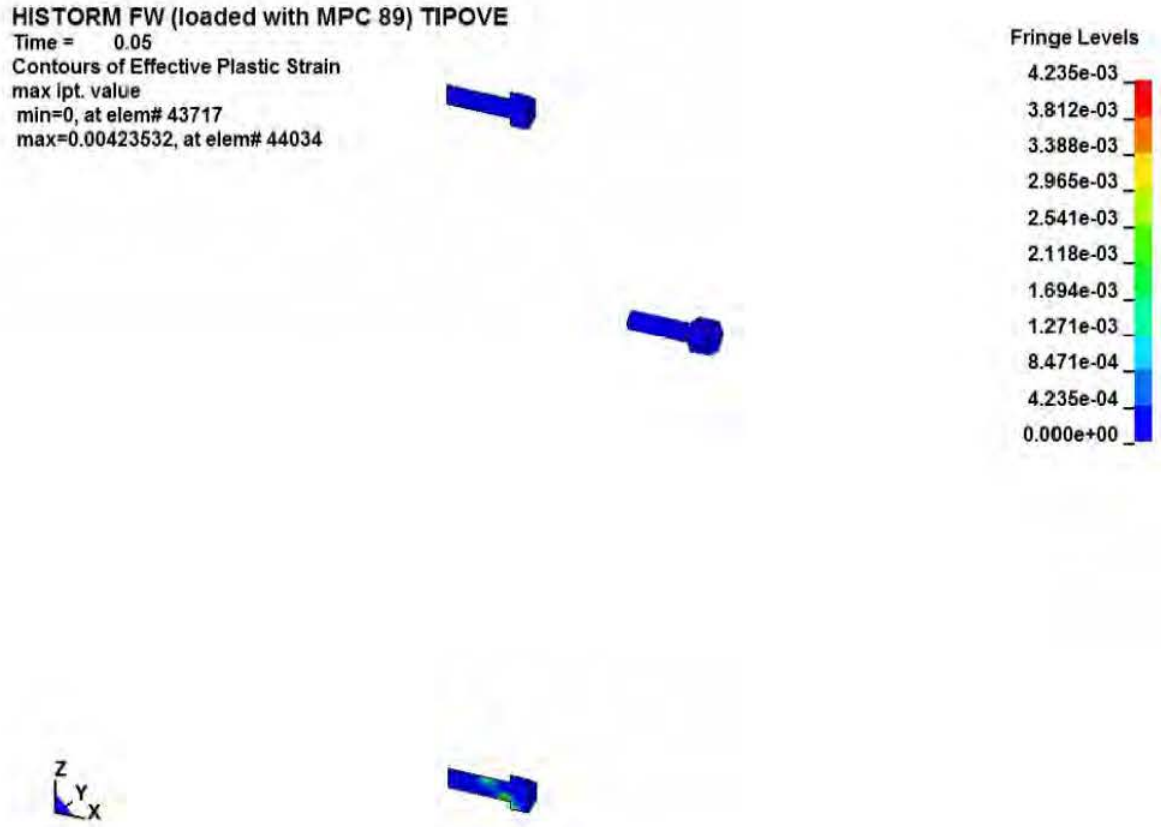

Figure 3.4.18B: Maximum Plastic Strain –
HI-STORM FW Overpack (for MPC-37) Closure Lid Bolts

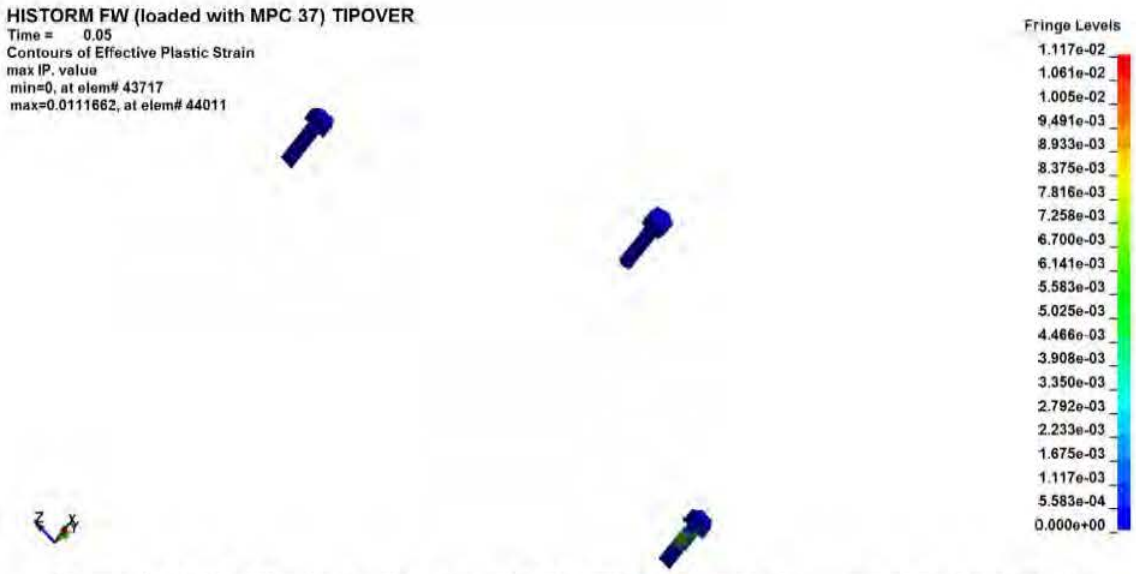

Figure 3.4.18C: Plastic Strain – HI-STORM FW Overpack Closure Lid Bolts (Case 1)

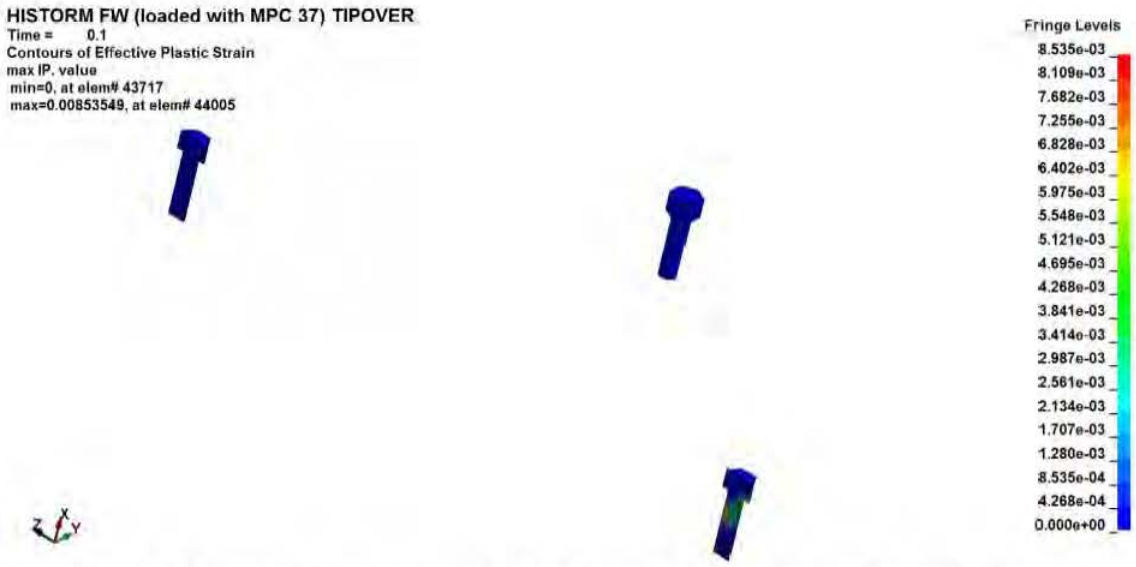

Figure 3.4.18D: Plastic Strain – HI-STORM FW Overpack Closure Lid Bolts Case 2

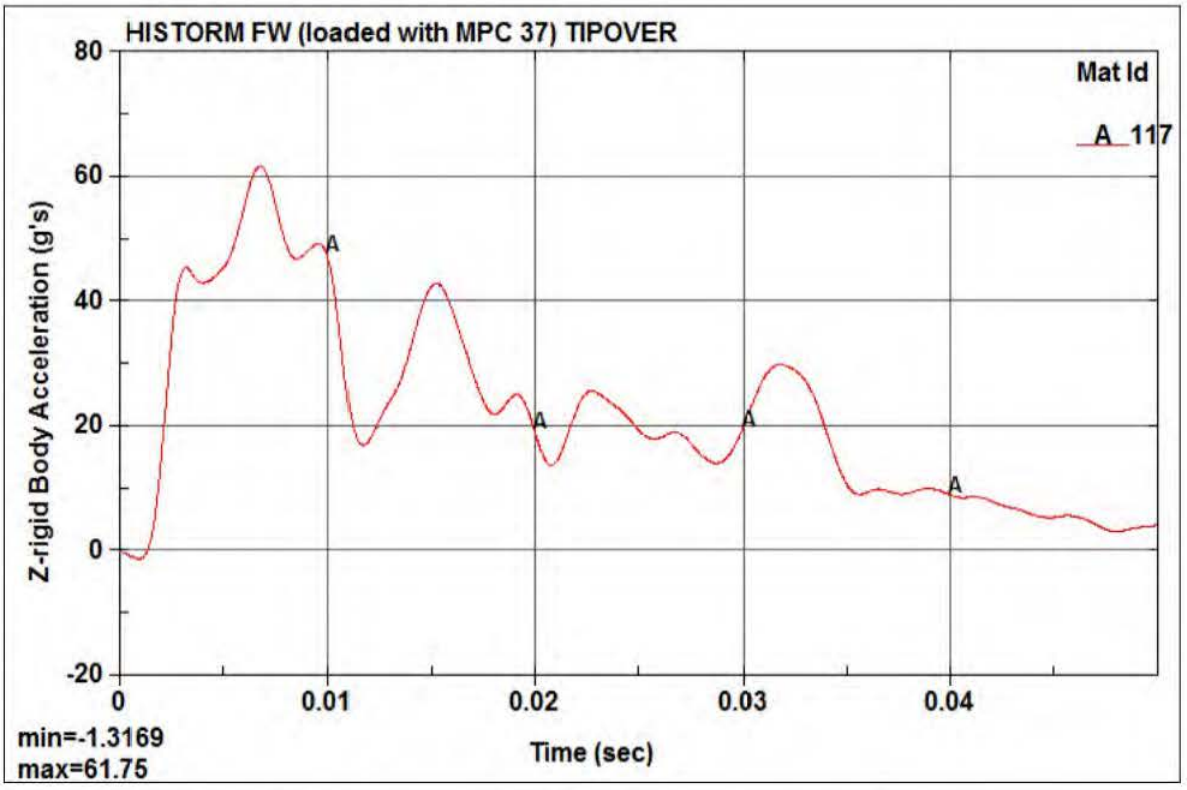

Figure 3.4.19A: Vertical Rigid Body Deceleration Time History –
Cask Lid Concrete (for HI-STORM FW Loaded with MPC-37)

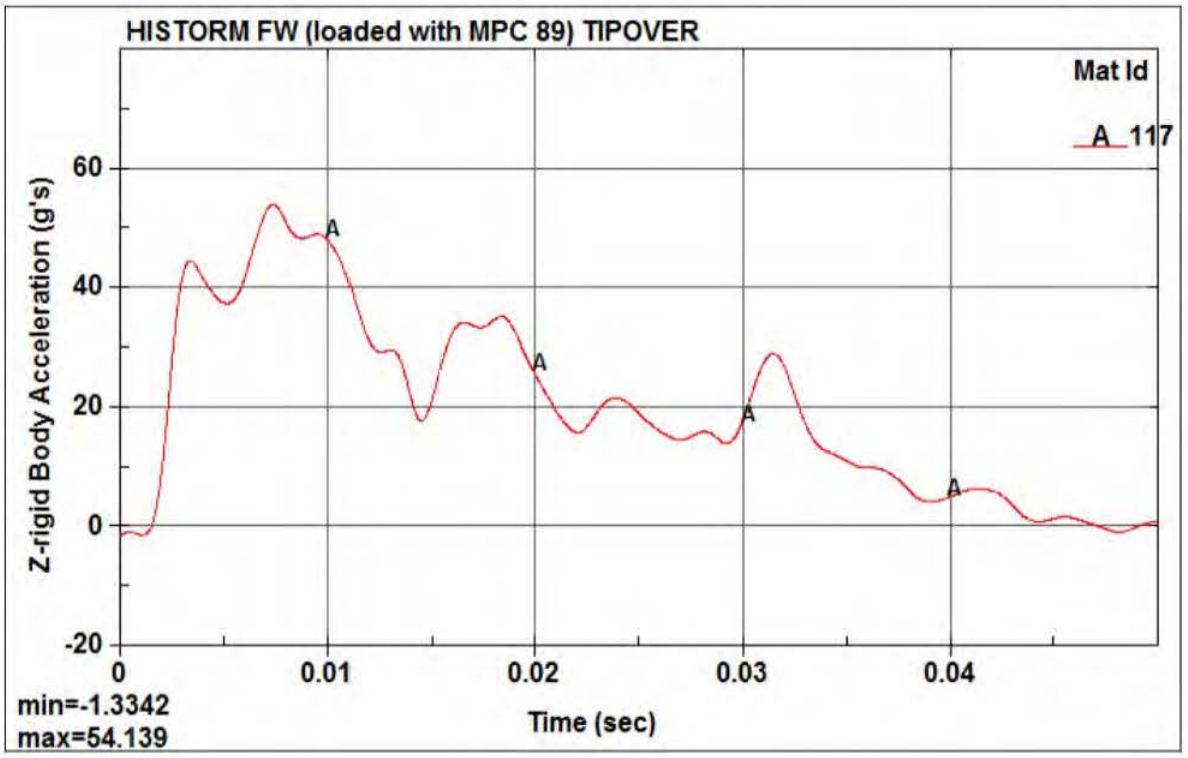

Figure 3.4.19B: Vertical Rigid Body Deceleration Time History –
Cask Lid Concrete (for HI-STORM FW Loaded with MPC-89)

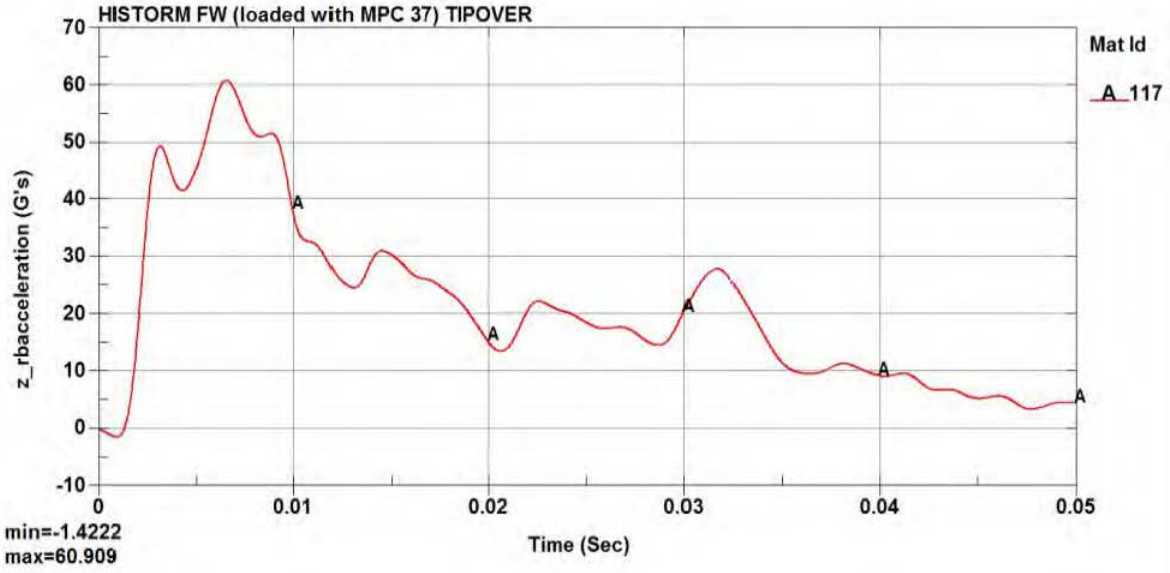

Figure 3.4.19C: Vertical Rigid Body Deceleration Time History –
Cask Lid Concrete for HI-STORM FW Loaded with MPC-37 (Case 1)

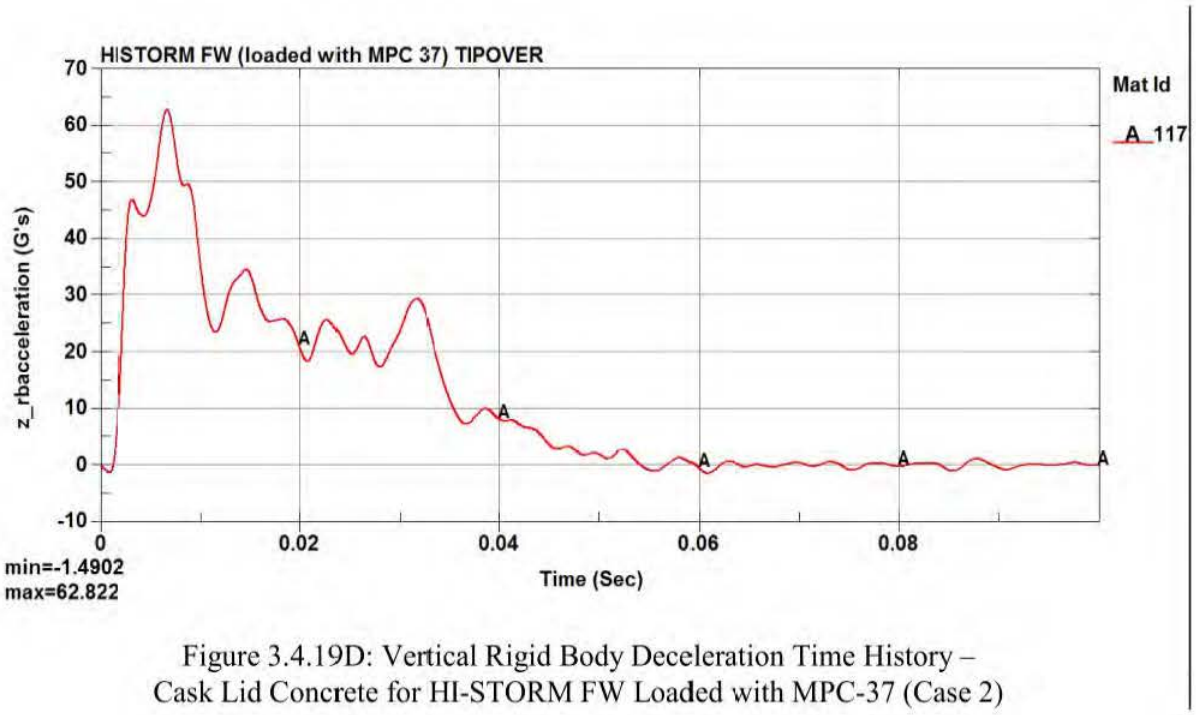

Figure 3.4.19D: Vertical Rigid Body Deceleration Time History –
Cask Lid Concrete for HI-STORM FW Loaded with MPC-37 (Case 2)

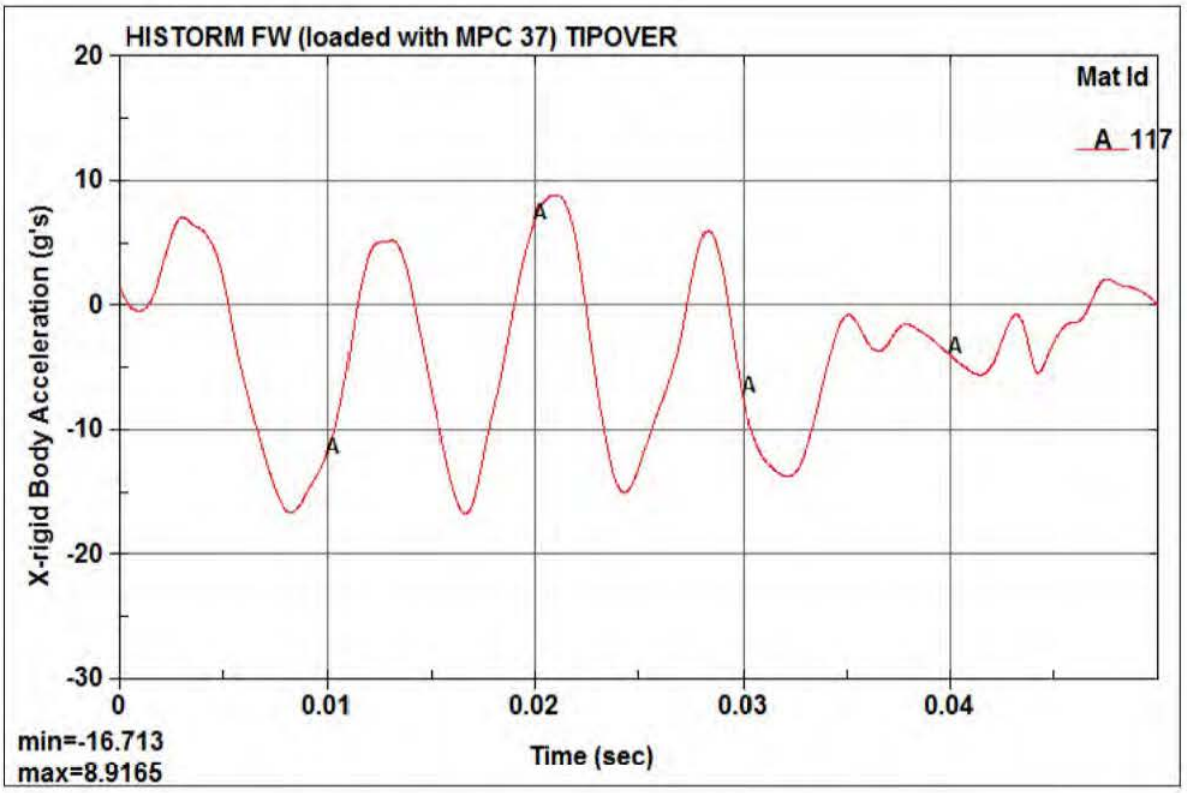

Figure 3.4.20A: Horizontal Rigid Body Deceleration Time History – Cask Lid Concrete (for HI-STORM FW Loaded with MPC-37)

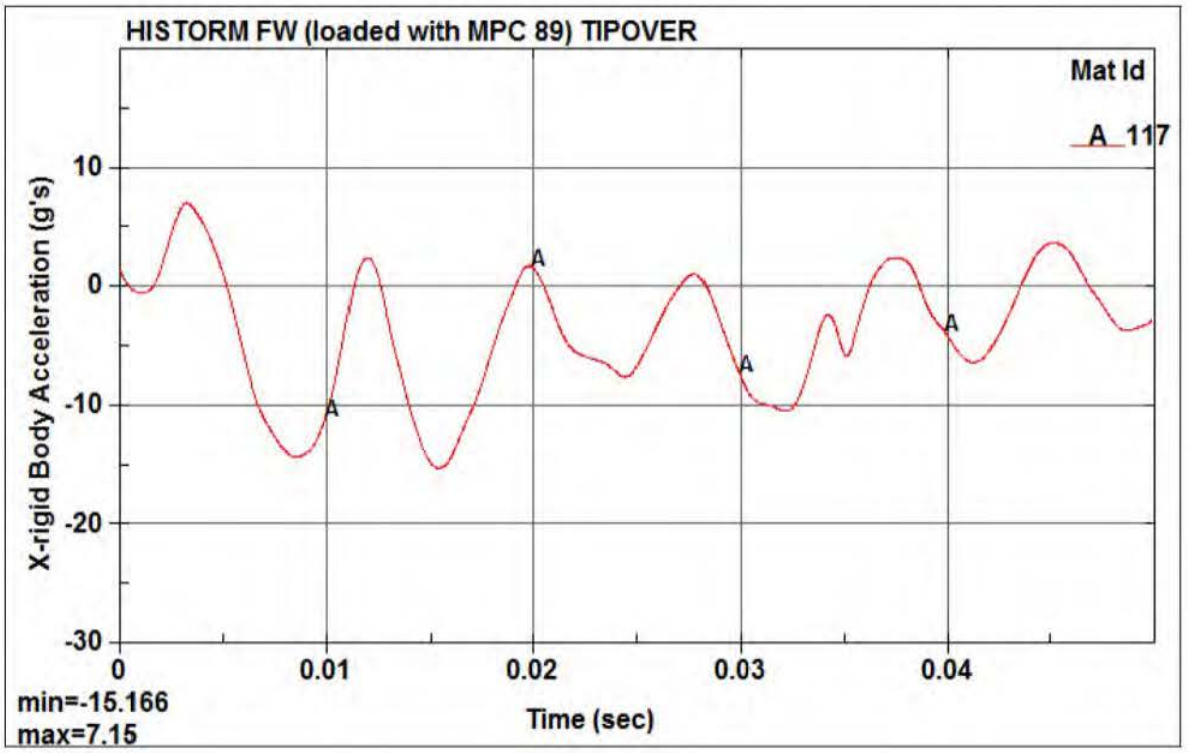

Figure 3.4.20B: Horizontal Rigid Body Deceleration Time History – Cask Lid Concrete (for HI-STORM FW Loaded with MPC-89)

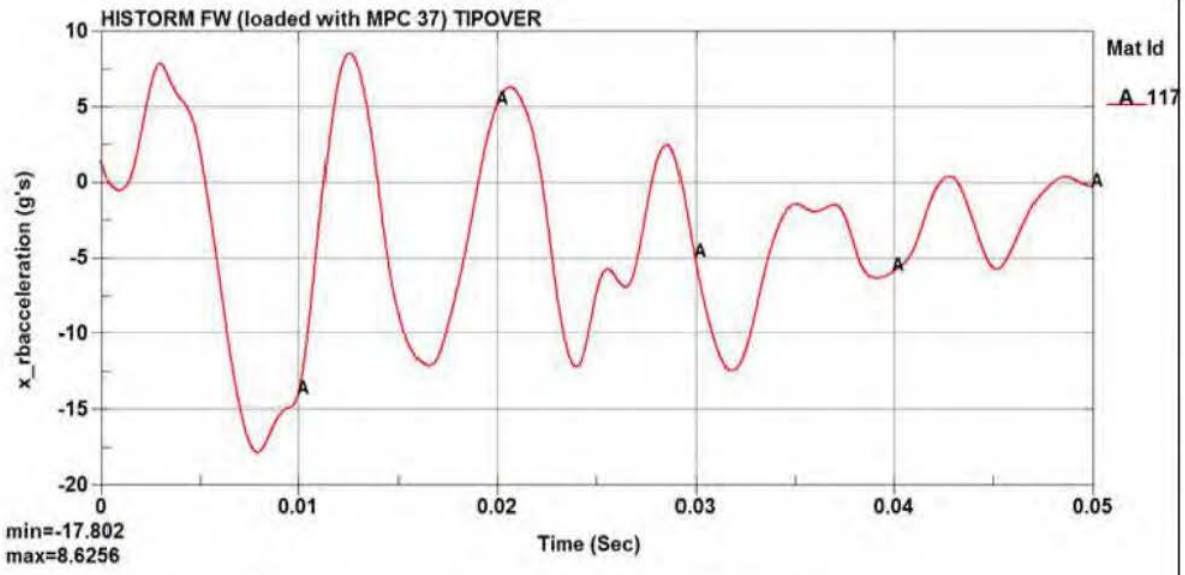

Figure 3.4.20C: Horizontal Rigid Body Deceleration Time History – Cask Lid Concrete for HI-STORM FW Loaded with MPC-37 (Case 1)

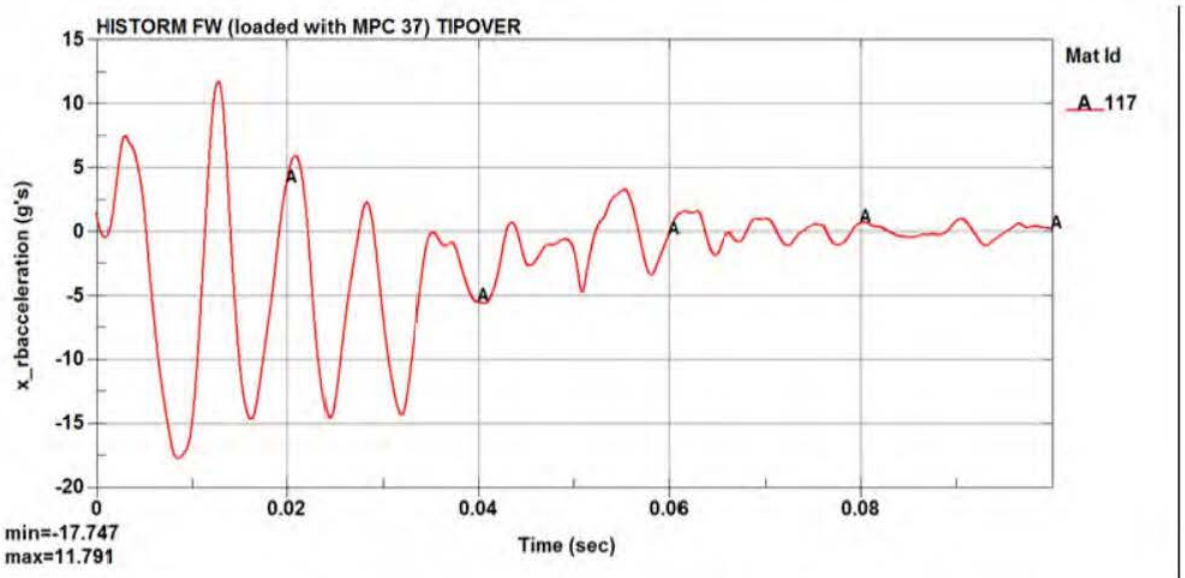

Figure 3.4.20D: Horizontal Rigid Body Deceleration Time History – Cask Lid Concrete for HI-STORM FW Loaded with MPC-37 (Case 2)

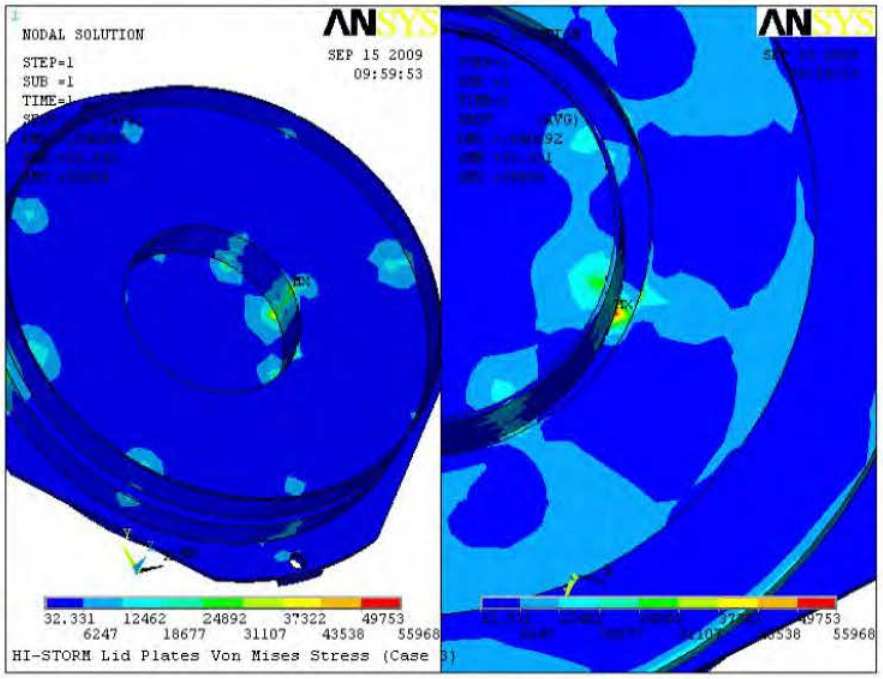

(a) Steel Weldment (Excluding Upper Shim Plates)

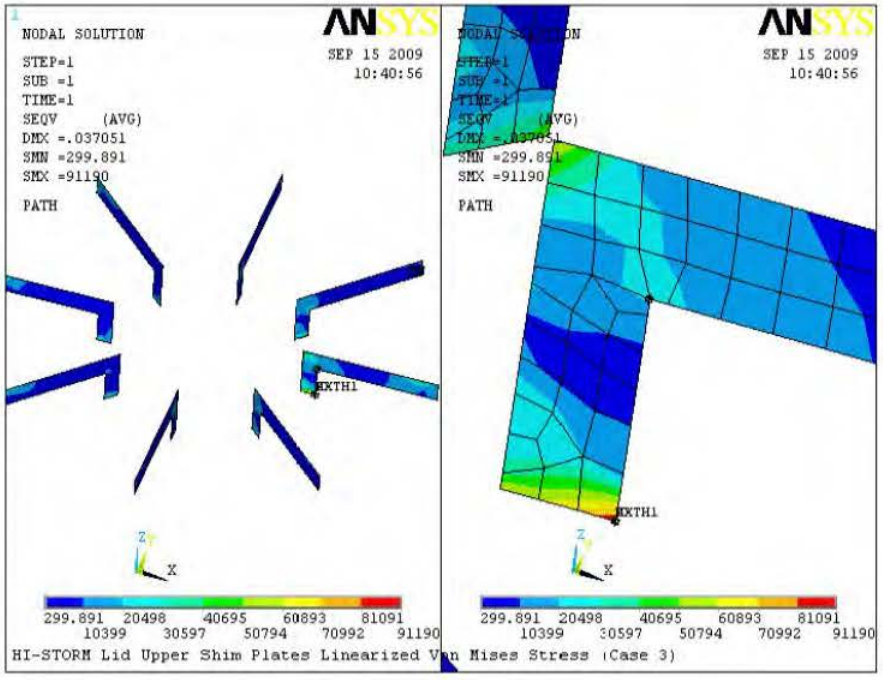

(b) Upper Shim Plates

Figure 3.4.21A: Stress Distribution in HI-STORM FW Lid – Non-Mechanistic Tipover

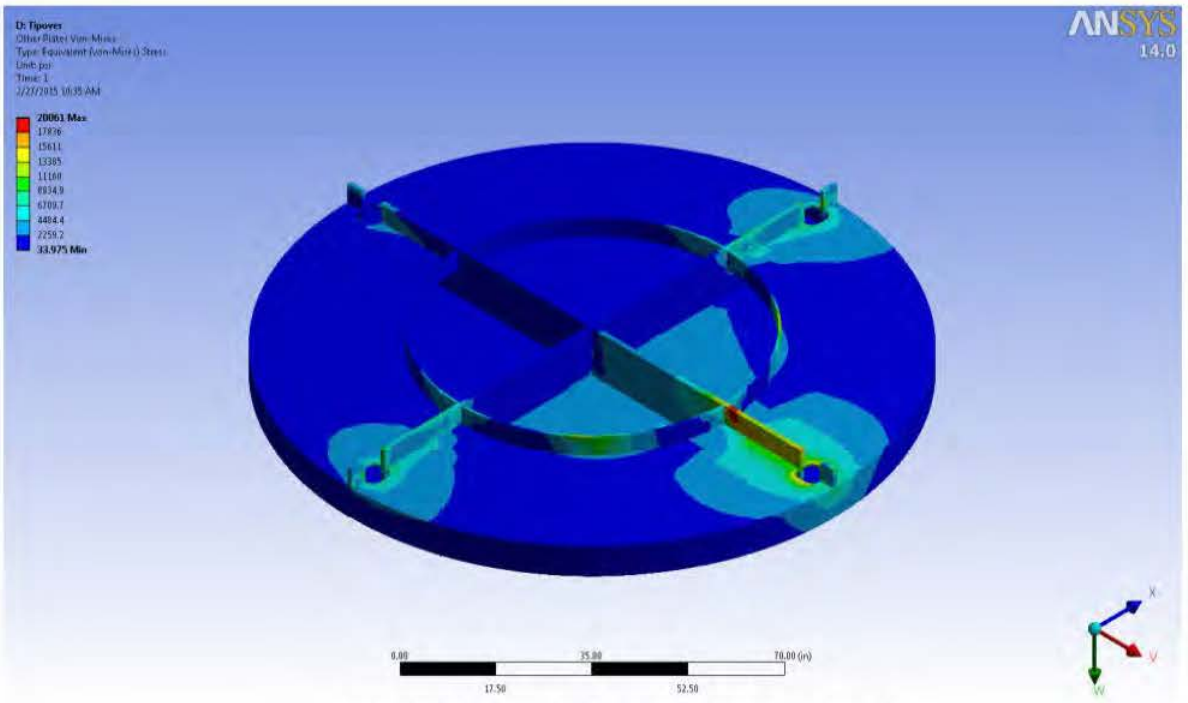

(a) Steel Weldment (Excluding Lid Base Plate)

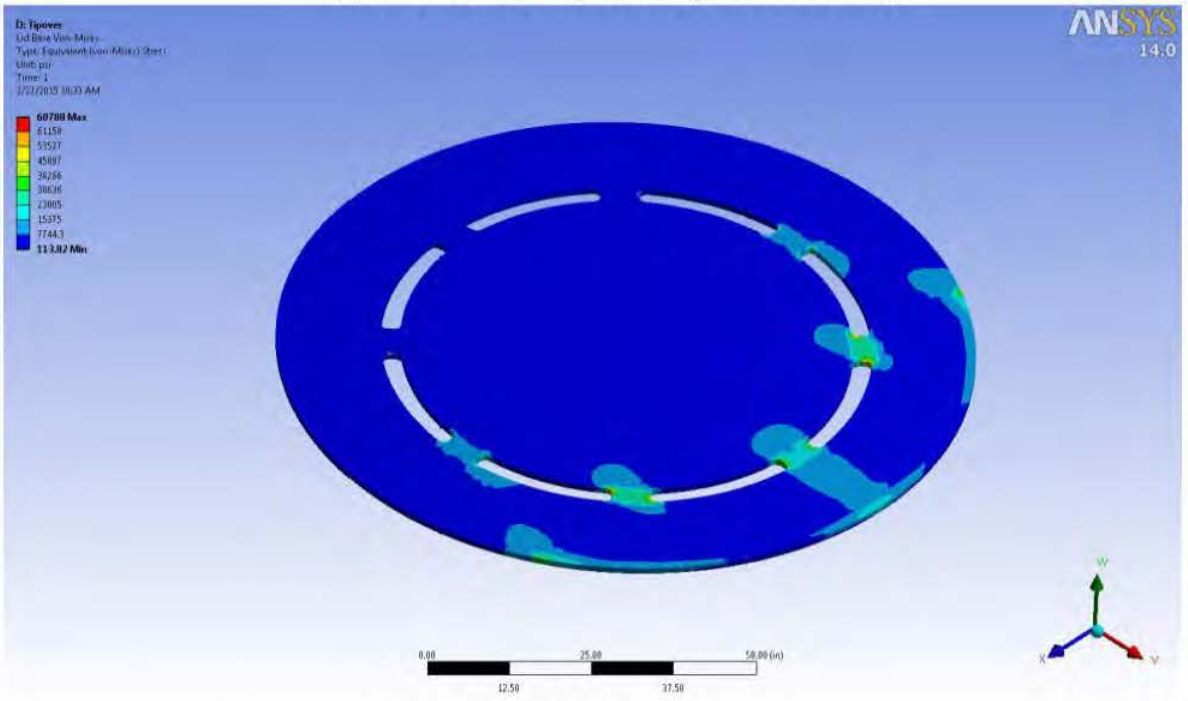

(b) Lid Base Plate

Figure 3.4.21B: Von-Mises Stress Distribution in HI-STORM FW Version XL Lid – Non-Mechanistic Tipover

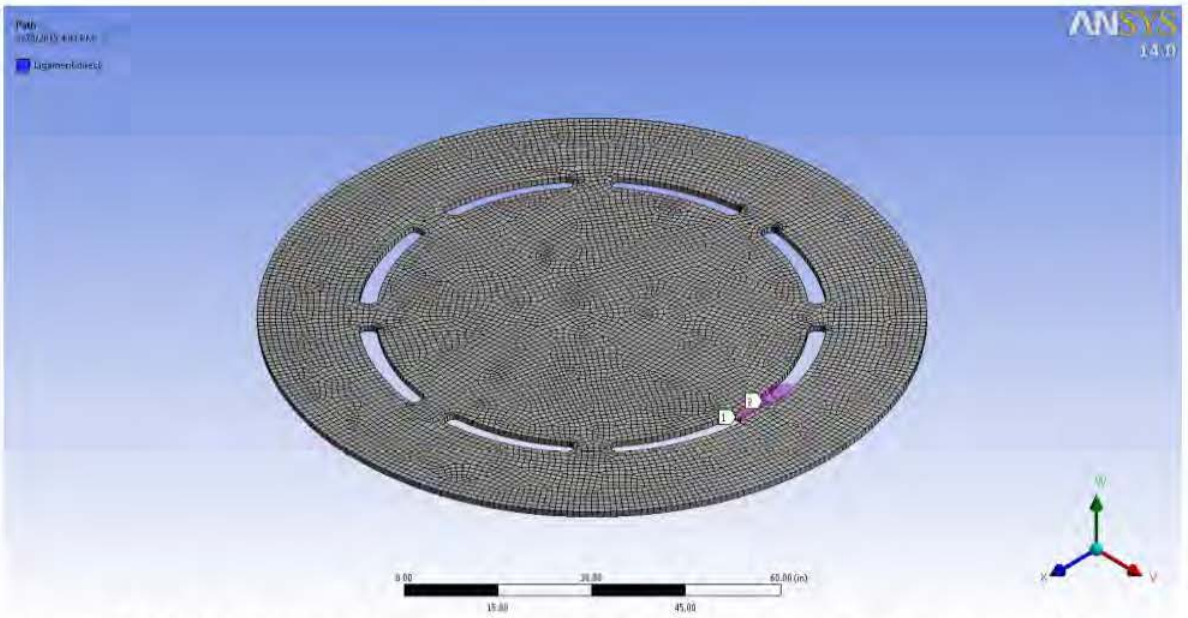

Figure 3.4.21C: HI-STORM FW Version XL Lid Base Plate Path – Non-Mechanistic Tipover

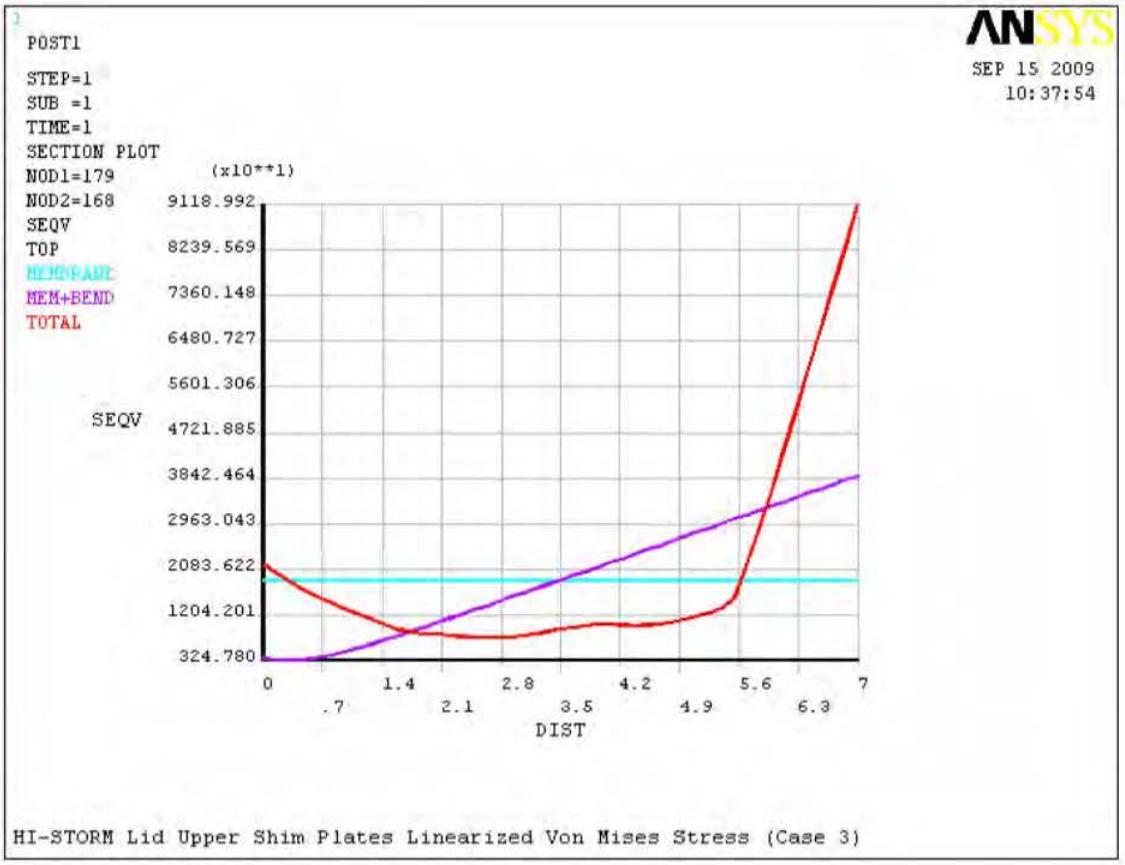

Figure 3.4.22A: Linearized Stress Results for Upper Shim Plate – Non-Mechanistic Tipover

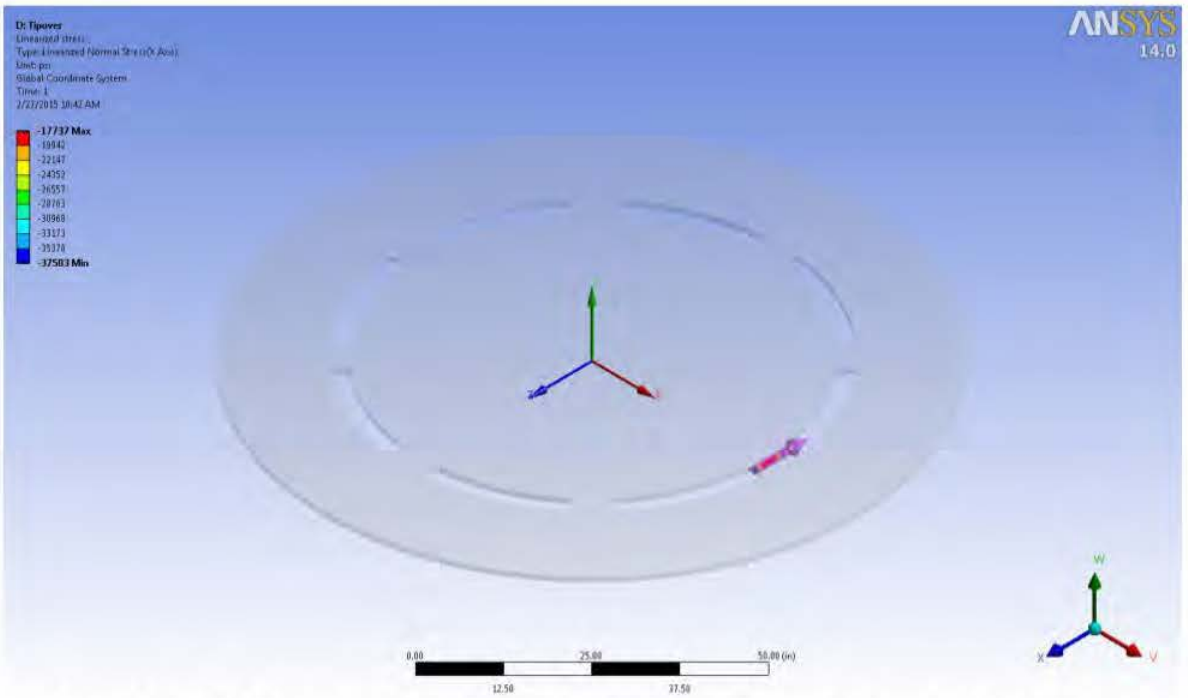

Figure 3.4.22B: Linearized Stress Results for Lid Base Plate – Non-Mechanistic Tipover

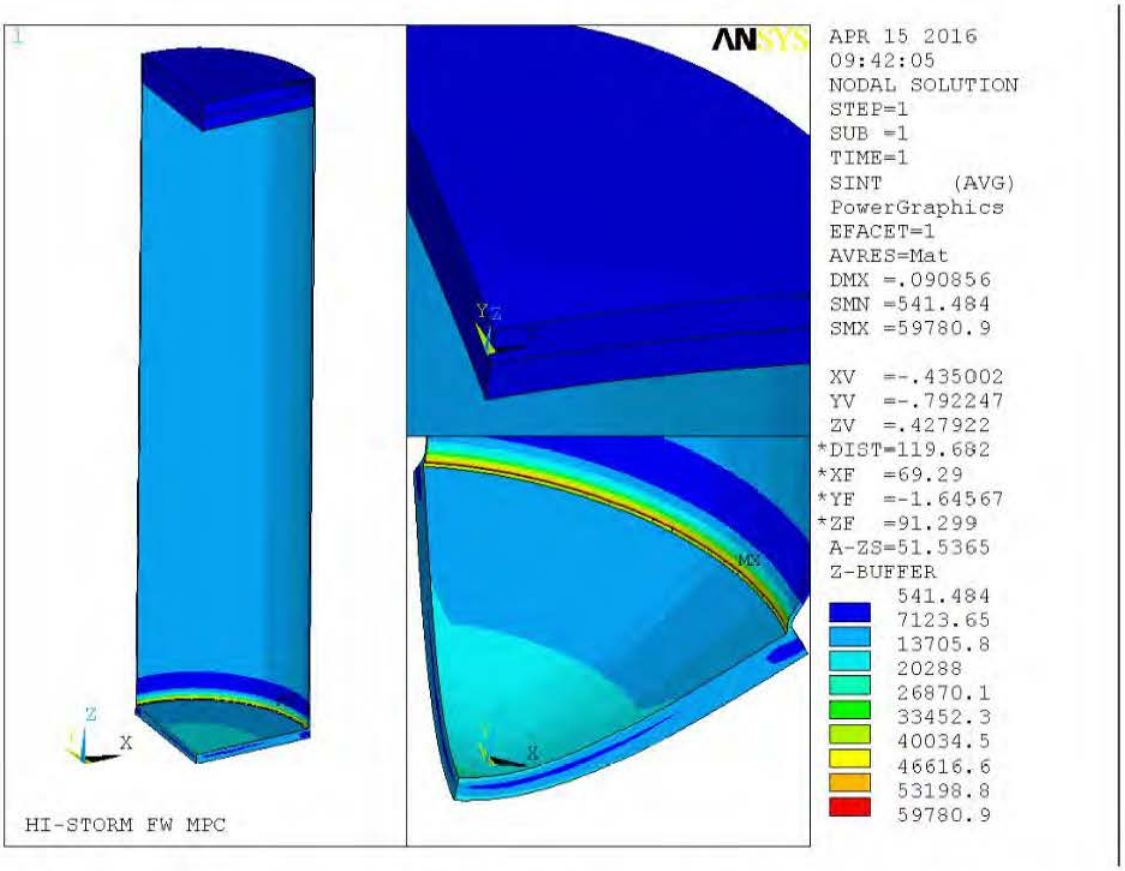

Figure 3.4.23: Stress Intensity Distribution in MPC Enclosure Vessel – Design Internal Pressure

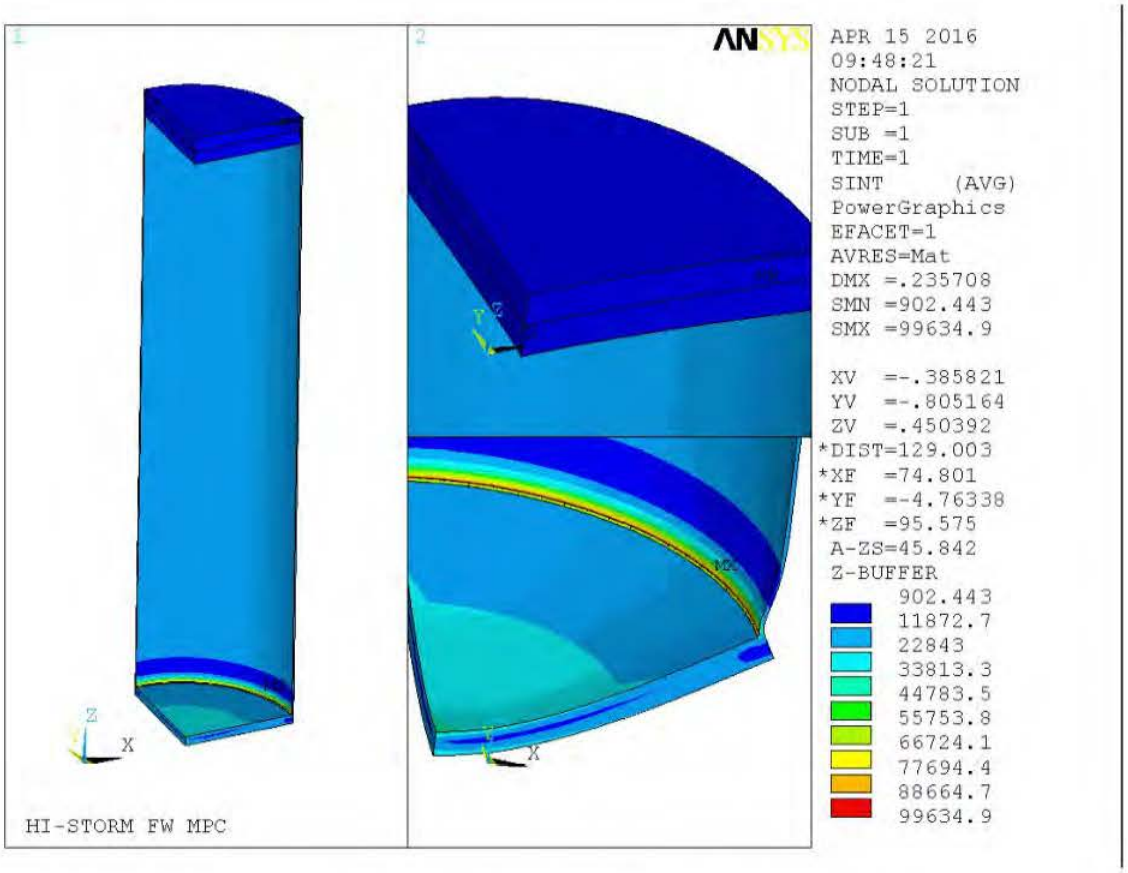

Figure 3.4.24: Stress Intensity Distribution in MPC Enclosure Vessel – Accident Internal Pressure

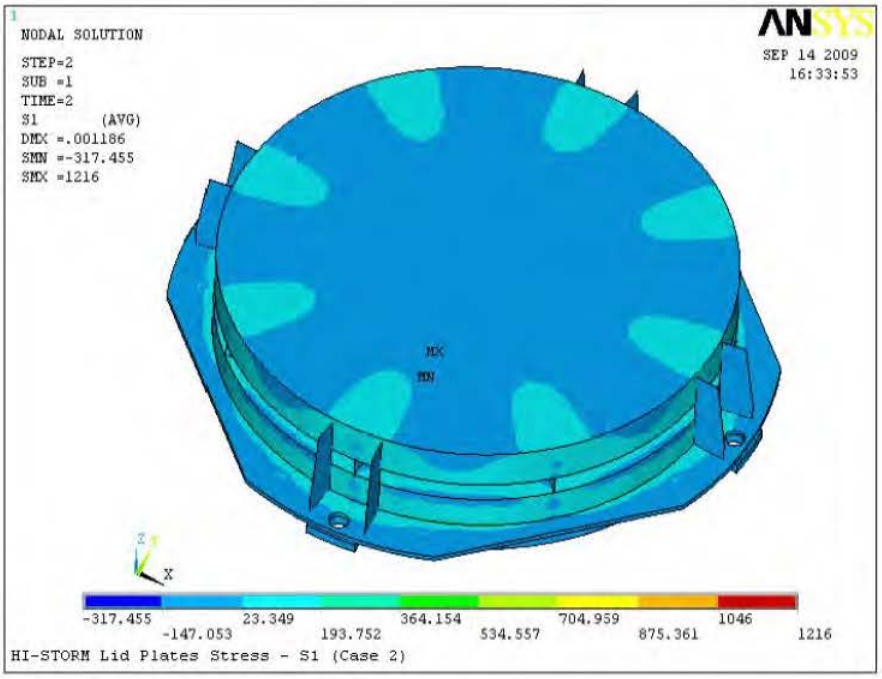

(a) S1 Principal Stress

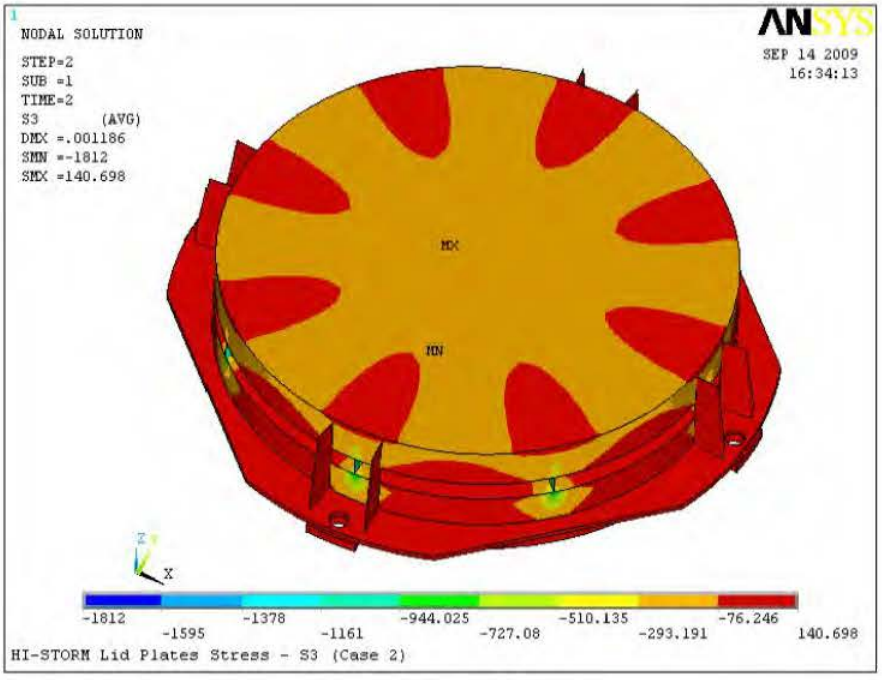

(b) S3 Principal Stress

Figure 3.4.25A: Stress Distribution in HI-STORM FW Lid – Snow Load

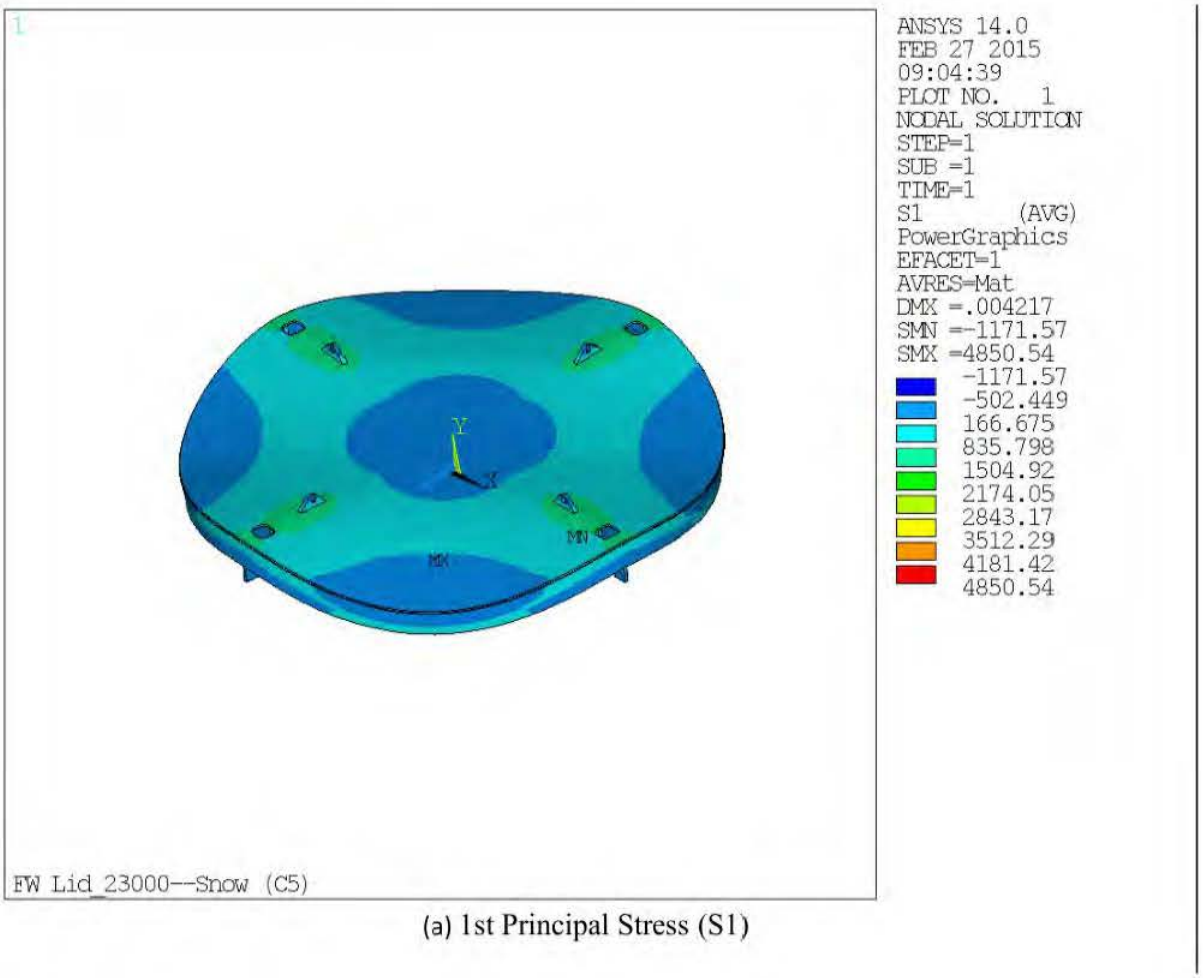

(a) 1st Principal Stress (S1)

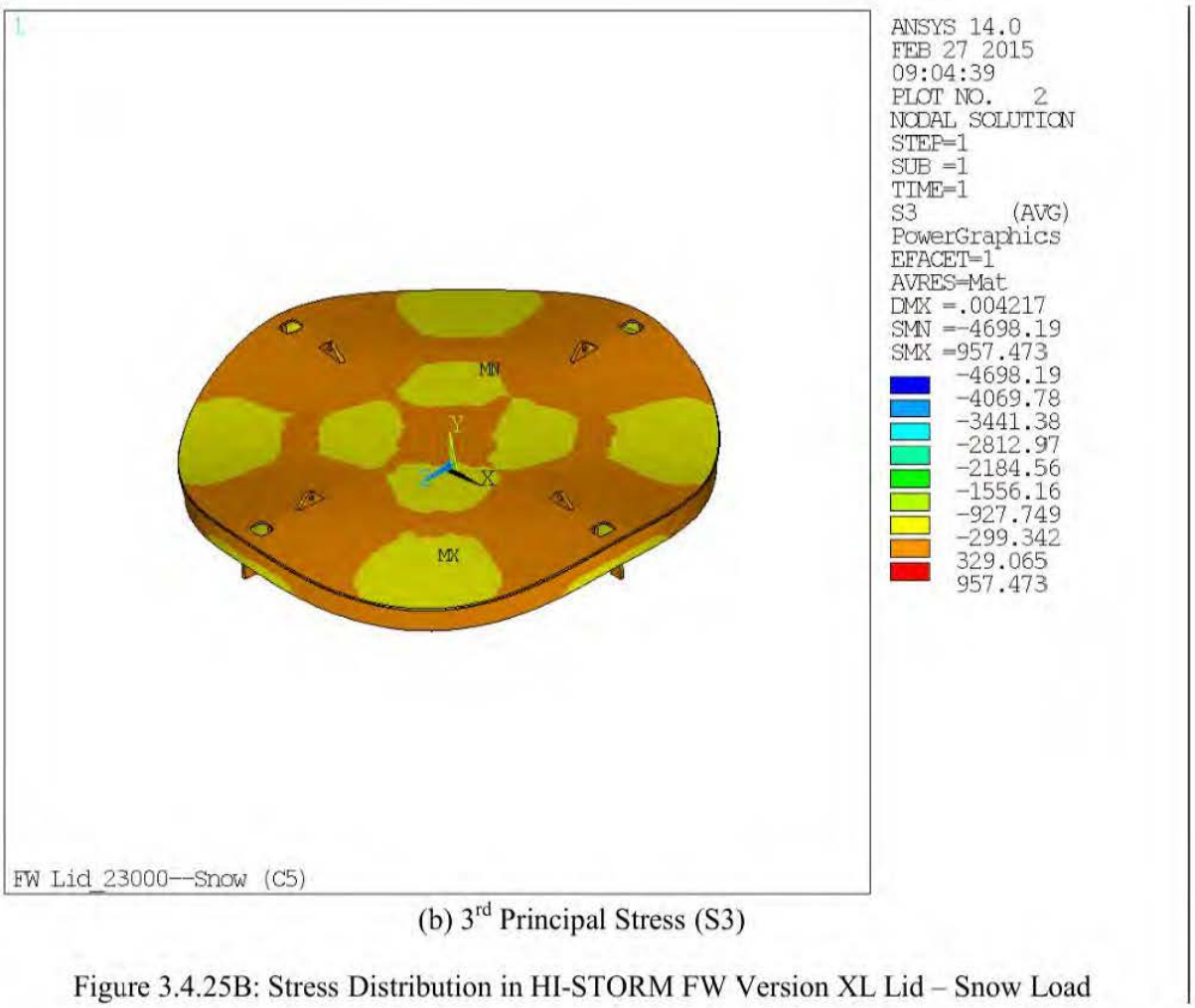

(b) 3rd Principal Stress (S3)

Figure 3.4.25B: Stress Distribution in HI-STORM FW Version XL Lid – Snow Load

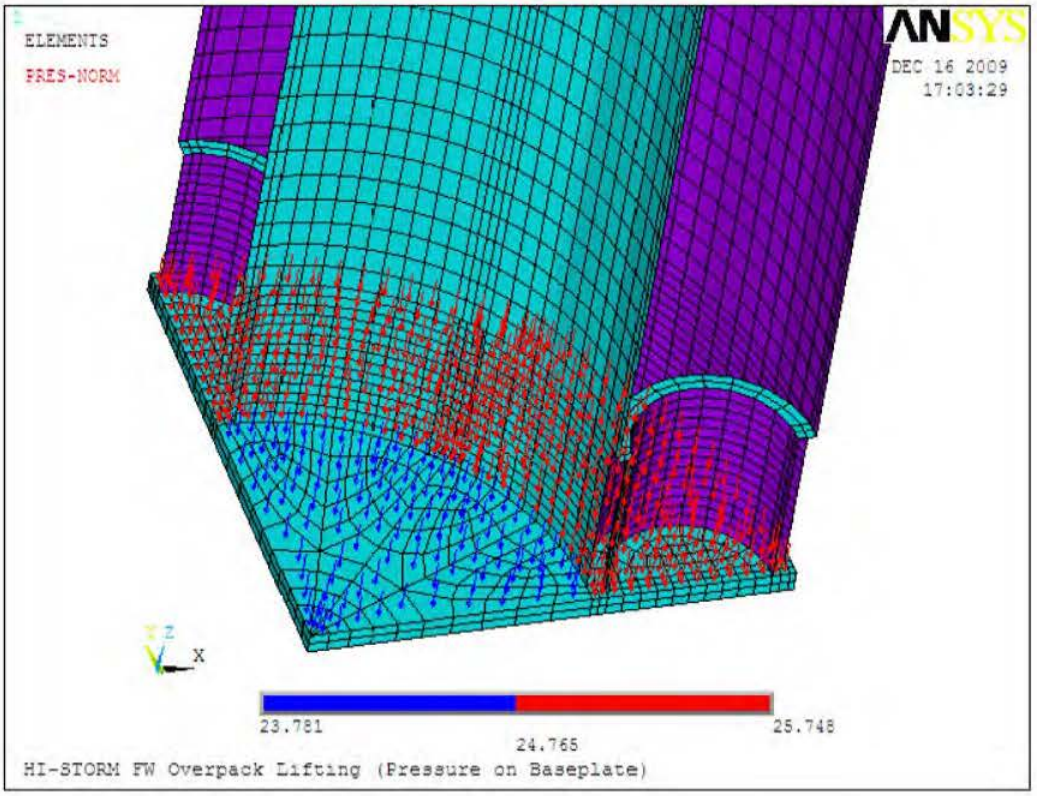

Figure 3.4.26: Applied Pressure on HI-STORM Baseplate Simulating Concrete Shielding and Loaded MPC

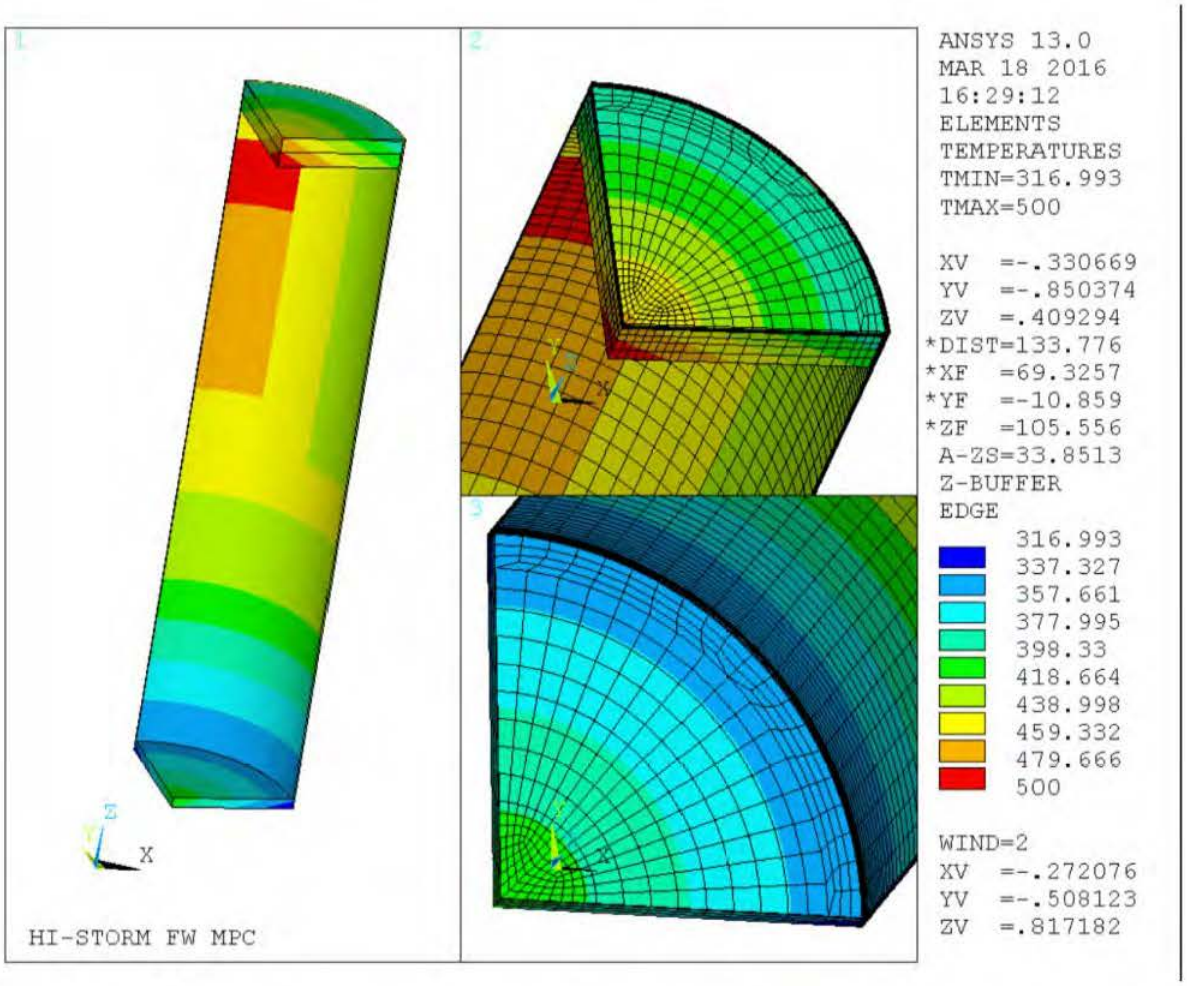

Figure 3.4.27: Short-Term Normal Condition Temperature Distribution in MPC Enclosure Vessel

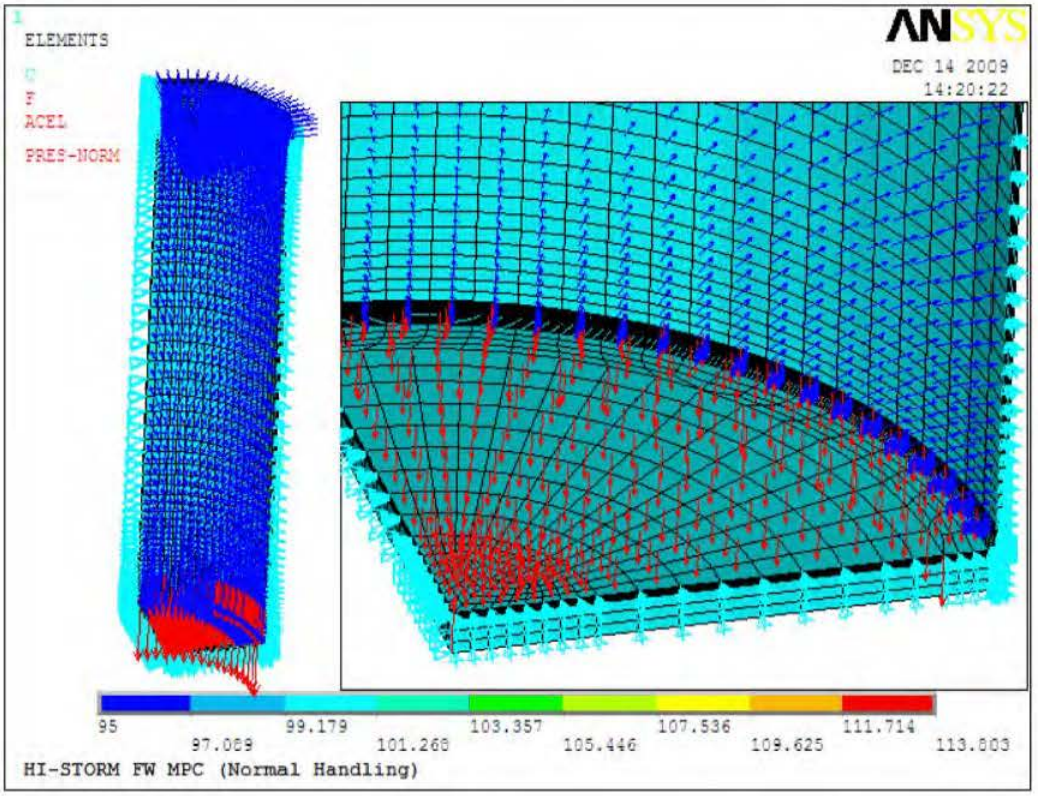

Figure 3.4.28: Normal Handling of MPC Enclosure Vessel –
Boundary Conditions and Applied Loads

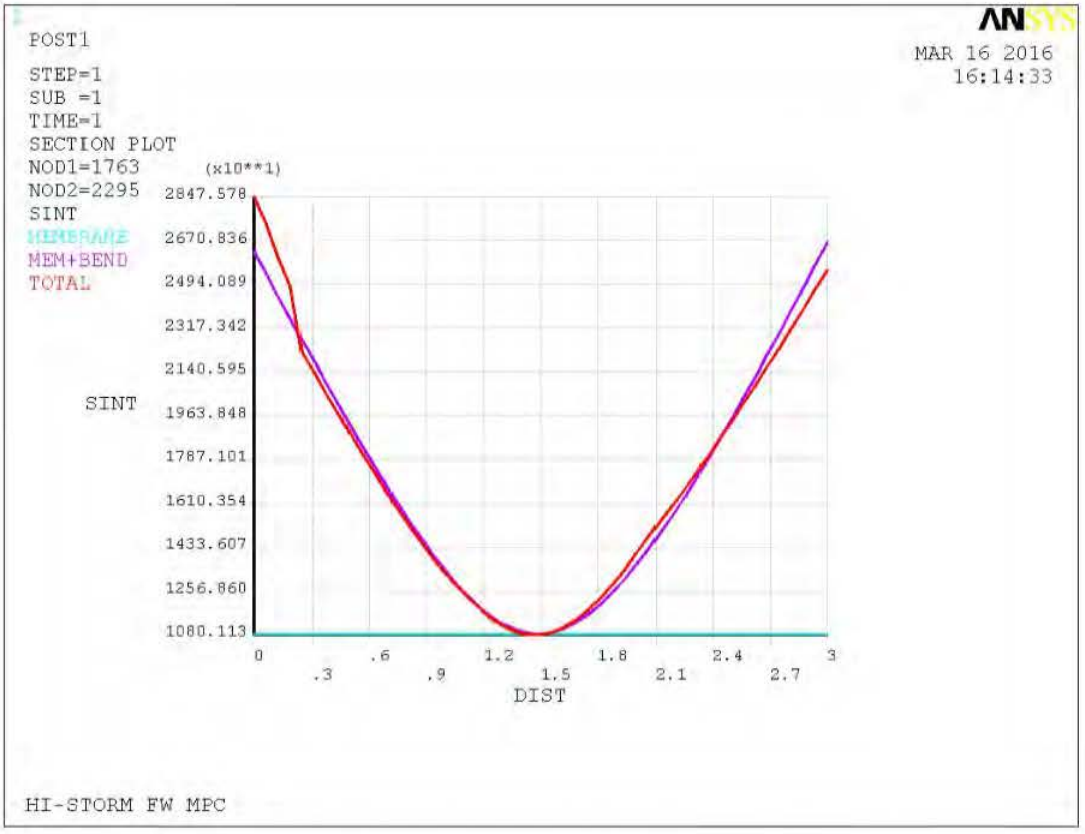

Figure 3.4.29: Normal Handling of MPC Enclosure Vessel –
Thru-Thickness Stress Intensity Plot at Baseplate Center

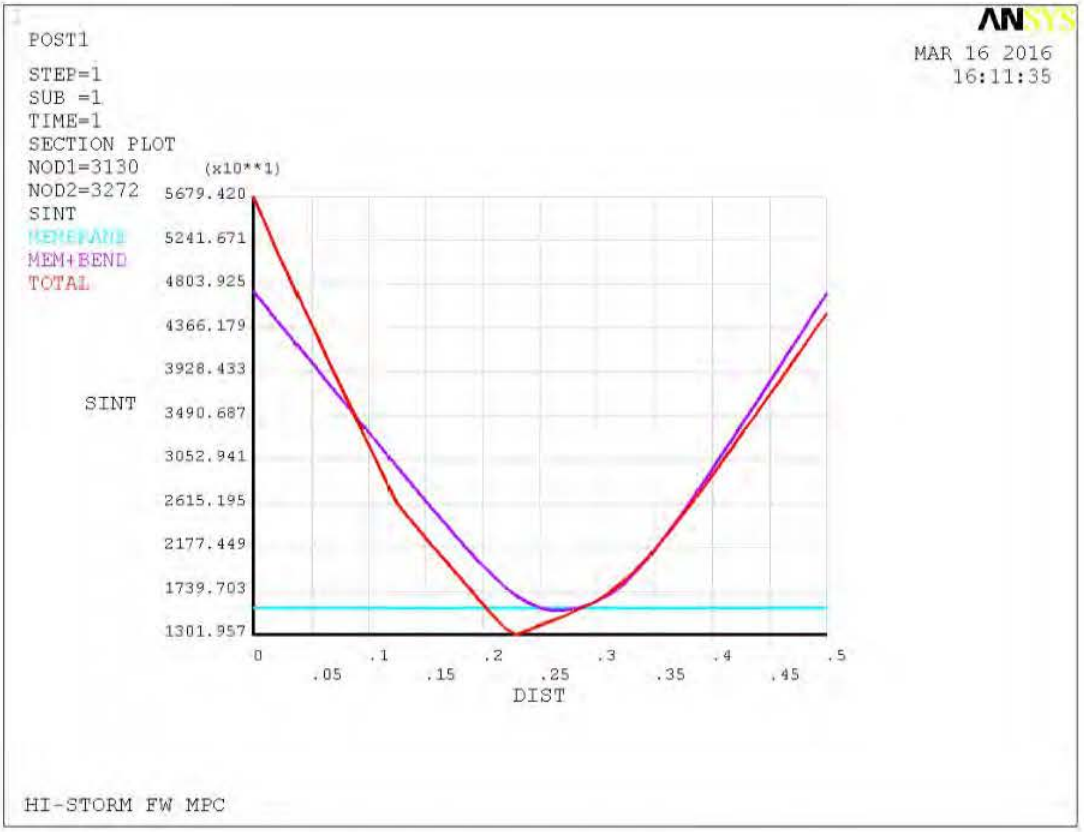

Figure 3.4.30: Normal Handling of MPC Enclosure Vessel –
Thru-Thickness Stress Intensity Plot at Baseplate-to-Shell Juncture

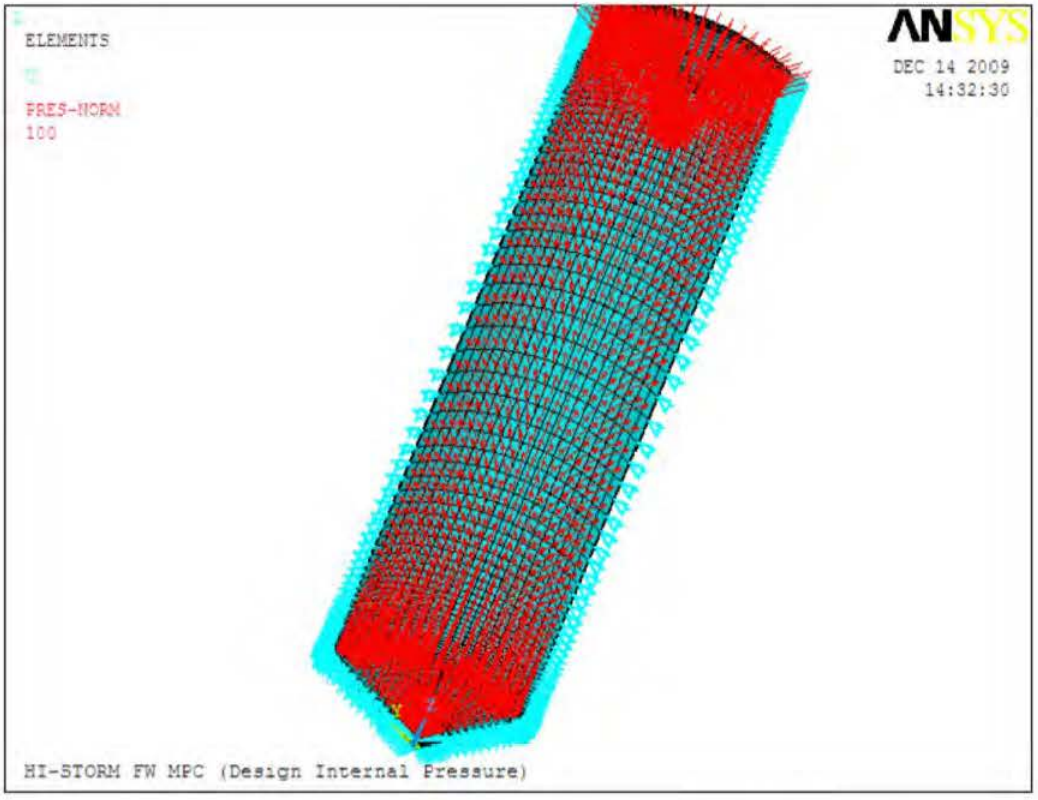

Figure 3.4.31: MPC Design Internal Pressure (Load Case 5) –
Boundary Conditions and Applied Loads

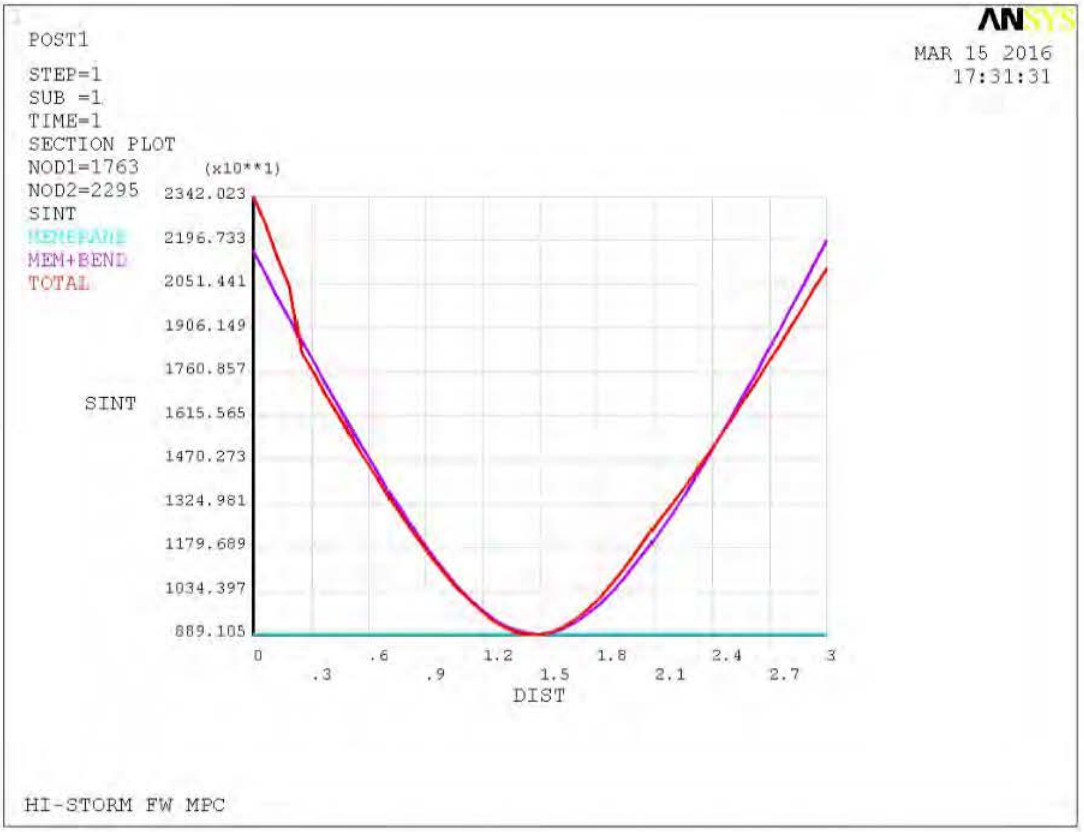

Figure 3.4.32: MPC Design Internal Pressure (Load Case 5) – Thru-Thickness Stress Intensity Plot at Baseplate Center

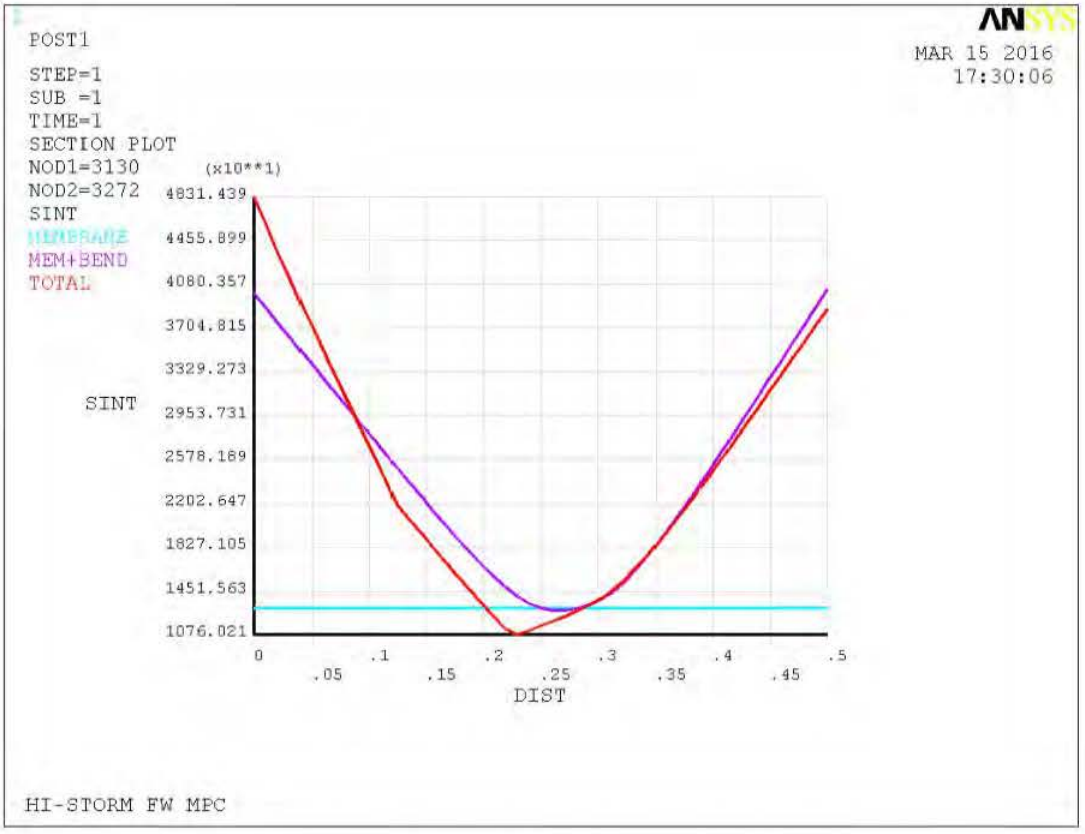

Figure 3.4.33: MPC Design Internal Pressure (Load Case 5) –
Thru-Thickness Stress Intensity Plot at Baseplate-to-Shell Juncture

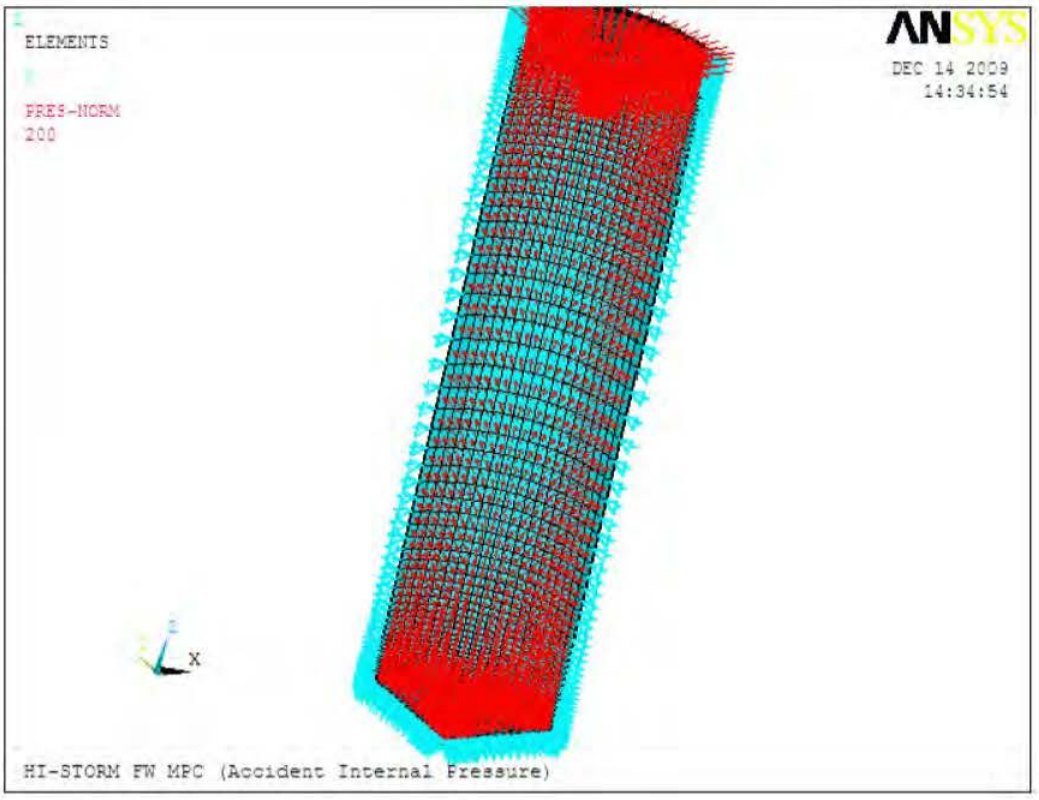

Figure 3.4.34: MPC Accident Internal Pressure (Load Case 6) – Boundary Conditions and Applied Loads

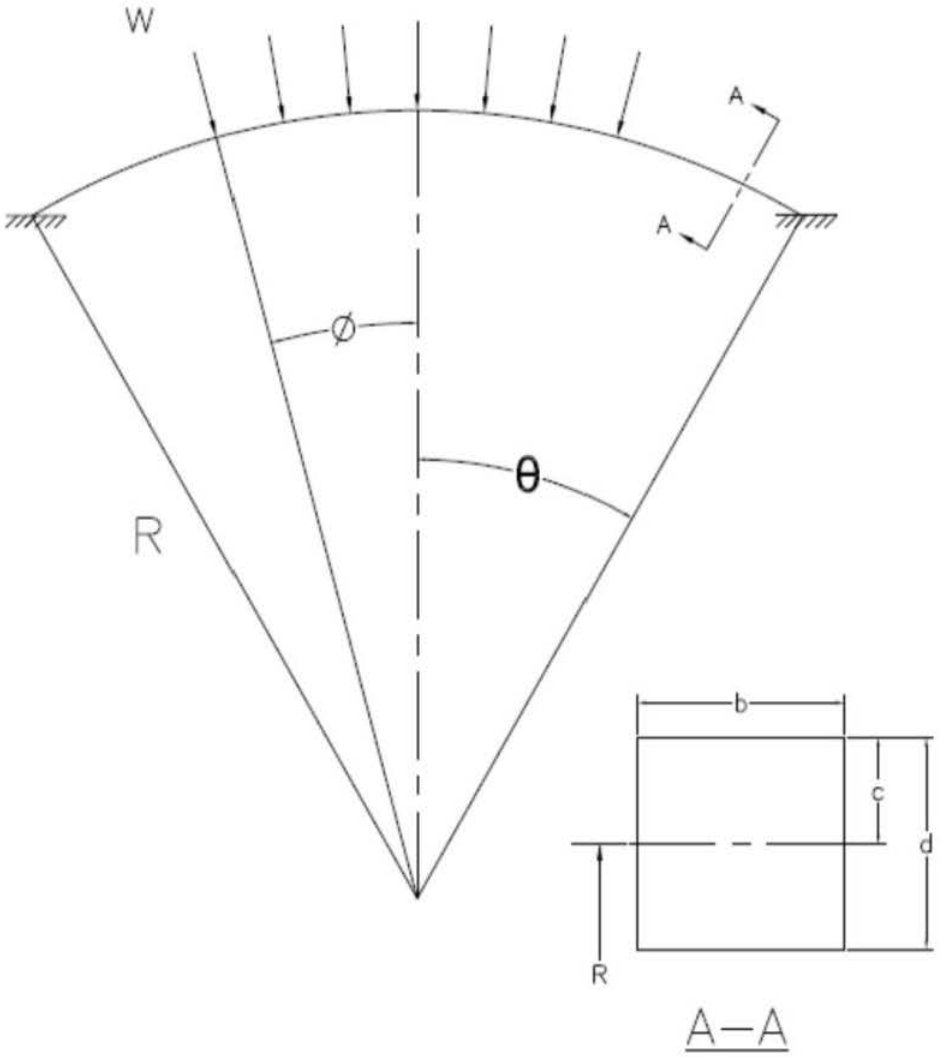

Figure 3.4.35: Analytical Model of HI-TRAC Water Jacket Shell (Load Case 8)